

The Influence of Counterparty Risk on Financial Stability in a Stylized Banking System

Annika Birch

A dissertation submitted in partial fulfillment
of the requirements for the degree of
Doctor of Philosophy
of
University College London.

Department of Computer Science
University College London
January 13, 2016

I, Annika Birch, confirm that the work presented in this thesis is my own. Where information has been derived from other sources, I confirm that this has been indicated in the work.

Abstract

In this thesis, we investigate the influence of counterparty risk on financial stability in a banking system. Banks are exposed among each other via loans, credit derivatives, repayment agreements, commercial bonds and other financial products. Losses caused by counterparty failure can potentially result in a bank's insolvency since a bank cannot expect to retrieve the full value of any obligation to an insolvent counterparty. The interconnectedness between institutions, in the form of exposure from one institution to another, can propagate insolvency from one bank to another, create further insolvencies, and eventually bring down the entire financial system.

We study a cascade counterparty risk model of interacting banks using liabilities and assets to define banks' balance sheets, which are further divided into interbank assets and liabilities, modelling direct dependencies between banks. We further assume that the balance sheet parameters are random variables. We simplify the system by assuming that banks can be in two states: solvent or insolvent. The state of a bank changes from solvent to insolvent whenever its liabilities are larger than the bank's assets, the so-called balance sheet test of insolvency. This creates a stylized banking system that is analogous to the Random Field Ising model, a well-known model in the statistical physics literature.

We solve the counterparty risk model semi-analytically by applying a mean-field assumption that homogenizes the banking system for different location-scale distributions. We call this simplified version of the counterparty risk model the *mean-field model*. The mean-field assumption allows us to conduct an analysis of the balance sheet parameters to evaluate the stability of the banking system. We observe the development of a fragile state where small perturbations to banks' capital reserves can trigger a sudden system failure. The parameter analysis further allows us to calculate minimum capital requirements for banks ensuring a stable system, and to quantify the cost of rescuing a defaulted banking system.

Two simulation models are used to test for the robustness of the results of the mean-field model. For the first simulation model, we consider a highly stylized banking system and verify that the mean-field model is robust for a variety of standard network topologies and random distributions. More specifically, we find that the interbank network is essential for the insolvency propagation. However, the structure of the interbank network does not play a critical role for the distribution of counterparty insolvency. We further show that diversification does not necessarily reduce the risk of system failure.

We also compute the critical balance sheet values for the stylized banking system in the mean-field model, at which the fragile state occurs. For the second simulation model, we use UK regulatory data to initialize the model. We show that a more realistic heterogeneous system with different bank types and a complex underlying interbank network calibrated on UK data also has systemic failures around similar sized shocks to banks' capital as computed for the stylized homogeneous system.

A network analysis on the exposure networks created using regulatory reports reveals a core-periphery topology with large internationally operating banks in the center of the exposure network and smaller regional banks in the periphery. By aggregating the fraction of surviving banks to specific bank types, we show that the behaviour of banks towards failure is independent of the size of their balance sheets or their position in the interbank network. This shows that bank-size heterogeneity and network complexity play a marginal role in the mechanism leading to systemic failure. However, we also observe significant differences. Insolvencies in the heterogeneous system start at smaller sized shocks than in the homogeneous system, and the residual fraction of surviving banks ends at a larger value in the heterogeneous system than in the homogeneous system.

In conclusion, we demonstrate that a simple counterparty risk model replicates the behaviour of more complex simulation-based stress test models of a heterogeneous banking system. This is significant because it allows for a better understanding of the spread of system-wide insolvency, to draw policy implications such as the cost of rescuing an insolvent banking system, and to specify capital requirements that ensure a stable banking system that can be computed analytically using the mean-field model.

Acknowledgements

First and foremost, I like to thank my supervisor Tomaso Aste for his help and advice while conducting the research for this thesis. I also like to thank the Centre for Doctoral Training in Financial Computing and Analytics and the Engineering and Physical Sciences Research Council for providing funding that enabled me to work on my research for the last four years but also to appreciate the advantages that come with living in London; and the Centre for Systemic Risk for offering access to data and seminars on systemic risk. I also like to take this opportunity to express gratitude to Zijun Liu and other employees at the Bank of England for their help in completing my research. I am also sincerely thankful to Philip Treleaven and Yonita Carter for their help while conquering the administrative jungle at UCL and providing great networking opportunities, and to my friends at the CDT for their mental support during coffee breaks in the common room and gatherings in the pub.

I am also grateful to my parents, Kerstin and Michael Wipprecht, for their unceasing encouragement, and support; my husband, Nathan Birch, for his support during the emotional ups and downs during my PhD (also for being the most patient proof reader that ever existed); and my dog, Bertrand, who tried to help write this thesis and add valuable words like: “asddddddffff” by pawing on the keyboard.

Contents

Contents	8
List of Figures	11
List of Tables	12
1 Introduction	13
2 Literature Review	21
2.1 Cascade Counterparty Risk Models	21
2.1.1 Simulation-Based Studies	21
2.1.1.1 This Thesis in Relation to the Literature on Simulation-Based Studies of the Cascade Counter- party Risk Model	22
2.1.2 Analytic Solutions of the Cascade Counterparty Risk Model . .	23
2.1.2.1 This Thesis in Relation to the Literature on Analytic Solutions of the Cascade Counterparty Risk Model . .	24
2.2 Literature on the Topology of Interbank Networks	26
2.2.0.1 This Thesis in Relation to the Literature on Interbank Networks	30
2.3 Short Overview of Other Systemic Risk Models	30
3 The Cascade Counterparty Risk Model	33
3.1 Counterparty Risk Model	33
3.2 Mean-Field Model	37
3.2.1 The Ratio of Interbank Assets to Total Assets, θ	41
3.3 Simulation-Based Counterparty Risk Model	42
3.3.1 Differences in the Assumptions of the Simulation Models . . .	44

3.3.2	Changes in the Value of Balance Sheet Quantities Over Time . . .	45
3.4	The Initial Shock to Banks' Balance Sheets	46
3.5	Conclusion	47
4	Mean-Field Model Results	48
4.1	Fixed Points	48
4.2	Change in the Number of Surviving Banks Induced by One Bank Failure	54
4.3	Parameter Analysis	54
4.4	Relation Between a and b	57
4.5	Leverage, γ	57
4.6	The Fraction of Mean Liabilities, f_L	58
4.7	Values for Other Location-Scale Distributions	59
4.8	Analysis of Real Banking Systems Using Balance Sheet Data	65
4.9	Conclusion	71
5	Comparison of Simulation and Mean-Field Model of Stylized Banking Systems	73
5.1	Initialization of Theoretical, Simulation-based Banking System	73
5.2	Random Distributions	76
5.2.1	Normal and Student's t Distributions	76
5.2.2	Non-Location Scale Distributions	80
5.3	Network Influence	83
5.3.1	Size of the Banking System, N	83
5.3.2	The Average Degree, \bar{z}	84
5.3.3	The Influence of the Variance, σ , on Diversification of Inter- bank Assets	86
5.3.4	Network Topology	89
5.4	Recovery Rate	91
5.5	Changes in Liabilities and Assets During the Insolvency Propagation . .	92
5.6	Conclusion	97
6	Empirical Analysis of Counterparty Failure in the UK Banking System	99
6.1	Data Analysis	99

6.1.1	Description of Regulatory Datasets	99
6.1.2	Data Analysis of Balance Sheets	102
6.1.3	Topology of the UK Interbank Network	104
6.1.3.1	Connected Component Analysis	105
6.1.3.2	Degree Analysis	105
6.1.3.3	Weight Analysis	107
6.1.3.4	Associativity Coefficients Analysis	109
6.2	Model Calibration	110
6.2.1	Calibration of Homogeneous Mean-Field Model	110
6.2.2	Calibration of the Heterogeneous Simulation	110
6.3	Stress Simulation Results and Comparison with Homogeneous Solutions	111
6.3.1	Inducing System Stress by Increasing Average Liabilities	111
6.3.2	Frequency Distribution for Fixed f_L	115
6.3.3	Inducing Stress by Increasing Direct Exposure of Large Banks	118
6.4	Minimum Leverage Ratio	121
6.5	Conclusion	122
7	Conclusions	124
	Appendices	131
A	Propositions and Lemmas Needed for Fixed Point Analysis	131
B	Emperical Information on Interbank Network	134
C	Additional Figures of Empirical Counterparty Risk Analysis of the UK Banking System	139
D	Variable Description	145
E	Abbreviations	147
	Bibliography	149

List of Figures

3.1	Stylised balance sheet of bank i	34
4.1	Graphs of $F(p)$ and $p - F(p)$ against p for fixed values of a and b	50
4.2	Graphs of $F'(x)$ and $x - F(x)$ against x for $a = 2.5$ and $b = 5$	51
4.3	Graphs of $x - F(x)$ against x for fixed values of b and changing values of a	53
4.4	Fraction of surviving banks as a function of a for different values of b . . .	55
4.5	Heat map of the fraction of surviving banks for different values of a and b	56
4.6	Minimum Leverage as a function of θ for different values of σ	58
4.7	Graphs of $F'(x)$ and $x - F(x)$ against x for different Location-Scale Distributions.	62
4.8	Graphs of $a_{1,2}$ against b for different Location-Scale Distributions. . . .	63
4.9	Minimum leverage for different Location-Scale Distributions.	64
4.10	Mean-field model calibrated with UK balance sheet data for 2007 and 2012.	68
4.11	Heat map of fractions of surviving banks for changing a and b including equilibrium fractions of surviving banks for UK balance sheet data. . . .	69
4.12	Mean-field model calibrated with US balance sheet data for 2007 and 2012.	70
5.1	Fraction of surviving banks for different distributions.	77
5.2	Frequency distribution for banking systems initialized with Normal and Student's t distribution.	79
5.3	Fraction of surviving banks for banking systems initialized with Nor- mal, Log-Normal, Logistic and Log-Logistic distribution.	80
5.4	Frequency distribution for banking systems initialized with Normal, Log-Normal, Logistic and Log-Logistic distribution.	81

5.5	PDFs for the average initial capital of a bank given that the banking system is initialized with Normal, Logistic, Log-Normal and Log-Logistic distributions.	82
5.6	Error between mean-field and simulation solution for banking systems of different sizes.	84
5.7	Error between mean-field and simulation solution for interbank networks with changing average degrees.	85
5.8	Fraction of insolvent banks for banking systems initialized with Normal distributions with different σ	86
5.9	Heat map of fraction of surviving banks for varying a and b and the equilibrium solutions of Figure 5.8 for different values of σ	87
5.10	Fraction of surviving banks for different network topologies.	89
5.11	Fraction of surviving banks for different recovery rates.	91
5.12	Rounds of insolvency including asset devaluation.	93
5.13	Graphs of $x - F(x)$ for different values of $a''(r)$	94
5.14	Fraction of surviving banks for changes in the value of liabilities during insolvency propagation.	96
5.15	Graphs of $x - F(x a')$ for two different a'	97
6.1	Interbank network.	104
6.2	Average degrees and weights for different bank types.	106
6.3	Fraction of surviving banks for banking systems calibrated with 2013 H1 data.	112
6.4	Fraction of surviving banks of different bank types for banking systems calibrated with 2013 H1 data.	113
6.5	Frequency distribution of simulation model calibrated with 2013 H1 data.	116
6.6	Fraction of surviving banks for increased exposure network for banking systems calibrated with 2013 H1 data.	117
6.7	Frequency distribution for increased exposure network for 2013 H1 data.	118
6.8	Minimum leverage requirement for 2013 H1 UK exposure network.	121
A.1	Graphs of $x - F(x)$ for fixed $a = 2$ and various values of b	133
C.1	Fraction of surviving banks for banking systems calibrated with 2011 H2 and 2012 H2 data.	140

C.2 Fraction of surviving banks aggregated to bank type level for banking systems calibrated with 2011 H2 and 2012 H2 data. 141

C.3 Frequency distribution for banking systems calibrated with 2011 h2 and 2012 H2 data. 142

C.4 Fraction of surviving banks for increased exposure network for banking systems calibrated with 2011 H2 and 2012 H2 data. 143

C.5 Frequency distribution for increased exposure network for banking systems calibrated with 2011 H2 and 2012 H2 data. 144

List of Tables

3.1	Variables of bank i at time t used in the balance sheet model.	35
4.1	The table states the values of $F(x)$, $F'(x)$, b_c , $x_{1,2}$, $a_{1,2}$ and γ_{\min} given that the random variables L_i and \hat{A}_i are drawn from Normal distributions.	60
4.2	The table states the values of $F(x)$, $F'(x)$, b_c , $x_{1,2}$, $a_{1,2}$ and γ_{\min} given that the random variables L_i and \hat{A}_i are drawn from Cauchy distributions.	60
4.3	The table states the values of $F(x)$, $F'(x)$, b_c , $x_{1,2}$, $a_{1,2}$ and γ_{\min} given that the random variables L_i and \hat{A}_i are drawn from Logistic distributions.	60
4.4	The table states the values of $F(x)$, $F'(x)$, b_c , $x_{1,2}$, $a_{1,2}$ and γ_{\min} given that the random variables L_i and \hat{A}_i are drawn from Student's t distributions with two degrees of freedom.	61
4.5	Summary of balance sheet information from Bankscope of the UK and US banking systems in the years 2007 and 2012.	66
5.1	Values of Variables as used in the simulation and mean-field model.	74
5.2	Input variables of Normal, Log-Normal, Logistic and Log-Logistic as derived from a Normal distribution's mean and standard deviation.	75
6.1	Number of UK banks used for calibration.	101
6.2	Arithmetic mean of the value of assets for different bank types.	102
6.3	Arithmetic mean of the value of Tier 1 capital for different bank types.	103
6.4	Average leverage ratio for different bank types.	103
6.5	Average interbank assets to total assets for different bank types.	108
B.1	Average in-weight aggregated by bank types.	135
B.2	Average out-weight aggregated by bank types.	136
B.3	Average in-degree aggregated by bank types.	137
B.4	Average out-degree aggregated by bank types.	138

Chapter 1

Introduction

In recent years, it became evident that the structure of the modern financial system can cause severe danger to financial stability by spreading insolvency through obligations on the interbank markets to other banks in the banking system (Haldane, 2009). The risk that banks impose on others through interconnectedness is called counterparty risk (Upper, 2011) and is the subject of this thesis.

In 2006, the US housing market started collapsing. This event induced a global financial crisis with the aftermath still visible in 2015. Low interest rates provided by the Federal Reserve enabled US banks to offer mortgages to people without deposits and uncertain income. These mortgages were bundled with less risky mortgages and sold as mortgaged backed securities to other banks and financial companies worldwide. The idea was to diversify risk, grouping mortgage holders prone to failure with less risky mortgage holders, thereby lowering the overall risk. In 2006, the Federal Reserve raised its interest rate to 6% from a former low of 0.75% in 2002 (Kolb, 2010). Banks raised interest rates of mortgages with adjustable interest rates as a consequence to cover their increased cost of funding the mortgages. This caused numerous holders of mortgages with adjustable interest rates to declare bankruptcy as they were not able to maintain their mortgage payments. In turn, banks faced large losses due to credit failure on their portfolios. The collapse of the US housing market resulted in a global financial crisis.

Mortgage-backed securities became an alternative funding source in addition to more traditional liabilities such as deposits and corporate bonds. In general, the market for asset-backed securities increased tremendously. More specifically, the Financial Crisis Inquiry Commission records in their report on the financial crisis:

“By 1999, when the market was 16 years old, about \$900 billion worth of securitizations ... were outstanding.” (Financial Crisis Inquiry Commission and others, 2011)

Securitization was only one way to fund the excessive growth of banks' balance sheets and mergers of banks that happened in the 90s and early 2000s. Interbank loans and particularly over-night loans also formed an integral part of banks' funding strategy. The Financial Crisis Inquiry Commission notes on the issue:

“For example, at the end of 2007, Bear Stearns had \$11.8 billion in equity and \$383.6 billion in liabilities and was borrowing as much as \$70 billion in the overnight market.” (Financial Crisis Inquiry Commission and others, 2011)

Over-night loans were used to satisfy banks' liquidity needs but were also used as financing for assets with maturity dates in the far future. Other ways for banks to obtain funding were repurchase agreements (repos). A bank sold a security to a counterparty and agreed to buy the security at an agreed date. Finally, banks were highly exposed to each other via derivatives. The Financial Crisis Inquiry Commission states that

“... the notional amount of OTC [Annot.: over-the-counter] derivatives outstanding globally was \$95.2 trillion, and the gross market value was \$3.2 trillion. In the seven and a half years from then until June 2008, when the market peaked, outstanding OTC derivatives increased more than seven-fold to a notional amount of \$672.6 trillion; their gross market value was \$20.3 trillion.” (Financial Crisis Inquiry Commission and others, 2011)

Banks and other financial firms were highly interconnected through interbank exposure and overlapping portfolios with the health of one company depending on the solvency of others. Losses from mortgage providers easily spread to other parts of the financial industry via mortgage backed securities and resulted in major uncertainty about the future of financial firms. As a result, governments started bail-out programs providing capital for struggling banks, and central banks initiated quantitative easing programs to inject liquidity into the system, but also to give banks time to restructure their portfolios to less risky products. For example,

“the [Annot.: US] government ultimately committed more than \$180 billion because of concerns that AIGs collapse would trigger cascading losses throughout the global financial system.” (Financial Crisis Inquiry Commission and others (2011))

Even though the major banks were rescued and loans from governments to failing banks were settled, the impact on the real economy and on society is still visible in 2015 with rates of unemployment high, and austerity measures in place intended to stabilize economies (Kolb, 2010; Claessens et al., 2013).

In this thesis, we show that interconnectedness can accelerate the failure of a banking system. We restrict our investigation to how counterparty failure influences financial stability disregarding the influence of market risk. We acknowledge that market risk played an important role during the financial crisis. However, for the moment, the goal of this thesis is to provide a better understanding of how the insolvency cascade process influences financial stability of a banking system. Having a better understanding of this allows us to provide restrictions on banks' balance sheet quantities to ensure a more stable banking system.

An active literature modelling counterparty risk in banking systems using network science and statistical modelling has emerged studying the impact of bank failure on the stability of the banking system (Allen and Gale, 2000; Eisenberg and Noe, 2001; Furfine, 2003; Nier et al., 2007; Gai and Kapadia, 2010; May and Arinaminpathy, 2010; Cont et al., 2010; Battiston et al., 2012a; Fouque and Langsam, 2013). These models are similar in that banks' balance sheets consist of liabilities and assets. The balance sheets are further divided into interbank assets and liabilities modelling direct dependencies between banks. The interbank assets and liabilities create an interbank network with banks being the nodes and interbank exposure forming the links of the network. In these models, a bank is considered insolvent if its liabilities are larger than the bank's assets, which is called the balance sheet test of insolvency (Goode, 2010). The insolvency of a bank can be triggered by a random event (an initial bank failure, reduction of asset values) that reduces banks' loss absorbing capital and brings about counterparty failure. In this thesis, we also introduce and study a cascade counterparty risk model of interacting banks. In our model, banks can be in either of two states: solvent or insolvent. This creates a stylized banking system that is analogous to the Random

Field Ising model, a well-known model in the statistical physics literature. In our stylized banking system, the balance sheet variables (assets, liabilities and loss absorbing capital) are random variables. We also divide assets and liabilities into interbank and non-interbank categories. The interbank assets and liabilities form the connection between banks. This allows us to also represent the interbank exposure using interbank networks. We shock the system by lowering a fraction of all banks loss-absorbing capital initially. This causes some initial insolvencies. The interbank network propagates the insolvency from one bank to another creating further insolvencies, and eventually bringing down the entire system given a large enough shock.

We use a mean-field assumption to solve the insolvency cascade model semi-analytically as well as numerically using simulation means. The mean-field assumption homogenizes the banking system. This enables us to compute the equilibrium fraction of surviving banks for fixed location and scale parameters of the balance sheet values using a fixed point analysis. The fixed point analysis allows us to detail the parameter ranges of balance sheet quantities that lead to a stable or unstable system. Because of this, we can determine restricting ratios between loss absorbing capital and assets, the leverage ratio, to ensure a stable banking system. We state this ratio for a variety of location-scale distributions used to initialize banks' balance sheets. The most dominant feature of the mean-field solution is the occurrence of a fragile state, where one bank can trigger the default of the entire banking system. This fragile state has been observed in other studies (Gai and Kapadia, 2010; Amini et al., 2012; Hurd and Gleeson, 2011). We find that the important quantities regulating the fragile state are the ratios of interbank assets to total assets, and loss absorbing capital to total assets. Moreover, we quantify the costs of potential rescue attempts to re-direct an unstable system into a stable region. We use balance sheet data for 2007 and 2012 to initialize the homogeneous counterparty risk model showing that the US and UK banking systems in 2007 were more prone to failure than in 2012.

To solve the counterparty risk model analytically, we make some restricting assumptions. In particular, we assume an infinitely large banking system, where banks are of similar size, and have equal-sized exposure to other banks. Additionally, we assume that the value of non-interbank assets and liabilities do not change during the insolvency propagation. To address the effects of these assumptions, we test for robust-

ness and generality of the mean-field solution by solving the counterparty risk model numerically. In particular, we change the structure of the exposure network and apply different random distributions to initialize the balance sheet parameters. We argue that, given a shock that causes the balance sheet parameters to shift into the unstable region, the precise underlying topology of the exposure network is secondary for the propagation of insolvency. Furthermore, we discuss how diversification of interbank assets affects the fragile state. We do so by showing that if the reaction of banks to an external shock to their balance sheet quantities results in similar losses of average capital, then the fragile state can still be observed even for a highly diversified portfolio of interbank assets. We also create banking systems of different sizes and compare the simulation solution with the mean-field solution, concluding that for systems of all sizes the mean-field solution is a fair approximation. Finally, we change the banks' values of liabilities and non-interbank assets during the insolvency propagation using (arbitrary) functions to reduce non-interbank assets proportional to the fraction of surviving banks, and decrease the value of liabilities by injecting external capital into the banking system. We discuss how the simulation results can be interpreted in the mean-field setting.

In the final part of this thesis, we use regulatory data of the UK banking system to initialize both a simulation-based model as well as the mean-field model. Initializing the simulation-based model with the UK regulatory data results in a highly heterogeneous banking system. Therefore, we call this model the heterogeneous model. The heterogeneous model replicates a more realistic picture of a banking system than the mean-field model. In both models, the system is stressed by artificially decreasing loss absorbing capital. We observe in both models the occurrence of the fragile state and the consequent systemic collapse and jump to a state where most banks are insolvent. We demonstrate that in the heterogeneous model the systemic collapse happens around the same values predicted by the mean-field model. Hence, we demonstrate that a simple insolvency cascade model of a homogeneous banking system replicates the behaviour of a more complex simulation-based stress test model of a heterogeneous banking system. This is significant since it allows us to better understand the spread of system-wide insolvency, to draw policy implications such as the cost of rescuing an insolvent banking system, and to specify capital requirements that ensure a stable banking system from a simple counterparty risk model of a homogeneous banking system.

As part of Chapter 6, we conduct a brief data analysis of the UK regulatory data sets. The UK regulatory data sets consist of information about banks' balance sheet quantities used to initialize the model, namely, the value of banks' total assets and Tier 1 capital. We conclude that the UK banking system consists of a wide variety of banks with balance sheet sizes that differ by orders of magnitude. In addition, we examine the structure of three exposure networks of the UK banking system constructed from regulatory reports on bilateral exposure collected in 2011, 2012 and 2013. We show that multinational banks are in the centre of the exposure network with regional banks and small subsidiaries of foreign banks forming the periphery of the exposure network.

The results of the data analysis should be considered with caution as the data still only provides a subset of the complete interbank network. Banks are required to only report exposure to 20 counterparties worldwide. In the model, we only use the exposure of UK banks to other UK banks to create the interbank network. The average links UK banks have to other UK banks is seven. This reduces the ratio of interbank assets to total assets considerably in comparison to values observed in other studies. For this reason, the shock to banks' loss absorbing capital has to be fairly large resulting in very low leverage ratios ensuring a stable banking system. We address the low values of interbank assets by increasing the exposure of banks artificially, thereby increasing the average ratio of interbank assets to total assets of the entire system to values observed in other studies.

We discuss in more detail the literature on cascade counterparty risk models in Chapter 2, and we also state in more detail how the results in this thesis improve those in on the literature in that chapter. The literature on cascade counterparty risk models can be divided into two branches. The first branch solves the counterparty risk model using simulations. Notable examples of studies of simulation-based cascade counterparty risk models include Furfine (2003), Müller (2006), Nier et al. (2007) and Gai et al. (2007). The second branch solves the model analytically. Notable examples of analytic solutions of the model are Gai and Kapadia (2010), May and Arinaminpathy (2010), Hurd and Gleeson (2011), Amini et al. (2012) and Glasserman and Young (2015).

The majority of studies (both simulation based and analytical) only investigate the cascade process. That excludes shocks to banks' capital caused by fluctuations in asset and liability values. The initial shock in most studies is caused by a reduction of a bank'

asset side of the balance sheet or one insolvent bank initially. In such studies the impact of counterparty failure to the stability of the banking system is minimal (Müller, 2006; Battiston et al., 2012c). Whereas solving the counterparty risk model using the mean-field approach as done in this thesis can incorporate fluctuations to all banks' capital. This is significant because we are able to show that depending on the initial shock to banks' capital the banking system can shift into an unstable region, in which most of the banks become insolvent. Using fluctuations to banks' capital seems a more realistic approach as the initial shock because shocks in financial markets are experienced by most banks in the financial system.

Furthermore, in most studies, and simulation-based studies in particular, banks have identical balance sheets. In these studies (Gai and Kapadia, 2010) diversification of interbank assets lowers counterparty risk. However, we show that in a banking system where banks have different ratios of capital to assets, diversification does not necessarily lower counterparty failure. This is in line with the results in Battiston et al. (2012b) and Garnier et al. (2013). We argue that in a system where banks have multiple counterparties, the probability of being connected to an insolvent bank also increases, and therefore the risk of failure still exists.

We simulate the diversification of banks' capital by assuming that the balance sheet quantities are random variables during the initialization process. Because of that, for each simulation we allow for small variations in banks' capital. This seems like a more reasonable assumption because it can be expected that banks' balance sheets change during daily business. Hence, even balance sheet data reported to regulators most likely is outdated shortly after reporting. Thus, when using random distribution of the balance sheet parameters, we can test the stability of the banking system for a range of parameters close to the observed values.

Finally, we show that the UK interbank network has a core-periphery structure using exposure data from the Bank of England. Other studies (Boss et al., 2004; Fricke and Lux, 2015; van Lelyveld et al., 2012; Langfield et al., 2014) also determined that interbank networks have a core-periphery structure. This result is not too surprising as part of the dataset used in this thesis was also studied in Langfield et al. (2014). Nonetheless, we extend on the study of Langfield et al. (2014) by providing more data on the position of specific bank types in the interbank network.

The thesis is structured as follows: Chapter 2 summarizes the current literature on studies on cascade counterparty risk models and on the topology of interbank networks and how the results of this thesis compare with those in the literature. Furthermore, we briefly outline work on other systemic risk measures not strictly related to cascade insolvency risk models. We do this because counterparty risk is part of systemic risk, i.e. risk that can contribute to system failure. This is followed by Chapter 3, where we state the cascade counterparty risk model used in this thesis, the assumptions leading to the homogeneous mean-field model and the algorithms used to propagate insolvency failure in the simulation-based models. In Chapter 4, we discuss the results of the mean-field model. A comparison of the mean-field model and the solution of simulation counterparty risk models are given in Chapter 5. A description and analysis of the regulatory data forms the first part of Chapter 6. The comparison of counterparty failure in heterogeneous and homogeneous banking systems initialized with the UK data is presented in the second part of Chapter 6. The conclusions are given in Chapter 7.

Chapter 2

Literature Review

2.1 Cascade Counterparty Risk Models

As stated in Staum (2013):

”via contagion, the default of one firm is a cause contribution to default of another.”

To test direct contagion effects, a literature on stylised banking systems has emerged using network science and stylized balance sheets, modelling the dependencies of interbank relationships (Eisenberg and Noe, 2001; Furfine, 2003; Cifuentes et al., 2005; Nier et al., 2007; Gai and Kapadia, 2010; May and Arinaminpathy, 2010). Assets and liabilities of banks are divided into interbank and non-interbank categories. The interbank assets and liabilities form the links between the banks, and henceforth, are the channels of default contagion.

2.1.1 Simulation-Based Studies

Most of the studied cascade counterparty risk models are simulation-based. Banks' balance sheets are initialized using an arbitrary algorithm and the underlying interbank network is constructed artificially using a standard network structure (i.e. Erdős-Rényi, Small-World (Watts and Strogatz, 1998) or Scale-Free (Barabási and Albert, 1999) networks). Some influential studies, that use this theoretical approach are: Nier et al. (2007); Gai et al. (2007); Heise and Kühn (2012); Anand et al. (2012). Other studies, for example, Furfine (2003); Upper and Worms (2004); Mistrulli (2005); Elsinger et al. (2006); Van Lelyveld and Liedorp (2006); Müller (2006); Iori et al. (2006); Degryse and Nguyen (2007); Memmel and Stein (2008); Cont et al. (2010); Mistrulli (2011);

Solorzano-Margain et al. (2013), use real world data of banks' balance sheets and real-world interbank networks to test for the resilience of a banking system.

2.1.1.1 This Thesis in Relation to the Literature on Simulation-Based Studies of the Cascade Counterparty Risk Model

We also use simulation-based models in Chapters 5 and 6. The simulation-based risk models in the later chapters use the same algorithm distributing insolvency through the banking system as used in studies presented above, for example, Furfine (2003) and Müller (2006). In Chapter 5, we show that the solution of the mean-field model can be replicated with simulation-based models for various network topologies and underlying random distributions for the balance sheet parameters.

Instead of using fixed values for assets and liabilities, we initialize our banking system, assuming that the balance sheet quantities are random variables. This initialization process of banks' balance sheets differs from other studies. In some studies, banking systems are initialized such that banks have the same balance sheets (for example, Nier et al. (2007); Gai et al. (2007)). This initialization process creates highly homogeneous banking systems. Real world banking systems, however, consist of banks that vary largely in size. In other studies, real-world balance sheet values are extracted from banks' annual reports and used to initialize the cascade process. We also use real-world balance sheet data in Chapter 6. However, in our initialization process, the real-world balance sheet data are used as the mean-values of the random distribution used to initialize the balance sheets. The stochasticity in our model allows us to introduce some diversity in banks' initial capital, and causes banks to react slightly differently in each stress test simulation. Because of the stochasticity, a shock can have different effects to the banking system depending on the distribution of banks' initial capital, whereas in deterministic initialization processes the same shock will lead to the same result. The stochastic method is more realistic because banks' balance sheets and capital reserves change continuously during operation. Because of this, any measurements of banks' balance sheets are already inaccurate the next day.

In simulation-based stress tests, it is easy to add extra algorithms to make the stylized banking system more realistic. For instance, Cifuentes et al. (2005), Müller (2006) and May and Arinaminpathy (2010) test the effects of liquidity shortage; in Gai et al.

(2011) unsecured claims, repurchase agreements and haircuts are included in the simulation; and in Anand et al. (2012) banks can choose to withdraw their funds (foreclose) early to a counterparty to limit losses in the event of insolvencies. We also use additional functions to change the values of interbank assets and liabilities in Section 5.5. As in the literature, we observe that a reduction in the value of interbank-assets during the insolvency cascade can result in or accelerate system failure. Additionally, we explain the effects of the functions in our mean-field setting.

2.1.2 Analytic Solutions of the Cascade Counterparty Risk Model

Simplifying the model set-up allows one to extract information about the insolvency propagation analytically. For example, in Gai and Kapadia (2010) banks' balance sheets are said to be identical. The interbank network is the source of randomness in their model. That is, the total interbank assets of a bank are divided by the out-degree of the bank creating different weighted exposure links between banks. Applying this simplification, they used a method combining probability generating functions of degree distributions with the probability of a bank being connected to an insolvent bank (discussed in more detail in Watts (2002)) to determine the probability of default of the banking system conditional on the out-degree of banks. They show that if banks diversify their interbank assets to many other banks, then the probability of default of the entire banking system is reduced. The result in Gai and Kapadia (2010) is to some extent confuted by Battiston et al. (2012b) and Garnier et al. (2013), where they allow balance sheet quantities (non-interbank assets and liabilities) to differ. The heterogeneity causes diversification of interbank exposure and does not necessarily stop the system from defaulting. This was also indicated in Iori et al. (2006), where both models of homogeneous and heterogeneous banking systems were studied using simulation means calibrated on data of the Italian Money Market. In Amini et al. (2012) and Amini et al. (2013), they generalise the results of Gai and Kapadia (2010) using asymptotic analysis on insolvency cascades on networks. They show that there exists a point, at which one bank can trigger entire system default. Another investigation of the influence of diversification is found in Hurd and Gleason (2011). There, they find that the size of a shock to the capital that causes system failure. Glasserman and Young (2015) also use connection probabilities to evaluate banks' risk of insolvency. They

compare these to banks' idiosyncratic risk of failure due to market effects. They determine that only if the idiosyncratic risk is high, interbank connectivity can result in insolvency propagation.

In May and Arinaminpathy (2010), a mean-field approach homogenizing the banking system is used to determine the fraction of insolvent banks after 3 rounds of insolvency. Gleeson et al. (2013) constructs an iterative cascade model and replicates the results of Nier et al. (2007), Gai et al. (2007) and May and Arinaminpathy (2010) by finding some fixed points of an iteration function. The conclusions relevant for regulators based on the model discussed in May and Arinaminpathy (2010) are discussed in Haldane and May (2011). In that paper, they argue for new sets of leverage/capital ratios and increasing the regulatory requirements of systemically important banks.

Finally, some measures of systemic risk have been proposed using as their foundation the cascade counterparty risk model. For example, Debrank (Battiston et al., 2012c) determines the impact of a single or multiple banks insolvency on the rest of the banking system using an iterative process. This causes the overall losses due to counterparty risk to be relatively small. In addition to pure counterparty failure, the contagion index (Cont et al., 2010) also includes external shocks to banks capital reserves, which leads to a risk measure that incorporates potential capital losses that increases the probability of insolvency of single banks.

2.1.2.1 This Thesis in Relation to the Literature on Analytic Solutions of the Cascade Counterparty Risk Model

The counterparty risk model studied in this thesis is based on the balance sheet model used by Nier et al. (2007) and Gai et al. (2007). Furthermore, we assign a state to each bank that determines whether a bank is insolvent or not, which bears similarities to the set-up in Solorzano-Margain et al. (2013). More specifically, we say, bank i is solvent if its state is one, and zero if the bank is insolvent. Because of that the model presented in this thesis is analogous to the Lattice Gas model (Griessen, 1983), (Richards, 1984), a model used to represent the motion of atoms. The state of the banks depends on interbank exposure but also the values of non-interbank assets and liabilities. This assumption leads to a stylized banking system that is analogous to the Random Field

Ising model (Dahmen and Sethna, 1996), (De Dominicis and Giardina, 2006).¹ The application of this kind of model in the context of economic and financial behaviour has been reviewed in Bouchaud (2013), and its application to credit default models has been discussed in Hatchett and Kuehn (2009). RFIM can be solved analytically using a mean-field assumption as is done in this thesis. The solution of the RFIM adopted to represent the dynamics in a banking system in this thesis is a modified version of the Curie-Weiss solution of the RFIM. The Curie-Weiss solution at zero temperature of the RFIM shows a first order phase transition (de Matos and Perez, 1991), (Bouchaud, 2013) that in the context of the adaptation of the model to a banking system explains the fragile state where the majority of banks change their state from solvent to insolvent or vice versa.

In general, the mean-field approach allows us to calculate the stability of the banking system for a wide variety of balance sheet parameters. In Chapter 4, we apply a mean-field assumption that is similar to the one simplifying the cascade model in May and Arinaminpathy (2010). Thereby, we assume that the interbank exposure between banks is the same, disregard the interbank network, and consider banks with similar sized balance sheets only. In our model, liabilities and non-interbank assets are random variables, and because of this, our banking system differs from the banking system constructed in May and Arinaminpathy (2010). In May and Arinaminpathy (2010), the balance sheet quantities of banks are the same values for all banks. Assuming random assets and liabilities allows us (i) to determine the fraction of banks that survive an external shock to their balance sheets and (ii) to conduct a parameter analysis, which reveals the regions, where a fragile state becomes possible. Our results are in line with the findings in Gai and Kapadia (2010), Amini et al. (2012) and Hurd and Gleeson (2011). We also observe a fragile state, at which the majority of banks in banking system change from solvent to insolvent, given a shock to banks' initial capital.

Furthermore, we replicate the results of Gai and Kapadia (2010) in Chapter 5 and discuss diversification of interbank assets within the setting of our methodology. We show that for a particular range of parameters, diversification becomes less significant in order to prevent the fragile state.

¹The Ising model (Ising, 1925) was first used to model ferromagnetic spins that can either be in two states: up or down. The lattice Gas model is a specific version of the Ising model where the state is either one or zero.

Most of the models (Gai and Kapadia, 2010; May and Arinaminpathy, 2010) studying counterparty risk consider counterparty risk on its own, disregarding the influence of potential losses in system-wide capital (notable exceptions are Elsinger et al. (2006), Cont et al. (2010), Amini et al. (2012), Hurd and Gleeson (2011) and Glasserman and Young (2015)). Instead, they discuss counterparty risk given that the initial shock is represented by the loss of one bank in the banking system or a value reduction of one bank's assets. A reason why it is important to consider considerable capital losses when dealing with not only counterparty risk but systemic risk in general is formulated in Acharya et al. (2014):

“If a firm fails in isolation, other financial firms will step in and take over its activities. However, in a period of aggregate stress where the whole financial sector is undercapitalized, financial firms cannot find the resources to take over other firms' activities; thus, failing firms impose negative externalities to the real economy.”

In Glasserman and Young (2015), they even show that without shocks to banks' capital reserves system-wide, the insolvency hardly ever propagates through the interbank network. Furthermore, we calculated the size of the average shock to banks' capital that causes a system crash, and we find that only within the vicinity of the fragile state one bank can trigger counterparty failure.

The results of the mean-field model are published in Birch and Aste (2014).

2.2 Literature on the Topology of Interbank Networks

Studies of direct contagion in a banking system are related to the study of the topology of exposure networks. Interbank exposure networks can be constructed from information on payments systems, interbank lending, or other exposure such as derivatives and repayment products. Interbank exposure and its effects on counterparty risk have led to an active study of interbank exposure networks, where direct obligations between banks are depicted as graphs. Among the first theoretical studies on interbank markets are the works conducted by Rochet and Tirole (1996), Allen and Gale (2000) and Freixas et al. (2000). The networks in these early studies are relatively small consisting of only a small number of banks. Basic concepts such as risk diversification and liquidity needs

are discussed theoretically. Since then, multiple studies on the structure of real-world interbank networks - consisting of a couple of hundred banks, were carried out, e.g. in Müller (2006) and Upper (2011). Some of these studies challenged the results of these early studies. For example, when increasing the number of banks and considering a heterogeneous system, diversification of interbank assets does not always lead to a stable system (Battiston et al., 2012b; Garnier et al., 2013) as suggested in Allen and Gale (2000).

This highlights the importance of empirical studies of the topology of interbank networks. However, studies of real world interbank networks are restricted due to limited access to bilateral exposure data. Bilateral exposure data are mostly collected by banking regulators and are not publicly available, since they are classified as market changing information. Langfield and Soramäki (2014) state regarding the opaqueness of interbank exposure data:

“...links between financial institutions are typically unobserved by market participants. Banks chief risk officers know their employer’s counterparty risk exposures, but not the counterparty risk exposures of their employer’s counterparties. Large broker-dealers typically have some information regarding their clients’ exposures, but uncertainty nonetheless dominates.”

In particular, banks report their bank-to-bank exposure² to their regulatory authority. Other sources of bilateral exposure include electronic trading platforms such as e-MID (electronic market for interbank deposits) (e MID, 2014; Iori et al., 2006) or the Fedwire Funds Services (Board of Governors of the Federal Reserve System, 2014; Soramäki et al., 2007). Regulatory reports and credit registers have restricted access due to their sensitive nature. Thus, most studies on interbank lending are conducted by central banks or bank regulators sometimes in cooperation with academics (for example, Hungary (Lublóy, 2005), Italy (Mistrulli, 2005, 2011; Delpini et al., 2013; Bargigli et al., 2015), Austria (Elsinger et al., 2006), Mexico (Solorzano-Margain et al., 2013; Martínez-Jaramillo et al., 2014) and Brazil (Cont et al., 2010)). In most cases, the interbank networks created from regulatory data contain information on banks belonging to the country of the regulators, excluding foreign banks because these do not fall into

²For example, in the UK the Prudential Regulation Authority, a division of the Bank of England, is responsible for collecting bilateral exposure reports.

the geographic area of the regulator's responsibility. When studying the topology of interbank networks, the exclusion of foreign banks can cause distortions. For example, in the European Union an active cross-border market is present. However, each country collects information on bilateral exposure for banks only that are situated in its jurisdiction (European Systemic Risk Board, 2015).

In other studies of country specific interbank networks, datasets are used to construct interbank networks of a variety of financial products (i.e. interbank credit, derivatives, repayment products and other securities), which are restricted either by a limit on the number of counterparties that banks have to report, or only include exposure above a certain threshold. Thus, the incomplete information on interbank networks restricts studies on the influence of interbank exposure on counterparty risk. This is because models calibrated with incomplete interbank networks underestimate counterparty risk. Examples of studies of incomplete interbank networks include the UK (Langfield et al., 2014), Germany (Van Lelyveld and Liedorp, 2006; Memmel and Stein, 2008; van Lelyveld et al., 2012), Switzerland (Müller, 2006), and Austria (Boss et al., 2004). In Chapter 6, we use UK interbank exposure data first studied in Langfield et al. (2014) to calibrate both the mean-field model as well as a heterogeneous simulation model of counterparty risk.

Datasets on payment flows are used to reconstruct payment and money market networks in the USA (Soramäki et al., 2007; Bech and Atalay, 2010; Battiston et al., 2012a) using data on Fedwire; in Denmark (Amundsen and Arnt, 2005; Rørdam and Bech, 2008) using regulatory reports; and in the Euro-area (Arciero et al., 2014) using TARGET2 (Trans European Real-time Gross settlement Express Transfer) data. In these datasets, transactions between banks are monitored. That is, if a bank A conducts a transfer to a bank B, and bank B returns that transfer (plus interest) at a later time, then it is assumed that bank A was exposed to bank B.

The literature on interbank networks suggests that there exists a core-periphery structure with internationally operating banks forming the core of the interbank network and a periphery consisting of smaller banks that operate on a national basis (Boss et al., 2004; De Masi et al., 2006; Craig and Von Peter, 2010; Wetherilt et al., 2010; Langfield et al., 2014). Specifically, it has been observed that the density of interbank networks are relatively low with small clustering coefficients and disassortative mixing

of the degree (Upper, 2011). In Cocco et al. (2009), it is argued that the core-periphery structure in a country specific interbank market occurs because smaller regional banks have limited access to international markets and tend to use the domestic interbank markets via large internationally operating banks.

Another category of studies on interbank networks uses banks' balance sheet reports and algorithms to infer interbank networks. An early algorithm used to construct an approximated interbank network is the entropy maximization algorithm, as used by Upper and Worms (2004) and Degryse and Nguyen (2007). Information about banks total interbank assets and liabilities to or from other banks is distributed using maximum entropy. This creates an interbank network where obligations are spread as equally as possible creating a fully connected graph. However, this algorithm disregards any community structure and low density as observed in real networks, and therefore was not deemed suitable to create interbank networks, as it underestimates the impact of counterparty risk (Mistrulli, 2011; Mastromatteo et al., 2012). The maximum entropy algorithm is tweaked in Mastromatteo et al. (2012) where they adopt the maximum entropy algorithm by tuning the degree of sparsity by bounding the maximum possible degree of sparsity to create a more realistic network.

In Musmeci et al. (2012), a bootstrapping method is used to reconstruct the topology of financial networks. This algorithm can be used provided there is information given about the connectivity of a small subset of nodes. To construct the network, they use an exponential random graph model that has to satisfy constraints provided from the initial seed network and other information.

The core-periphery algorithm in an interbank setting (Craig and Von Peter, 2010) is also used to construct exposure networks. The algorithm creates a network, where banks can be classified into two groups: core and periphery banks. In a perfect core-periphery network, periphery banks are only connected to core banks. Whereas, core banks are connected to periphery banks but also other core banks. The core-periphery algorithm was studied in Craig and Von Peter (2010), Fricke and Lux (2015) and Langfield et al. (2014). The studies reveal that the networks produced using the core-periphery algorithm provide a better fit to real world networks than networks constructed using the maximum entropy algorithm.

2.2.0.1 This Thesis in Relation to the Literature on Interbank Networks

We refrain from using any of the algorithms discussed above to construct the interbank network, as we were able to obtain real-world exposure data to construct our networks in Chapter 6. Nonetheless, we think that due to a lack of publicly available data, algorithms are needed to replicate the the core-periphery form of interbank networks. Hence, we intend to redirect our future research to the fine tuning of these algorithms and, for this and other reasons, provide more network measures in Section 6.1.3 to obtain a better understanding of the topology of interbank networks.

In alignment with the literature on interbank networks, we find that the exposure data studied in this thesis also produces core-periphery interbank networks. This is not surprising because part of the data (2011) used to produce the interbank networks was already studied in Langfield et al. (2014).

2.3 Short Overview of Other Systemic Risk Models

Financial contagion can occur via indirect and direct channels. Insolvency propagation via interbank exposure is only one (direct) channel of insolvency contagion in a banking system. An other channel is asset price fluctuations. In this thesis, we focus on the effects of direct exposure from one bank to another and how this effects the stability of a banking system. For completeness, this section gives a brief overview of works on systemic risk, where asset price fluctuation and correlated portfolios are considered the source for an unstable banking system. Fouque and Langsam (2013) provide a more detailed collection of papers and an extensive review of the most current literature on systemic risk.

Influential studies examining indirect channels include, for example, the measure: Conditional Value at risk (CoVar) by Adrian and Brunnermeier (2011), a variation of the Value at Risk (VaR³). CoVar uses the quantile function, measuring whether a bank is at its VaR conditional on other institutions being at their VaR. The Systemic Expected Shortfall (SES) by Acharya et al. (2010), a variation of the Expected Shortfall (ES⁴), measures "... the amount a bank's equity ... drops below its target level ... in

³VaR states the value of a quantile function of loss distributions that a bank is likely to lose over a time period given a certain confidence interval.

⁴Acharya et al. (2010) defines ES as: "... the expected shortfall is the average of returns on days when the portfolio's loss exceeds its VaR limit."

case of a systemic crisis” (Acharya et al., 2010). The distress insurance premium measure introduced by Huang et al. (2009) and Huang et al. (2012) is “based on credit default swap (CDS) spreads of individual banks and the co-movements in banks equity returns”(Huang et al., 2012). The three measures rely on time series analysis of banks’ portfolios.

In Billio et al. (2012) correlation and causality measures on financial institutions’ returns are used to quantify systemic risk. They conclude “that linkages within and across all four sectors [Annot.: banking, insurance companies, hedge funds and broker/dealers] are highly dynamic over the past decade, varying in quantifiable ways over time and as a function of market conditions. Over time, all four sectors have become highly interrelated, increasing the channels through which shocks can propagate throughout the finance and insurance sectors” (Billio et al., 2012).

Segoviano and Goodhart (2009) calculate the banking system’s portfolio multivariate density, which characterizes “both the individual and joint asset value movements of the portfolio of banks representing the banking system” (Segoviano and Goodhart, 2009), by computing the joint probability of distress of the banking system. A similar approach is used in Tsatskis (2012), where he solves for the distribution of insolvent banks using multi-name latent variable models. Specifically, he uses normal distributions for the underlying balance sheet variables. The outcome in both papers depends on the choice of the underlying copulas used to combine the default probabilities of single banks and might vary greatly for different random distributions.

Banks and asset classes form the set of nodes of bipartite networks in Caccioli et al. (2014), where the Galton-Watson process is used to determine the influence of overlapping portfolios on financial stability. In both Tsatskis (2012) and Caccioli et al. (2014), asset prices are reduced proportional to the number of insolvent banks. This causes the banking system to turn from a stable system to an unstable system, given variations in capital. Thus, the interconnectedness of banks causes a fragile state similar to the one observed in the cascade counterparty risk models.

Agent-based models have been used to model banking and other financial systems (Lux and Marchesi, 2000; Hommes, 2006; Farmer and Geanakoplos, 2009). In agent-based models of systemic risk, banks (or other financial companies) form the agents. An algorithm models the strategy and interaction of banks in the system. This results

in macro-economic observable behaviour of the banking system. The simulation-based nature of agent-based models allows for testing of different strategies, for example banks having additional information on other banks' systemic risk influence (Thurner and Poledna, 2013), the inclusion of a central bank (Geanakoplos et al., 2014), or testing new regulations such as the influence of a transaction tax (Poledna and Thurner, 2014), or the effects of a bail-out of an insolvent bank (Klimek et al., 2014).

Finally, stress test platforms like the Systemic Risk Monitor (Boss et al., 2006), the Risk Assessment Model for Systemic Institutions (Alessandri et al., 2009) and the V-Lab (Acharya et al., 2014) incorporate cascade models based on balance sheets and interbank networks, and various other risk measures, like CoVar and SES, when evaluating the stability of financial systems.

Chapter 3

The Cascade Counterparty Risk

Model

Summary *The chapter details a description of the counterparty risk model studied in this thesis. Stylized balance sheets contain information about banks' assets, liabilities and capital. If banks' assets are smaller than banks' liabilities, the bank is said to be insolvent. The insolvency propagates through an interbank exposure network. Insolvent banks reduce the asset side of their counterparties causing further insolvencies. The chapter also includes the assumptions and derivations of the mean-field model - a variation of the counterparty risk model that can be solved semi-analytically by creating a homogeneous banking system. Finally, the assumptions and the insolvency algorithm of a simulation-based counterparty risk model are described.*

3.1 Counterparty Risk Model

The counterparty risk model studied in this thesis investigates the insolvency propagation caused by counterparty failure in a banking system following an initial shock to banks' assets or liabilities.

In our model, we consider N banks. A bank i is assigned a state, $S_i(t)$, displaying whether the bank is solvent or insolvent at time t :

$$S_i(t) = \begin{cases} 1 & \text{if bank } i \text{ is solvent} \\ 0 & \text{if bank } i \text{ is insolvent} \end{cases} . \quad (3.1)$$

We adopt the stylized balance sheet introduced by Nier et al. (2007) and Gai et al. (2007), considering liabilities and assets. A schematic diagram of a simple balance

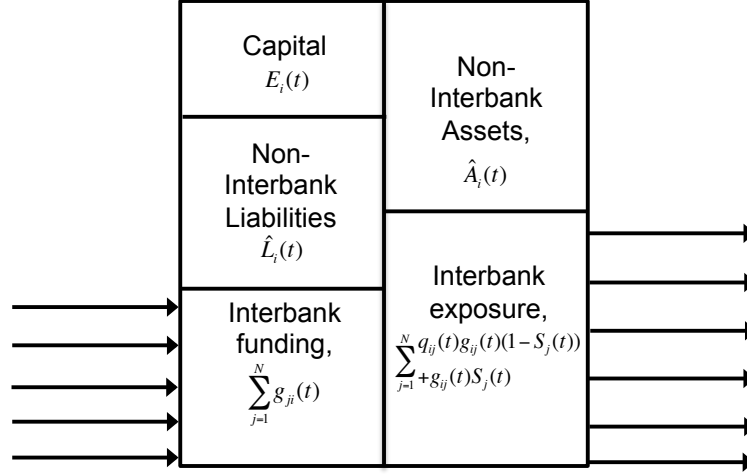


Figure 3.1: This figure represents a stylised balance sheet of bank i . The total liabilities of bank i at time t , $L_i(t)$, is the sum of the bank's non-interbank liabilities, $\hat{L}_i(t)$, and interbank funding, $\sum_{j=1}^N g_{ji}$. The total assets of bank i at time t , $A_i(t)$, is the sum of non-interbank assets, $\hat{A}_i(t)$ and interbank exposure, $\sum_{j=1}^N g_{ij}(t)S_k(t)$. Additionally, the value of exposure to an insolvent bank is considered by introducing a recovery rate, $q_{ij}(t)$ such that the term $\sum_{j=1}^N q_{ij}(t)g_{ij}(t)(1-S_j(t))$ states the value of any exposure to insolvent banks j . The difference in the bank's total assets and liabilities is the bank's capital $E_i(t) = A_i(t) - L_i(t)$. A bank is said to solvent if $A_i(t) \geq L_i(t)$. If $A_i(t) < L_i(t)$, the bank is said to be insolvent.

sheet of a bank ' i ' is given in Figure 3.1.

The balance sheet quantities are divided into interbank and non-interbank quantities. The exposure matrix $\mathbf{G} = \{g_{ij}(t)\}_{1 \leq i, j \leq N}$ describes the interbank network at time t ; interbank exposure is modelled by adding all the exposures of banks j at time t to a bank i , and multiplying each exposure to bank j with the state of bank j , i.e. $\sum_{j=1}^N g_{ij}(t)S_j(t)$. The state of a bank j indicates whether bank j is able to fulfill any obligation to bank i . In the event of a bank being insolvent and not being able to return the full amount of exposure to any loaner banks, the loaner bank can usually expect a reduced amount of the original value of the exposure during insolvency procedures. The fraction of the amount of exposure, that bank i receives from an insolvent bank, is called the recovery rate. In particular, we say matrix $\mathbf{Q}(t) = \{q_{ij}(t)\}_{1 \leq i, j \leq N}$, where $q_{ij}(t) \in [0, 1]$ contains the recovery rates $q_{ij}(t)$ at time t for any exposure $g_{ij}(t)$ from bank i to bank j , such that an additional term $\sum_{j=1}^N q_{ij}(t)g_{ij}(t)(1-S_j(t))$ models the value of an exposure of bank i to bank j at time t , when bank j is insolvent. The total assets of bank i at time t are the sum of non-interbank assets, $\hat{A}_i(t)$, and interbank

Table 3.1: The table states a list of variables of bank i at time t used in the balance sheet model. $S_i(t)$ describes the state of bank i , $g_{ij}(t)$ models the loan from bank i to bank j . Similarly, $g_{ji}(t)$ is the loan from bank j to bank i . The recovery rate of any defaulted exposure from bank i to bank j is given as $q_{ij}(t)$. The total interbank exposure from bank i to bank j is $\sum_{j=1}^N g_{ij}(t)S_j(t)$, and bank i receives funding on the interbank market of a total amount of $\sum_{j=1}^N g_{ji}$ from banks j . The value of defaulted exposure is $\sum_{j=1}^N q_{ij}(t)g_{ij}(t)(1 - S_j(t))$. The non-interbank assets are represented by $\hat{A}_i(t)$, and $\hat{L}_i(t)$ denotes non-interbank deposits, and $E_i(t)$ denotes the bank's loss absorbing capital. The total assets are $A_i(t) = \hat{A}_i(t) + \sum_{j=1}^N \left(g_{ij}(t)S_j(t) + q_{ij}(t)g_{ij}(t)(1 - S_j(t)) \right)$, and the total liabilities are $L_i(t) = \hat{L}_i(t) + \sum_{j=1}^N g_{ji}(t)$.

Variable	Description of variables
$S_i(t)$	State of bank i
$A_i(t)$	Total assets
$L_i(t)$	Total liabilities
$E_i(t)$	Capital
$\hat{A}_i(t)$	Non-interbank assets of bank i at time t
$\hat{L}_i(t)$	Non-interbank liabilities
$g_{ij}(t)$	Interbank loan from bank i to bank j
$\sum_{j=1}^N g_{ij}(t)S_j(t)$	Total interbank exposure
$\sum_{j=1}^N q_{ij}(t)g_{ij}(t)(1 - S_j(t))$	Total value of defaulted exposure
$\sum_{j=1}^N g_{ji}(t)$	Total interbank funding

assets at time t :

$$A_i(t) = \hat{A}_i(t) + \sum_{j=1}^N \left(g_{ij}(t)S_j(t) + q_{ij}(t)g_{ij}(t)(1 - S_j(t)) \right). \quad (3.2)$$

Similarly, the liabilities are the sum of non-interbank liabilities $\hat{L}_i(t)$ and interbank liabilities $\sum_{j=1}^N g_{ji}(t)$ such that the total liabilities of bank i at time t are:

$$L_i(t) = \hat{L}_i(t) + \sum_{j=1}^N g_{ji}(t). \quad (3.3)$$

The loss absorbing capital of bank i at time t is the difference between total assets and total liabilities, i.e.

$$E_i(t) = A_i(t) - L_i(t). \quad (3.4)$$

The above equation is the Balance Sheet Equation. Table 3.1 summarizes the variables used in this model.

The stress criteria are modelled by using the balance sheet test to determine insolvency, as outlined in Goode (2010). Namely, a bank is said to be insolvent if assets are less than liabilities at time t , i.e. the Insolvency Condition is:

$$A_i(t) < L_i(t). \quad (3.5)$$

In legal terms, a bank defaults if it is not able to pay back a loan upon maturity. Whereas insolvency occurs if a bank's liabilities are larger than a bank's assets (Goode, 2010). Thus, insolvency and default are not synonyms but describe two legal processes that can result in the bankruptcy of a bank. Nonetheless, we sometimes refer to "default" in this thesis when the correct term is insolvency. In particular, we use default if most banks of the entire banking system are insolvent and say the banking system defaulted.

Given that the state of a bank i is determined by the Insolvency Condition, Eq. 3.5, consequently the state of a bank at time $t + 1$ is

$$S_i(t + 1) = H_c(A_i(t) - L_i(t)), \quad (3.6)$$

where $H_c(x) = 1$ for $x \geq c$ and $H_c(x) = 0$ for $x < c$. For the purpose of this thesis, we set c to zero and omit writing the subscript from now on. In some countries, solvency procedures are started when the capital of a bank is still positive but when capital reaches a certain threshold of total assets.¹ In this case, c should be adjusted to the value at which solvency procedures start.

Note that, an insolvent bank ($S_i(t) = 0$) can recover and change its state to $S_i(t + 1) = 1$ if the difference between liabilities and total assets is positive: $A_i(t) > L_i(t)$. This possibility can occur whenever capital is introduced to a distressed bank, as done via quantitative easing (QE) or government bail-outs. The cost of returning to a stable system as well as more details about capital injections are discussed in Chapter 4.

Finally, the fraction of surviving banks, $p_{t+1} \in [0, 1]$, at time $t + 1$ is given by

$$p_{t+1} = \frac{1}{N} \sum_i^N H(E_i(t)). \quad (3.7)$$

In the Ising model literature describing spin systems, $E_i(t) = A_i(t) - L_i(t)$ is

¹For example, see regulations in Mexico (Solorzano-Margain et al., 2013).

called the ‘incentive function’ (De Dominicis and Giardina, 2006). The probability of bank i to be in a particular state, using the logit rule (which is a standard choice to determine the probability of a spin being in a particular state) is:

$$P(S_i(t) = 1 | E_i(t-1)) = \frac{1}{1 + \exp(-\beta E_i(t-1))}, \quad (3.8)$$

where β is the inverse temperature of the spin system. When β tends to zero (infinite temperature limit) the incentive does not influence the state of the bank. Hence, bank i is normally operating or under stress with probability $1/2$. Conversely, when β tends to infinity (zero temperature limit) then Eq. 3.6 is recovered. Thus, the map introduced in Eq. 3.7 belongs to the Random Field Ising models (RFIM) at zero temperature, a model in statistical physics that describes the spin of atoms (De Dominicis and Giardina, 2006). In addition, RFIM have been used to investigate the behaviour of other complex systems, where the state of actors can be modelled as a binary decision influenced by other actors in the system. For example, Weidlich (1994) used the model to study decision making, Newman (2002) for the development of epidemic spread and in Heise and Kühn (2012), it was used to investigate credit derivatives.

3.2 Mean-Field Model

The mean-field model is a simplified version of the counterparty risk model introduced in Sec. 3.1. In order to obtain a closed form expression of the fraction of surviving banks, assumptions are made that homogenize the banks in the banking system.

Furthermore, we are looking at the instantaneous stress imposed on a banking system given a particular distribution of non-interbank assets and liabilities. Hence, any change in the investment after the system is stressed is neglected. More specifically, it is assumed that the time to counteract a shock using other investment strategies is of larger order of time than the instantaneous stress imposed by insolvent banks to its creditors. Therefore, we consider most of the balance sheet quantities to be constant in time. Specifically, we consider that the process of stressing a bank and the consequent loss of the interbank exposure are much more imminent than the distribution of any assets belonging to an insolvent bank. Therefore, even if the creditor of a bank is insolvent, the bank still has to pay any outstanding loans towards the insolvent bank.

Furthermore, we assume that transfers of assets belonging to the insolvent bank to counterparties are excluded. Hence, we say that the liabilities of bank i , $L_i(t) = L_i$ are constant in t and vary from bank to bank as drawn from a random distribution.

The non-interbank assets $\hat{A}_i(t) = \hat{A}_i$ are also considered constant in t and drawn from a random distribution. This represents different investment decisions, and hence, different investment returns. Then Eq. 3.7 can be written as

$$p_{t+1} = \frac{1}{N} \sum_{i=1}^N H(\hat{A}_i - L_i + \sum_{j=1}^N (g_{ij} S_j(t) + q_{ij} g_{ij} (1 - S_j(t)))). \quad (3.9)$$

For interbank loans, we assume a mean-field, i.e. the average amount bank i is exposed to all other banks, $\sum_{j=1}^N g_{ij} S_j(t)$, is approximated with zgp_t , where z is the average number of banks that bank i is exposed to and assumed to be very large, g is the average loan borrowed from one bank to another and $p_t \in [0, 1]$ is the fraction of solvent banks at a given time t as before. Similarly, the recovery rate is averaged and constant in t : $q_{ij}(t) = q$. Then Eq. 3.9 changes to

$$p_{t+1} = \frac{1}{N} \sum_{i=1}^N H(\hat{A}_i - L_i + zgp_t + zqg(1 - p_t)). \quad (3.10)$$

A probability distribution belongs to the family of location-scale distributions, if for any random variable X with distribution function from such a family, one can find another random variable $Y = \mu + \sigma X$, where $\mu \in \mathbf{R}$ and $\sigma > 0$, with distribution function also in that family (Rinne, 2011). The parameter μ is called the location parameter and σ is the scale parameter. Furthermore, if X 's location parameter equals zero and it has a scale parameter of one, X is called the standardized variable.

Let us use the assumption here that \hat{A}_i and L_i are independent and follow distributions in the location-scale family with location parameters $\mu_{\hat{A}}$ and μ_L , and scale parameters $\sigma_{\hat{A}}$ and σ_L , respectively. The random variable $\hat{A}_i - L_i$ therefore has location parameter $\mu = \mu_{\hat{A}} - \mu_L$ and scale parameter $\sigma = \sqrt{\sigma_{\hat{A}}^2 + \sigma_L^2}$.

Normal distributions belong to the family of location-scale distributions. If \hat{A}_i and L_i are drawn from Normal distributions, the location parameter, μ , is the mean of the non-interbank assets minus the mean of liabilities and σ is the standard deviation, which represent the level of uncertainty of the expected value for non-interbank assets and liabilities.

To transform the CDF into a standard location-scale CDF, let $\hat{A}_i - L_i = \mu + \sigma\epsilon_i$, where the standardized variable ϵ_i is taken from a standard location-scale distribution. Then Eq. 3.9 changes to

$$p_r = \frac{1}{N} \sum_{i=1}^N P(\mu - \sigma\epsilon_i + zqg > -zg(1-q)p_{r-1}), \quad (3.11)$$

and the Insolvency Condition becomes

$$\epsilon_i < \frac{-\mu - zqg}{\sigma} - \frac{zg(1-q)}{\sigma} p_{r-1}. \quad (3.12)$$

For convenience, let us introduce the following two variables:

$$a = \frac{-\mu - qzg}{\sigma}, \quad (3.13)$$

and

$$b = \frac{zg(1-q)}{\sigma}. \quad (3.14)$$

By using the above assumptions and assuming that N is very large, we can simplify Eq. 3.11 and write the fraction of solvent banks after r rounds of insolvency as

$$p_r = F(p_{r-1}), \quad (3.15)$$

where $F(x) = 1 - P(a - bx)$ is a cumulative distribution function (CDF). The term $a - bp_{r-1}$ states the average capital of a bank in round r . The function described in Eq. 3.15 is a monotone increasing function on a compact set. This ensures that the map in Eq. 3.15 has at least one stable fixed point (Smith, 2008). We present a more detailed analysis of the fixed points in Chapter 4. Given an initial fraction, p_0 , of surviving banks (note that p_0 can differ from one), the solution of Eq. 3.15 is a fixed point probability satisfying $p = F(p|p_0)$. Hence, the fraction p represents the probability of the survival of the banking system.

In the RFIM literature, the parameter b models the influence of agents on other agents. In our model, b describes the average exposure minus the average expected value of defaulted exposure divided by the scale parameter, σ , of the sum of non-

interbank assets and liabilities, and hence b is always positive. When b is negative, banks would have to pay their loaners to keep the exposure. When b equals zero, then, whether a bank is insolvent, depends solely on the distributions of the non-interbank assets and liabilities. If the standardized variable ϵ_i is drawn from a standard Normal distribution, it is to be expected that half the banks are insolvent when a and b equal zero. Conversely, when b becomes larger, i.e. when the average total interbank exposure becomes larger, or when the recovery rate becomes smaller, or the scale parameter of the sum of non-interbank assets and liabilities becomes smaller, then, for a fixed a , the system is more resilient. However, we will see in Chapter 4, there exists a critical value b_c , at which the behaviour of the system changes from a smooth decline in normally operating banks to a sudden decrease, which we call the fragile state of the banking system.

The parameter a is the difference between the location parameters of liabilities and non-interbank assets, μ , and the average recovery value of defaulted exposure, qzg , divided by the scale parameter of non-interbank assets and liabilities, σ . If a is negative, then the location value of non-interbank assets and expected recovery term are larger than the liabilities. The denominator of a is the scale parameter, σ . If a is negative and σ tends to zero, then a tends to minus infinity, leading to a more stable system. However, if a is positive, then $\sigma \ll 1$ leads to a more unstable system. Instead, if the location parameter of non-interbank assets is sufficient to counter the liabilities, i.e. $a \ll 0$, a large σ would imply that for some banks, their non-interbank assets would not be enough to satisfy the Solvency Condition, Eq. 3.5. Therefore, if the interbank loans are not sufficient, these banks are insolvent. Conversely, if $a \gg 0$, then a large σ is desirable, as this implies that for some banks, their non-interbank asset value is higher than the expected value. Thus, these banks can satisfy the Solvency Condition, Eq. 3.5, and will operate normally.

These assumptions homogenize the system, but it should be noted that banking systems in most countries are far from a homogeneous system. Indeed, banks' balance sheets differ greatly. In particular, we discuss the size of UK banks in more detail in Section 6.1, showing that some banks' balance sheets only contain a few hundred Mil. GBP, especially smaller regional building societies, and other banks' assets are worth a few trillion GBP (large internationally operating banks headquartered in the UK).

We study a homogeneous system because it can be solved semi-analytically. A reason why a homogeneous solution of a heterogeneous system can still be of interest is the particular structure of the interbank network. It has been shown that in some countries the interbank network structure can be described as a tightly connected core with international banks in the centre and smaller regional banks in the periphery (Müller, 2006; Fricke and Lux, 2015). We reach the same conclusion in Section 6.1, where we investigate an interbank exposure network constructed from UK regulatory reports. In the core-periphery structure, the larger international banks in the core are of similar size. Therefore, we can argue that, for systemic risk, the most relevant part of the interbank network is the homogeneous core network of large banks, which can be modelled using the homogeneous mean-field model.

Furthermore, in Chapter 6, we compare a simulation-based model of a heterogeneous banking system with the homogeneous model solution, concluding that both models lead to similar results: we show that a fragile state, at which most of the banks in the banking system suddenly become insolvent occurs, for both models, with a similar sized shock to their balance sheet quantities. This suggests that a simple model of a homogeneous banking system sufficiently describes the main features of a more complex model of a heterogeneous banking system.

3.2.1 The Ratio of Interbank Assets to Total Assets, θ

For convenience, let us introduce here the ratio of interbank assets to total assets, θ . To derive the mean-field model solution containing θ , we use the same assumptions as above up to and including Eq. 3.10. We further assume $A_i(0)$ is drawn from a location-scale distribution with location parameter μ_A and scale parameter σ_A . We say that $z_g = \theta A_i(0)$ and $\hat{A} = (1 - \theta)A_i(0)$, and assume that p_0 equals one. Furthermore, we assume as before that L_i is drawn from a location-scale distribution with location parameter μ_L and scale parameter σ_L . Thus, we have

$$\begin{aligned} (1 - \theta)A_i(0) + \theta A_i(0) - L_i &= \mu_A - \mu_L + \sqrt{\sigma_A^2 + \sigma_L^2} \epsilon_i \\ &= (1 - \theta)\mu_A + \theta\mu_A - \mu_L + \sqrt{\sigma_A^2 + \sigma_L^2} \epsilon_i. \end{aligned} \quad (3.16)$$

Then Eq. 3.10 can be written for $r = 1$:

$$p_1 = \frac{1}{N} \sum_{i=1}^N P\left((1 - \theta)\mu_A + \theta\mu_A - \mu_L + \sqrt{\sigma_A^2 + \sigma_L^2}\epsilon_i < 0\right), \quad (3.17)$$

where $P(\cdot)$, as before, is the CDF of the location-scale distribution. The fraction of operating banks after r iterations then can be written as:

$$p_r = \frac{1}{N} \sum_{i=1}^N P\left((1 - \theta)\mu_A + \theta\mu_A p_{r-1} + q\theta\mu_A(1 - p_{r-1}) - \mu_L + \sqrt{\sigma_A^2 + \sigma_L^2}\epsilon_i < 0\right), \quad (3.18)$$

For $N \rightarrow \infty$, the above equation can be simplified further to:

$$p_r = 1 - P\left(a' - b'p_{r-1}\right), \quad (3.19)$$

where we reduced the multi-parameter system to the following two parameters given

$$\sigma' = \sqrt{\sigma_A^2 + \sigma_L^2}:$$

$$a' = \frac{-(1 - \theta)\mu_A + \mu_L - q\theta\mu_A}{\sigma'}, \quad (3.20)$$

and

$$b' = \frac{(1 - q)\theta\mu_A}{\sigma'}. \quad (3.21)$$

We have two reasons for introducing θ . First, we use θ to calibrate the simulation-based model of counterparty failure described in the next section. When comparing the simulation solution with the solution of the mean-field model, a' and b' are used to calculate the mean-field solution. Second, estimates for θ can be obtained from other studies (Müller, 2006; Upper, 2011). Whereas it is more difficult to retrieve zp from publicly available data.

3.3 Simulation-Based Counterparty Risk Model

The mean-field assumption of the interbank market implies that each bank lends the same amount to all other banks and that the size of banks' balance sheets are roughly the same, with similar capital reserves to counteract a shock to banks' non-interbank assets and liabilities. In Chapter 5, we test the robustness of the results of the mean-

field model by comparing it with a simulation-based model. In Chapter 6, we use two regulatory datasets from the BoE to calibrate a simulation-based model.

The banking system discussed in Chapter 5 is still highly stylised using standard network structures and random distributions to initialize the banking system. Whereas when constructing the banking system studied in Chapter 6, we use real-world exposure networks and balance sheet data. For this reason, the initialization processes of the simulation-based models are stated in the beginning of Chapters 5 and 6 in more detail. However, the assumptions about balance sheet variables during the insolvency propagation are mostly the same in both simulation models and outlined in the following.

For both simulation-based models, the number of banks N is fixed and, as in the general model layout, each bank i is assigned a state $S_i(0) \in \{0, 1\}$, stating whether bank i is solvent ($S_i(0) = 1$) or not ($S_i(0) = 0$). As in the mean-field model, we also consider the instantaneous impact of counterparty failure. Hence, we assume liabilities, $L_i(t) = L_i$, non-interbank assets, $\hat{A}_i(t) = \hat{A}_i$, interbank exposure, $g_{ij}(t) = g_{ij}$, and recovery rates, $q_{ij}(t) = q_{ij}$ do not change in time. The total liabilities, L_i , and the initial value of total assets, $A_i(0)$, of bank i are assumed to be random variables.

For the same reasons as in the mean-field model, we assume that interbank liabilities to insolvent banks have to be returned also to an insolvent bank. Hence, we use total liabilities, L_i , in the simulation models only. Interbank assets are the sum of the exposure from bank i to bank j multiplied by the state of banks j plus the recovery value of the exposure: $\sum_{i=1}^N g_{ij}S_j(0) + q_{ij}g_{ij}(1 - S_j(0))$. The total assets of bank i in round r are then

$$A_i(r) = \hat{A}_i + \sum_{i=1}^N g_{ij}S_j(r) + q_{ij}g_{ij}(1 - S_j(r)) \quad (3.22)$$

The insolvency cascade algorithm describes the propagation of insolvency of banks in the banking system. Specifically, we use a similar algorithm as proposed in Furfine (2003), where at each iteration round r :

1. The total assets, $A_i(r)$, are calculated using Eq. 3.22 for each bank i .
2. For all banks i , the difference between total liabilities, L_i , and total assets, $A_i(r)$, is calculated, simultaneously.

3. For any bank i with negative capital, $A_i(r) - L_i$, the state of bank i is set to zero.
4. The iteration is repeated until no bank changes its state.

When the process stops, all surviving banks are counted and the fraction of surviving banks, p , is computed as the total number of surviving banks divided by the total number of banks.

3.3.1 Differences in the Assumptions of the Simulation Models

In Chapter 5, each bank i is initially calibrated with liabilities L_i and assets $A_i(0)$ drawn from random distributions with location μ_L and scale σ_L for liabilities, and location μ_A and scale σ_A for total assets.

We construct the interbank network using standard network structures (Erdős-Rényi networks, Small-World networks (Watts and Strogatz, 1998) and a Barabási-Albert networks (Barabási and Albert, 1999)). The adjacency matrix of the standard network, $\mathbf{X} = \{\chi_{1 \leq ij \leq N}\}$, indicates whether a bank i is exposed to a bank j (i.e. $\chi_{ij} = 1$) or not (i.e. $\chi_{ij} = 0$). The total interbank assets of a bank i are computed using a fixed fraction, $\theta \in (0, 1)$, of interbank assets to total assets, such that the total interbank exposure is: $\theta A_i(0)$. To extract the value g_{ij} of interbank assets from bank i to bank j , $\theta A_i(0)$ is divided by the degree of bank i , $z_i = \sum_{j=1}^N \chi_{ij}$. Hence, the individual loan from bank i to its neighbouring banks j is $\theta A_i \chi_{ij} / z_i$. The difference between total initial assets, $A_i(0)$, and total interbank assets, $\theta A_i(0)$, are the non-interbank assets, \hat{A}_i , of bank i .

The recovery rate is constant for all exposures from bank i to bank j , such that an element of the recovery matrix \mathbf{Q} can be written as $q_{ij} = q$. Hence, the value of recovered loans are given as $q\theta A_i(0)g_{ij}$.

In Chapter 6, each bank i is initially calibrated with liabilities L_i and assets $A_i(0)$ drawn from random distributions with location μ_{L_i} and scale σ_{L_i} for liabilities, and location μ_{A_i} and scale σ_{A_i} for total assets, i.e. $\mu_{A_i}, \mu_{L_i}, \sigma_{A_i}$ and σ_{L_i} are chosen individually for each bank. This creates a highly heterogeneous banking system where banks vary greatly in the size of their balance sheets.

The value of interbank exposure, g_{ij} , from bank i to bank j is taken from the regulatory data. The non-interbank assets, \hat{A}_i , are the difference between the total initial assets, $A_i(0)$, and the sum of bank i 's exposure to other banks, $\sum_{j=1}^N g_{ij}$.

We disregard the recovery rate, q_{ij} , in the simulation model of the heterogeneous banking system. The reason for this is quite practical: we do not have data on the recovery rate of exposure between specific banks. Thus, the recovery rate is set to zero.

3.3.2 Changes in the Value of Balance Sheet Quantities Over Time

Fire-sales, QE, bank runs and bail-outs are examples that potentially change the value of banks' balance sheet quantities during the insolvency propagation. To investigate the effects of value changes in time of balance sheet quantities, we incorporate functions that alter the value of assets or liabilities following the initial shock to banks' balance sheets.

For the simulation model in Chapter 5, we apply a function that changes the balance sheet values of a bank i at time t . If a bank becomes insolvent, its assets are liquidated to satisfy debtors demands. This might cause a change in the price value of specific assets due to an over supply of these assets. When mark-to-market accounting is used to evaluate the value of the asset side of balance sheets, other banks experience a shock to their balance sheets because of asset devaluation. In particular, we use an inverse demand curve for the illiquid asset to simulate a reduction in the asset value caused by the insolvency of banks:

$$\hat{A}_i(r+1) = \exp(-\kappa_1(1-p_r))\hat{A}_i(r), \quad (3.23)$$

where $\kappa_1 \in [0, 1]$ is a constant. Thus, $\exp(-\kappa_1(1-p_r))$ reduces the value of non-interbank assets of a bank i in round r proportional to the fraction of insolvent banks, $1-p_r$.

Eq. 3.23 captures the effect of asset value reduction by multiplying the initial value of non-interbank assets with the exponential function. It should be noted that there is no evidence that a price reduction indeed corresponds to an exponential function that is proportional to the fraction of insolvent banks. We nonetheless use this form as it is in accordance with the literature. Other studies (Cifuentes et al., 2005; Müller, 2006; May and Arinaminpathy, 2010; Tsatskis, 2012) use the same function to investigate the impact of price reduction of assets and liquidity shortages.

To model a reduction in the value of the liability side of the balance sheet, we use

the following function:

$$L_i(r + 1) = (1 - \kappa_2)L_i(r), \quad (3.24)$$

where $\kappa_2 \in [0, 1]$ is a constant as before. Eq. 3.24 is a simple linear reduction of the liability side of the balance sheet, which can be used to model a capital infusion to a bank i as done during government bail-outs.

For the simulation model, any function describing the movement of the value of the asset or liability side can be used. Other examples include the geometric random walk (Webber and Willison, 2011), which is usually used to model the price movement of assets. The functions used in this thesis are chosen to a certain extent arbitrarily as there is no evidence that the precise form of an asset reduction or capital infusion resembles an exponential or linear function. We chose the functions as they can be easily included into our model set-up, and the effects of the functions to the stability of the banking system can be explained using the equilibrium solutions of the mean-field model.

3.4 The Initial Shock to Banks' Balance Sheets

There are multiple ways to shock the banking system. Some studies consider the failure of one or multiple banks initially (Battiston et al., 2012c; Gai et al., 2011). Other studies (May and Arinaminpathy, 2010; Gai, 2013) shock banks' capital by reducing or increasing a fraction of banks asset or liability side of the balance sheet.

In this thesis, we vary the capital of banks to induce the initial shock. We do this for technical convenience when comparing different model solutions. A negative shock to banks' capital decreases the amount of the bank's capital by increasing the value of liabilities or decreasing the asset side of the balance sheet. A positive shock to banks' capital is achieved by a reduction of the bank's liabilities or an increase in the value of assets. In particular, we vary the liability side of banks' balance sheets to induce a shock to banks' liabilities. However, we could have equally chosen to reduce the asset side of banks' balance sheets. All the calculations and simulations can be repeated using a shock to banks' asset side and will lead to the same solution.

3.5 Conclusion

In this chapter, we outlined the general counterparty risk model that we study in this thesis to obtain a better understanding of counterparty risk in a banking system. We mapped a counterparty risk model to a RFIM by assuming that a bank can be either solvent or insolvent. Additionally, we use a mean-field assumption to simplify the counterparty risk model and obtain an iterative map stating the fraction of surviving banks in any iteration round. We call this simplified version the mean-field model. The iteration map is governed by two parameters: a and b that contain the information of the average balance sheet parameters of banks in the banking system. The parameter a states the difference between the averages of liabilities, and non-interbank assets and the recovery term of defaulted exposure divided by the variance of liabilities and non-interbank assets. The parameter b states the average interbank exposure (excluding the recovery value of exposure) of banks in the banking system divided by the variance of liabilities and non-interbank assets. Finally, we introduce the assumptions and algorithm of a more heterogeneous simulation-based version of the counterparty risk model.

Chapter 4

Mean-Field Model Results

Summary *The chapter contains a discussion of the equilibrium solutions of the mean-field counterparty risk model. A fixed point analysis of the iteration map describing the insolvency propagation reveals the occurrence of a hysteresis cycle for the equilibrium fraction of surviving banks. This implies that the solution of the iteration map is history dependent and allows one to calculate the cost of rescuing a defaulted banking system. Additionally, we conduct a parameter analysis of the balance sheet variables and their influence on the stability of the banking system. We show that below a specific leverage ratio, one bank can trigger the insolvency of most of the banks in the banking system. The calculations are repeated for multiple location-scale distributions to show that the results are robust. Finally, we use balance sheet data from UK and US banks to discuss the stability of each banking system in the years 2007 and 2012.*

4.1 Fixed Points

The counter party risk model presented in Chapter 3 is part of the Curie-Weis models. The analysis presented in this chapter uses the equilibrium solution of the Curie-Weis mean-field model at zero temperature to show a phase transition experienced by the banking system, whereby the banking system changes from a stable to an unstable state and vice versa. Curie-Weis models have been studied extensively in the past decades and the reader is directed to Weidlich (1971), de Matos and Perez (1991), Sethna et al. (1993), Dahmen and Sethna (1996), and Bouchaud (2013) for more details. To study the behaviour of the iteration map in Eq. 3.15 ($p_r = 1 - P(a - bp_{r-1}) = F(p_{r-1})$), we investigate the fixed points, p , of the iteration map $F(\cdot)$. The fixed point of an iteration map is reached when $p = F(p)$. The propositions and lemmas used in this Section can

be found in the Appendix, Chapter A. Using Lemma A.4.1 ensures that the iteration map in Eq. 3.15 has at least one fixed point since p_r, p_{r-1}, \dots, p_0 for $p_s \in [0, 1]$ is a monotone sequence, and $[0, 1]$ is a compact set. Using Eq. 3.15 and assuming $P(\cdot)$ is a standard Normal CDF, we can write:

$$F(x) = 1 - \Phi(a - bx), \quad (4.1)$$

where $\Phi(\cdot)$ is the standard normal CDF. Using a Normal distribution as the underlying random distribution for the balance sheet quantities is a standard choice in the RFIM literature. Note that the following discussion can be repeated with other location-scale distributions (see Section 4.7). The assumption to draw the random variables from location-scale distributions is not necessary. The sudden decline in the fraction of surviving banks can also be observed with other random distributions. For example, in Chapter 5, we initialize the balance sheet variables with Lognormal and Loglogistic distributions and obtained similar results. The advantage of using location-scale distributions is that it allows one to reduce the multi-parameter model into a two-parameter model, where the two parameters, a (the weighted average difference of liabilities, and the sum of non-interbank assets and the value of interbank exposure of insolvent counterparties) and b (the weighted average value of interbank assets minus the recovery term of insolvent exposure) are defined as stated in Eqs. 3.13 and 3.14.

In order to investigate the fixed points, we report in Figure 4.1 (first row) various plots of the iteration map $p_r = F(p_{r-1})$ for different values of a and b for r from $r = 0$ to $r = 100$. It becomes clear, that, given particular parameter values, and the same starting value, the fixed points change. This is better illustrated in the second row of Figure 4.1, where $p - F(p)$ is plotted, which crosses zero at the fixed point. This is of importance as the roots of $p - F(p)$ are the fixed points of $p_r = F(p_{r-1})$.

In Lemma A.4.2, we see that $x - F(x)$ undergoes a behavioural change at $b = b_c$. The critical parameter is a common result of the Curie-Weiss solution leading to the first order phase transition (Dahmen and Sethna, 1996), (Bouchaud, 2013). For the standard Normal CDF, b_c equals $\sqrt{2\pi}$. If $b < b_c$, then $x - F(x)$ is strictly increasing. However, if $b > b_c$, then $x - F(x)$ has a maximum x_1 and a minimum x_2 as shown in Lemma A.4.2. Depending on the position of $x_1 - F(x_1)$, $x_2 - F(x_2)$ and a , $p_r = F(p_{r-1})$ has

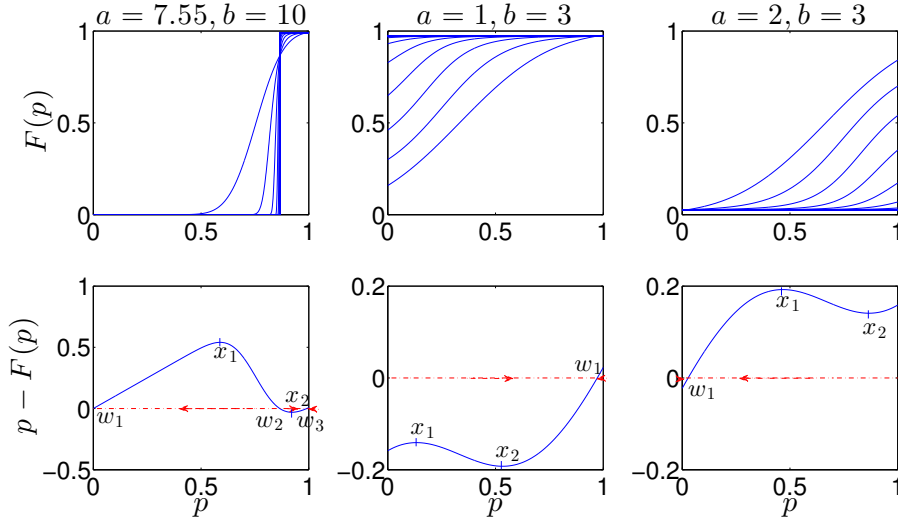


Figure 4.1: The first row of this figure shows $F(p)$ from Eq. 4.1 vs. p for $r = 0, \dots, 100$ with various combinations of parameters a and b . The second row shows plots of $p - F(p)$. The extreme values, x_1 and x_2 , of $p - F(p)$ are indicated with a cross and the corresponding fixed points, w_1, w_2 and w_3 are the points where $p - F(p)$ crosses zero. The arrows indicate which fixed point is reached starting at a particular p_0 .

up to three fixed points.

Substituting $x_1 = F(x_1)$ and solving for a , allows one to determine $a_1 = b + \sqrt{2 \ln \frac{b}{b_c}} - b\Phi(\sqrt{2 \ln \frac{b}{b_c}})$. Similarly, for $x_2 = F(x_2)$, the weighted, average difference of liabilities and non-interbank assets is $a_2 = b - \sqrt{2 \ln \frac{b}{b_c}} - b\Phi(-\sqrt{2 \ln \frac{b}{b_c}})$.

To be more specific, say $b > b_c$ and $a \in (a_1, a_2)$, we have $x_1 - F(x_1) > 0$ and $x_2 - F(x_2) < 0$. Thus, $x - F(x)$ has three roots, and therefore, $p_r = F(p_{r-1})$ has three fixed points: w_1, w_2 and w_3 , where $w_1 < x_1 < w_2 < x_2 < w_3$. Furthermore, the derivative of $F(x)$ is

$$F'(x) = \frac{b}{b_c} \exp\left(-\frac{(a-bx)^2}{2}\right) \quad (4.2)$$

Note that $F'(x_1) = 1 = F'(x_2)$. For $x \rightarrow \pm\infty$, we have $\exp(-\frac{(a-bx)^2}{2}) \rightarrow 0$. Thus, for $x < x_1$ or $x_2 > x$, $F'(x)$ tends to zero and is less than one. Using Proposition A.4.1, w_1 and w_2 are therefore stable fixed points. Because $F'(x)$ equals one only for $x = x_{1,2}$, $F'(w_2)$ has to be larger than one. Hence, using Proposition A.4.2, w_2 is an unstable fixed point.

To summarize, if the starting value p_0 is in the orbit $[0, w_1]$ or $[w_3, 1]$, then the attracting fixed points are w_1 or w_3 , respectively. If $p_0 \in [w_1, w_2]$, then w_2 is a repelling fixed point and w_1 is the attracting fixed point that is eventually reached. Similarly, if

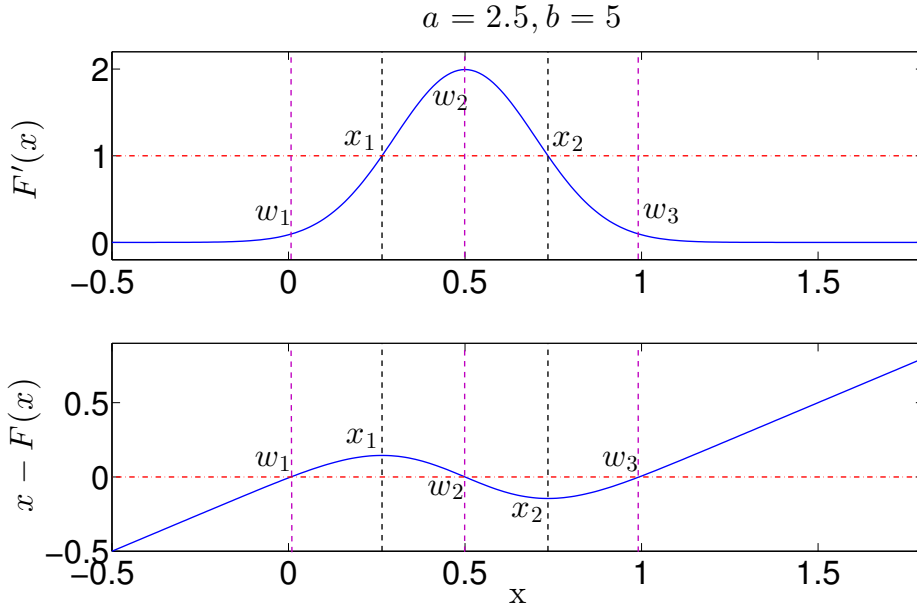


Figure 4.2: The figure shows two subplots. In the first row, the first derivative of $F(x)$, $F'(x)$, is plotted against x . In the second row, the function $x - F(x)$ is plotted against x . The parameters $a = 2.5$ and $b = 5$ are fixed for each plot. Additionally, the maximum (x_1 , vertical black line) and minimum (x_2 , vertical black line) of $x - F(x)$ as well as fixed points of $p_r = F(p_{r-1})$ (w_1, w_2 and w_3 , vertical purple line) are indicated. It becomes clear that for the chosen values of a and b , w_1 and w_2 are stable fixed points and w_3 is an unstable fixed point since $F'(w_1), F'(w_3) < 1$ and $F'(w_2) > 1$.

$p_0 \in [w_2, w_3]$, the fixed point eventually reached is w_3 .

To illustrate the occurrence of three fixed points, we plotted in Figure 4.2 $F'(x)$ (first subplot) and $x - F(x)$ (second subplot) against x for fixed $a = 2.5$ and $b = 5$. For $b = 5$, we have $a = 2.5 \in (a_1, a_2)$. We marked the maximum (x_1) and minimum (x_2) of $x - F(x)$ with vertical, black lines as well as the fixed points of $p_r = F(p_{r-1})$ with vertical, magenta lines. The horizontal, red line in the first subplot indicates where the y-axis is equal to one. In the second subplot, the horizontal, red line indicates where the y-axis equals zero. As in Figure 4.1, the intersections of $x - F(x)$ with zero in the second row represent the fixed points of $p_r = F(p_{r-1})$, namely w_1, w_2 and w_3 . It becomes clear that $F'(w_1)$ and $F'(w_3)$ are less than one and $F'(w_2)$ is larger than one for $a = 2$ and $b = 5$. Hence, w_1 and w_3 are stable and w_2 is unstable.

For $b > b_c$ and $a < a_1$, $x_1 - F(x_1)$ and $x_2 - F(x_2)$ are less than zero. But $x - F(x)$ tends to infinity as x tends to infinity. Hence, $x - F(x)$ has only one root. Similarly, for $a > a_2$, $x_1 - F(x_1)$ and $x_2 - F(x_2)$ are larger than zero and $x - F(x) \rightarrow -\infty$ for $x \rightarrow -\infty$. Thus, for $a < a_1$ and $a > a_2$, $x - F(x)$ has one root and $p_r = F(p_{r-1})$ has

one fixed point: w_1 , which is stable (by Lemma A.4.1).

For $a = a_1$ and $b > b_c$, $x - F(x)$ has two roots with one root being x_1 . That is because for $a = a_1$, $x_1 - F(x_1)$ equals zero. Furthermore, $x_2 - F(x_2)$ is less than $x_1 - F(x_1)$ because at x_2 , $x - F(x)$ is at its local minimum. Note that $\frac{\partial(x-F(x))}{\partial a} > 0$ for all a , which implies that for increasing a and fixed x , $x - F(x)$ increases. Let $0 < \epsilon < a_2 - a_1$ and consider the case $a = a_1 + \epsilon$ (then $a \in (a_1, a_2)$). Thus, $p_r = F(p_{r-1})$ has the three fixed points w_1, w_2 and w_3 . For $\epsilon \rightarrow 0$, w_2 tends to x_1 since $x - F(x)$ decreases for decreasing a . Similarly, w_1 tends to x_1 for decreasing a . Eventually, w_1 and w_2 merge at x_1 for $\epsilon = 0$. Thus, the left-hand side of x_1 is stable. Whereas the right-hand side of x_1 is unstable. Any iteration process with starting value p_0 in the orbit $[0, w_1 = w_2]$ will reach the fixed point w_1 . However, if $p_0 \in [w_1 = w_2, w_3]$, the fixed point reached is w_3 , which is a stable fixed point. For $p_0 \in [w_3, 1]$, the attracting fixed point is again w_3 .

A similar argument can be used to show that for $a = a_2$ and $b > b_c$, we have $w_2 = x_2 = w_3$, i.e. w_2 and w_3 merge at x_2 implying that if $p_0 \in [w_1, w_2 = w_3]$, then w_1 is the attracting fixed point. If $p_0 \in [0, w_1]$ or $p_0 \in [w_3, 1]$, then the fixed points reached are w_1 and w_3 , respectively.

Finally, if $b < b_c$, $x - F(x)$ is strictly monotonically increasing. Therefore, $p_r = F(p_{r-1})$ has only one fixed point, w_1 . By Lemma A.4.1, w_1 is stable.

In general, for at least three fixed points to become possible in the iteration process $p_r = F(p_{r-1})$, the following conditions need to be satisfied: $F'(x)$ is a positive real-valued, bell-shaped, continuous and differentiable probability distribution function; and the balance sheet parameters can be tuned such that $F'(x)$ is larger than one.

In Figure 4.3, we illustrate how the number of roots of $x - F(x)$ depends on a . The figure shows various plots of $x - F(x)$ for fixed $b = 3$ and varying $a \in [1.2228, 1.7772]$. Note that for $b = 3 > b_c$, we have $a_1 \approx 1.4228$ and $a_2 \approx 1.5772$. More specifically, for the magenta coloured graphs, $a \in [1.2228, a_1)$. For the red and blue line, a equals a_1 and a_2 , respectively. For $a \in (a_2, 1.7772]$, the graphs are coloured cyan. In addition, we plotted horizontal, dotted lines indicating the roots of the thicker graphs. It becomes clear that for $a \in [1.2228, a_1)$ and $a \in (a_2, 1.7772]$, $x - F(x)$ has one root. Hence, $p_r = F(p_{r-1})$ has one fixed point. For $a = a_1$ and $a = a_2$, $x - F(x)$ has two roots, and $p_r = F(p_{r-1})$ has two fixed points. The figure illustrated further that for $a \in (a_1, a_2)$,

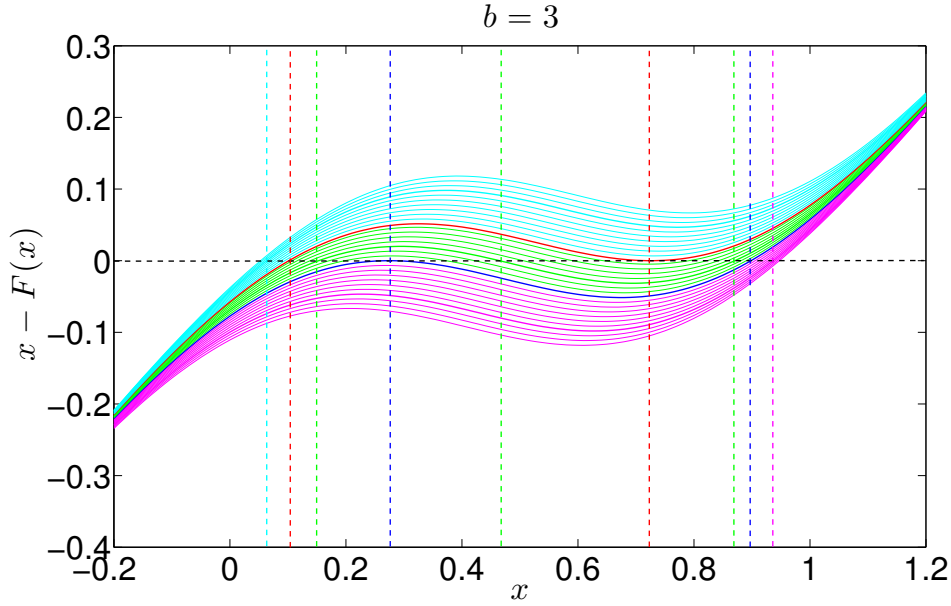


Figure 4.3: The figure shows $x - F(x)$ against x for fixed $b = 3 > b_c$ and $a \in [1.2228, 1.7772]$. Note that for $b = 3$, we have $a_1 \approx 1.4228$ and $a_2 \approx 1.5772$. Magenta coloured graphs indicate $x - F(x)$ for $a \in [1.2228, a_1)$, for the blue line $a = a_1$, for the green lines $a \in (a_1, a_2)$, for the red line $a = a_2$, and for the cyan lines $a \in (a_2, 1.7772]$. The dotted horizontal lines indicate the roots of the ticker graphs. For $a \in [1.2228, a_1)$ and $a \in (a_2, 1.7772]$, $x - F(x)$ has one root. For $a = a_1$ and $a = a_2$, $x - F(x)$ has two roots, and for $a \in (a_1, a_2)$, $x - F(x)$ has three roots. This is important as the roots of $x - F(x)$ are the fixed points of $p_r = F(p_{r-1})$.

$x - F(x)$ has three roots, and $p_r = F(p_{r-1})$ has three fixed points.

In terms of the stability of the modelled banking system, we note that for $b > b_c$ a barrier, represented by the unstable fixed point, can occur, such that the number of operating banks does not decrease below a certain value (or increases above a certain value). However, if there is a change in the parameter values, then it becomes possible that the entire system suddenly collapses (or becomes fully functional again). Hence, for $b < b_c$, the system is reversible, but for $b > b_c$, a hysteresis cycle occurs, such that the system becomes irreversible, and depends on its history. The hysteresis cycle is a well known phenomena in Curie-Weis models at zero temperature (Bouchaud, 2013). Therefore, a large amount of lending on the interbank market (i.e. large b when $p_0 = 1$) can help to stabilize the system, if the corresponding value for liabilities and mean value of non-interbank assets are such that $a < a_2$, because, in this case the barrier prevents an entire system failure.

4.2 Change in the Number of Surviving Banks Induced by One Bank Failure

For a small change from p_r to p_{r+1} , the change in the number of surviving banks is given by $NF'(p_r)$. Note that $F'(x)$ is the probability density function that $\epsilon_i = a - bx$. Thus, the number of banks becoming distressed as a consequence of one bank changing from operating normally to insolvent in the next iteration is (Dahmen and Sethna, 1996):

$$n = F'(x). \quad (4.3)$$

If n is less than one, any avalanche will eventually stop. This is because one insolvent bank triggers on average less than one bank to become insolvent. Whereas, if $n \geq 1$, one bank's insolvency can trigger an entire system failure. Starting with $p_0 = 1$, for $b > b_c$ and $x = x_1$, n is precisely one. The maximum of $F'(x)$ is reached when $x = a/b$. At this point the number of insolvent banks triggered by one bank in the following iteration is of order z suggesting that all the neighbouring banks of the initially insolvent bank become all insolvent as well.

4.3 Parameter Analysis

We have observed that when b becomes larger than the critical value b_c , the system passes from a reversible kind of dynamics to an irreversible one, where hysteresis cycles emerge. This is illustrated in Figure 4.4, where the fixed point probability values are plotted for varying a for various b ranging from $b = 0, \dots, 15$. The solid blue lines indicate the stable fixed points, whereas the blue dashed lines indicate the unstable fixed points. The hysteresis cycle is indicated by the red arrows.

We can observe that at $b = 0$, when banks are not lending to each other, the system is stable for negative values of a ; fluctuations in the asset side of the balance sheet equation can cause banks to fail and, at $a = 0$, half the banks in the system are insolvent. By lending money from one bank to another ($b > 0$), the system becomes more stable with smaller numbers of banks in distress for the same values of a .

If a increases further but b is kept constant, then more banks fail as the difference between the banks non-interbank assets and liabilities increases. Hence, the capital in the system is lowered (for constant σ and q). If b is below its critical value, then the

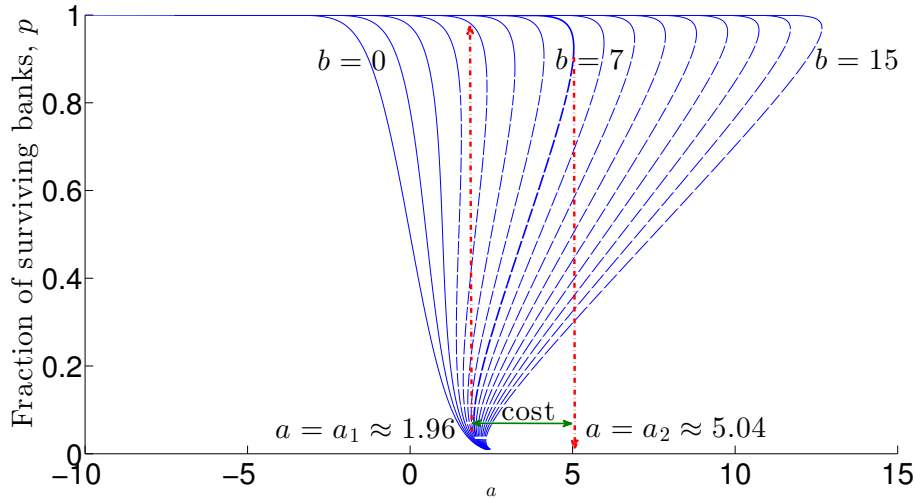


Figure 4.4: This figure shows the fraction of surviving banks as a function of the parameter a for given fixed values of b . The blue graphs are the solution of the iteration map 4.1 for different b values whereby $b = 1, \dots, 15$. The solid lines indicate stable fixed points whereas the dotted lines indicate unstable fixed points. If the fixed point is unique as in the case for $b = 1, 2$, no hysteresis occurs for decreasing or increasing a . For this value of $b > b_c$ and a particular range of a , three fixed points become possible leading to a hysteresis cycle. The thick blue line indicates the fixed points for $b = 7$. The red arrows indicate the hysteresis cycle that occurs for $b = 7$. Starting from $p_0 = 1$, the parameter a needs to increase to $a = a_2 \approx 5.04$ for the entire system to default. If the starting value is $p_0 = 0$ then a needs to decrease to $a = a_1 \approx 1.96$ for the banks to be operating. Thus, the path is history depended.

system is reversible and all fixed points are stable. If b becomes larger than the critical value b_c and $a < a_2$, almost the entire system is stable (if $p_0 = 1$) because of the barrier. However, if a increases above a_2 , then the whole system suddenly crashes. We call the sudden system failure the fragile state.

If a is constant but b decreases, then a sudden jump becomes possible as well. Let us here note that a decrease in b happens, if average interbank loans zg decrease, or the variance $\sigma = \sqrt{\sigma_A(t)^2 + \sigma_L(t)^2}$ increases. In Iori et al. (2012), it was shown that during the financial crisis, there was indeed a decrease in the amount of money loaned but the interest rates for loans also increased. Thus, b decreased, and a increased due to changes on the financial markets. In our stylized system, this is a mechanism that would create disastrous consequences unless $b < b_c$.

In order to return to a normally operating system after the crash, a needs to be reduced at least to a_1 . Then a sudden jump brings the whole system operative again. Hence, the cost of rescuing a banking system is given by the difference between

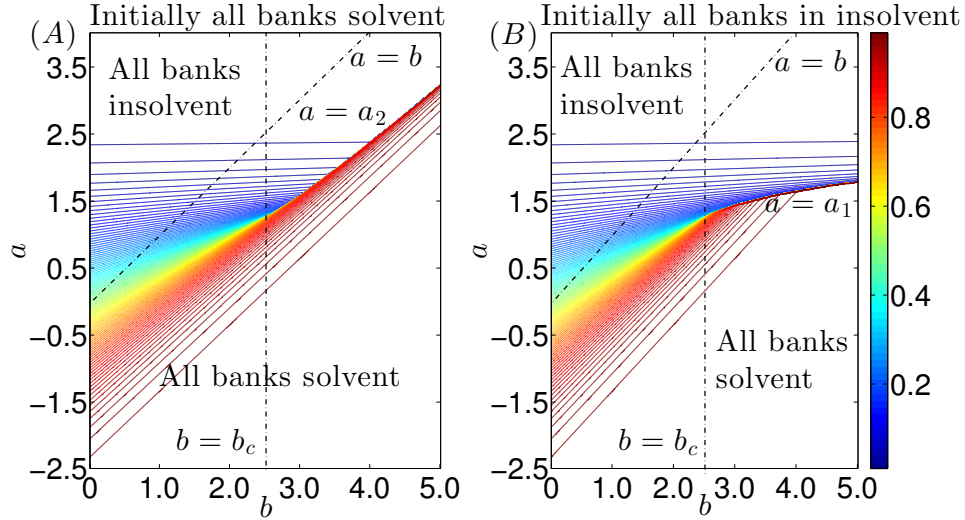


Figure 4.5: The figures show the fraction of operating banks for given a and b obtained by numerically solving the Iteration Function 4.1 starting from an initial value $p_0 = 1$ (plot A) and $p_0 = 0$ (plot B). The hysteresis behaviour becomes visible from the jump occurring in (A) at $a = a_2$ and in (B) at $a = a_1$.

$a_1(b(t))$ and $a_2(b(t + \delta t))$, where $b(t)$ is the value of b at the beginning of the crisis and $b(t + \delta t)$ the value of b at the time of rescue.

To be more specific, let us here discuss the case $b = 7$ and starting from fully operating banks (i.e. $p_0 = 1$). Here, the infinite avalanche occurs when a reaches $a_2 \approx 5.04$. Whereas, if one starts with all banks insolvent, a would need to be lowered to $a_1 \approx 1.96$, in order to return to a stable system. In Figure 4.4, this cost is indicated by the green arrow.

Figure 4.5 is a plot of the equilibrium fraction of surviving banks for different parameter values. The figure contains two plots: A and B, and depicts the solution of Eq. 4.1 for different values of a and b when the initial state of all banks is $p_0 = 1$ (plot A) or $p_0 = 0$ (plot B). Whenever $b = 0$, the fraction of surviving banks depends only on the CDF of non-interbank assets and liabilities. In the case of the standard normal CDF, for $a = 0$, half of the banks are expected to be under stress; at $a = -2.5$, the equilibrium fraction of operating banks is $p \approx 0.9938$; whereas for $a = 2.5$, the equilibrium fraction of operating banks is $p \approx 0.0062$. If $0 < b < b_c$, the system becomes more stable, which is obvious as the asset side of the balance sheet is increased and the interbank loans act as an extra asset. If a is kept constant, then either extra capital is introduced in the system or the values $\mu_L, \mu_{\hat{A}}, q, \sigma_L$ and $\sigma_{\hat{A}}$ change such that a stays constant. Further, for values of b in that range, the decline in the fraction of solvent banks for

increasing a is still smooth. When $b > b_c$, the fraction of solvent banks suddenly jumps from almost all banks solvent to almost all banks insolvent, which happens because of the occurrence of the multiple fixed points as outlined in Section 4.1.

4.4 Relation Between a and b

For fixed capital $E(p)$, the parameters a and b are dependent on one another such that the parameter a can be expressed in terms of b as:

$$a = -\frac{E(p)}{\sigma} + bp. \quad (4.4)$$

Thus, a change in a given a fixed b at the fixed point p can only happen when external capital is introduced to the system. There are multiple ways of increasing capital of a bank. For instance, a bank can raise capital by issuing shares (ECB, 2009; Fed, 2011a; Kollwe, 2011; ECB, 2011). Given the thread of insolvency, a government can intervene by inducing capital into the insolvent bank via government bailouts. Further, central banks use methods of QE by adjusting interest rates and lending to banks, or buying assets using open market operations (Singh, 2010; The Federal Reserve Board, 2011). Hence, QE can ensure that liabilities are reduced using central bank loans with smaller interest rates than otherwise required by the money market, and assets are liquidated above the market value, ensuring that capital is not needed to overcome losses when faced by liquidity shortages.

4.5 Leverage, γ

For a stable system (i.e. $p \approx 1$) with $b > b_c$, the ratios between assets and liabilities should ensure that $a \leq a_2$. Using a' and b' as defined in Eqs. 3.20 and 3.21,¹ and Eq. 4.4, the leverage ratio² - the ratio of capital to total assets (i.e. $\gamma = \frac{\mu_E}{\mu_A}$, where $\mu_E = \mu_A - \mu_L$), ensuring a stable banking system has to satisfy the following condition:

¹As a reminder, the random variables used to derive a and b are non-interbank assets and liabilities. Interbank assets are deterministic values. Whereas for a' and b' , the random variables are assets and liabilities, with interbank assets being a fraction θ of the total assets.

²There exists numerous definitions of the leverage ratio. We decided to use the ratio of loss absorbing capital to total assets in accordance with Acharya et al. (2014) and Bank for International Settlement (2014). Specifically, the leverage ratio in Bank for International Settlement (2014) is stated as the ratio of a capital measure to an exposure measure.

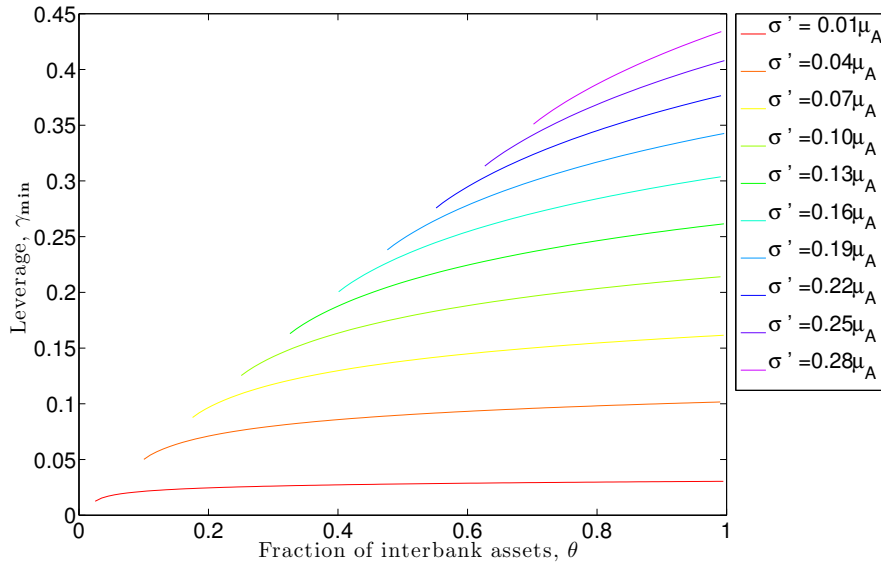


Figure 4.6: The figure shows the minimum leverage, γ_{\min} , for an average bank to ensure a stable banking system as a function of the fraction of interbank assets θ for $q = 0$. The different curves correspond to various σ' 's. From the figure, we can see that the larger σ' , the larger is θ at the instability and also the larger the minimum leverage.

$$\gamma \geq \gamma_{\min} = (1 - q) \frac{\theta_c}{b_c} \left(\sqrt{2 \ln \frac{\theta}{\theta_c}} + \frac{b_c}{\theta_c} \theta \Phi \left(-\sqrt{2 \ln \frac{\theta}{\theta_c}} \right) \right), \quad (4.5)$$

where $\theta_c = \frac{\sigma' b_c}{(1-q)\mu_A}$ and $q \neq 1$. When Eq. 4.5 reaches equality, the smallest leverage ratio, γ_{\min} , is recovered, at which the banking system is stable. Figure 4.6 is a plot of Eq. 4.5 depicting the minimum leverage, γ_{\min} , at which the system is stable as a function of θ , of interbank assets to total assets for given values of σ' . The value of σ' is chosen to be a fraction of the mean total assets for each graph as applicable in the accompanying legend. Any leverage value above and including γ_{\min} ensures a safe banking system given a particular σ' .

4.6 The Fraction of Mean Liabilities, f_L

Eq. 4.5 can be further simplified, without any loss of generality, by assuming that σ' is a fraction, $\sqrt{2}f_A$, of μ_A , i.e. $\sigma' = \sqrt{2}f_A\mu_A$. We chose to represent σ' in this way because Eq. 4.5 then becomes independent of μ_A .

In Chapter 6, we use a fraction f_L to stress the banking system. That is, we multiply μ_L by a fraction f_L to vary the average value of capital in the system. Define the parameter f_L^{MF} to be the fraction of mean liabilities, at which the fraction of surviving

banks, p , jumps from almost all banks solvent to almost all banks insolvent. Using Eq. 4.5, f_L^{MF} can be written as:

$$f_L^{MF} = \frac{\mu_A}{\mu_L} - \sqrt{2}f_A \frac{\mu_A}{\mu_L} \sqrt{2 \ln \frac{(1-q)\theta}{\sqrt{2}f_A b_c}} - \theta \frac{\mu_A}{\mu_L} (1-q) \Phi\left(-\sqrt{2 \ln \frac{(1-q)\theta}{\sqrt{2}f_A b_c}}\right). \quad (4.6)$$

Thus, the free model parameter becomes f_A . The fraction of the mean liabilities, f_L^{MF} , is influenced by f_A . The parameter, f_A , indicates how big the uncertainty of capital is, and thus indicates the size of a potential initial shock to banks' capital.

For Eq. 4.6 to have a solution, θ needs to be larger than or equal to $\frac{\sqrt{2}f_A b_c}{1-q}$. The maximal value of f_A is reached if θ tends to one. Thus, f_A tends to $\frac{1-q}{\sqrt{2}b_c}$. If $q = 0$, then f_A tends to approximately 0.2821.

It should be noted that σ' is the variance of the average, initial capital in the system. Therefore, for f_A larger than 0.2821, the capital reserves of individual banks differ greatly, such that some banks are safer than others. These banks form barriers stopping the insolvency from spreading via interbank exposure failure. Because of this, the interbank exposure network does not cause a sudden system failure, but rather the stability of the banking system relies on changes in the market, influencing the value of liabilities and assets.

If f_A tends to zero, then f_L^{MF} tends to $\frac{\mu_A}{\mu_L}$. For f_A equal to zero, all banks have the same value of capital initially because their balance sheets are identical. Then the initial shock causing one bank to become insolvent automatically causes all other banks to become insolvent as well. Hence, the average capital for system failure to occur is $\mu_A - \mu_L = 0$, which is equivalent to f_L^{MF} being equal to $\frac{\mu_A}{\mu_L}$. Thus, in a banking system with identical banks (i.e. all banks have the same balance sheet values), the underlying exposure network becomes irrelevant for systemic failure because the initial shock causes all banks to fail simultaneously.

4.7 Values for Other Location-Scale Distributions

The parameter analysis can be repeated with any location-scale distributions where the PDF, $F'(x)$, satisfies the properties stated in Section 4.3. In Tables 4.1-4.4, we state the iteration function, $F(x)$; its first derivative, $F'(x)$; the critical parameters, b_c and θ_c ; the extrema of $x - F(x)$, $x_{1,2}$; the parameters $a_{1,2}$, at which the jump occurs;

Table 4.1: The tables states the values of $F(x)$, $F'(x)$, b_c , $x_{1,2}$, $a_{1,2}$ and γ_{\min} given that the random variables L_i and \hat{A}_i are drawn from Normal distributions.

Normal Distribution	
$F(x)$	$\frac{1}{2} + \operatorname{erf}\left(\frac{a-bx}{\sqrt{2}}\right)$
$F'(x)$	$\frac{b}{\sqrt{2\pi}} \exp\left(-\frac{(a-bx)^2}{2}\right)$
b_c	$\sqrt{2\pi}$
θ_c	$\frac{\sigma' b_c}{(1-q)\mu_A}$
$x_{1,2}$	$b^{-1}\left(a \mp \sqrt{2 \ln \frac{b}{b_c}}\right)$
$a_{1,2}$	$b \pm \sqrt{2 \ln \frac{b}{b_c}} - b\Phi\left(\pm \sqrt{2 \ln \frac{b}{b_c}}\right)$
γ_{\min}	$(1-q)\frac{\theta_c}{b_c} \left(\sqrt{2 \ln \frac{\theta}{\theta_c}} + \frac{b_c}{\theta_c} \theta \Phi\left(-\sqrt{2 \ln \frac{\theta}{\theta_c}}\right)\right)$

Table 4.2: The tables states the values of $F(x)$, $F'(x)$, b_c , $x_{1,2}$, $a_{1,2}$ and γ_{\min} given that the random variables L_i and \hat{A}_i are drawn from Cauchy distributions.

Cauchy Distribution	
$F(x)$	$\frac{1}{2} - \frac{1}{\pi} \arctan(a - bx)$
$F'(x)$	$\frac{1}{\pi(1+(a-bx)^2)}$
b_c	π
θ_c	$\frac{\sigma' b_c}{(1-q)\mu_A}$
$x_{1,2}$	$\frac{a \mp \sqrt{\frac{b}{b_c} - 1}}{b}$
$a_{1,2}$	$\frac{b}{2} \pm \sqrt{\frac{b}{b_c} - 1} - \frac{b}{b_c} \arctan\left(\pm \sqrt{\frac{b}{b_c} - 1}\right)$
γ_{\min}	$(1-q)\frac{\theta_c}{b_c} \left(\frac{1}{2} \frac{b_c}{\theta_c} \theta + \sqrt{\frac{\theta}{\theta_c} - 1} + \frac{\theta}{\theta_c} \arctan\left(-\sqrt{\frac{\theta}{\theta_c} - 1}\right)\right)$

Table 4.3: The tables states the values of $F(x)$, $F'(x)$, b_c , $x_{1,2}$, $a_{1,2}$ and γ_{\min} given that the random variables L_i and \hat{A}_i are drawn from Logistic distributions.

Logistic Distribution	
$F(x)$	$\frac{1}{2} - \frac{1}{2} \tanh\left(\frac{a-bx}{2}\right)$
$F'(x)$	$\frac{b}{4} \operatorname{sech}^2\left(\frac{a-bx}{2}\right)$
b_c	4
θ_c	$\frac{\sigma' b_c}{\mu_A}$
$x_{1,2}$	$\frac{a \mp 2 \operatorname{arccosh}\left(\sqrt{\frac{b}{b_c}}\right)}{b}$
$a_{1,2}$	$2 \frac{b}{b_c} \mp \sqrt{b} \sqrt{\frac{b}{b_c} - 1} \pm 2 \operatorname{arccosh}\left(\sqrt{\frac{b}{b_c}}\right)$
γ_{\min}	$(1-q)\frac{\theta_c}{b_c} \left(\frac{1}{2} \frac{b_c}{\theta_c} \theta - \sqrt{\frac{b_c}{\theta_c}} \theta \sqrt{\frac{\theta}{\theta_c} - 1} + 2 \operatorname{arccosh}\left(\sqrt{\frac{\theta}{\theta_c}}\right)\right)$

Table 4.4: The tables states the values of $F(x)$, $F'(x)$, b_c , $x_{1,2}$, $a_{1,2}$ and γ_{\min} given that the random variables L_i and \hat{A}_i are drawn from Student's t distributions with two degrees of freedom.

Student's t Distribution, $\nu = 2$	
$F(x)$	$\frac{1}{2} - \frac{a-bx}{2\sqrt{2+(a-bx)^2}}$
$F'(x)$	$\frac{b}{(2+(a-bx)^2)^{3/2}}$
b_c	$2^{3/2}$
θ_c	$\frac{\sigma' b_c}{(1-q)\mu_A}$
$x_{1,2}$	$\frac{a \mp \sqrt{b^{2/3}-2}}{b}$
$a_{1,2}$	$\frac{b}{2} + \left(\mp \frac{b^{2/3}}{2} \pm 1 \right) \sqrt{b^{2/3} - 2}$
γ_{\min}	$(1-q) \frac{\theta_c}{b_c} \left(\frac{1}{2} \frac{b_c}{\theta_c} \theta - \left(\frac{1}{2} \left(\frac{b_c}{\theta_c} \theta \right)^{2/3} - 1 \right) \sqrt{\left(\frac{b_c}{\theta_c} \theta \right)^{2/3} - 2} \right)$

and the minimum leverage, γ_{\min} , to ensure a stable system, given that the random variables, (non-interbank) assets and liabilities, are drawn from Normal distributions (Table 4.1), Cauchy distributions (Table 4.2), Logistic distributions (Table 4.3), and Student's t distributions with two degrees of freedom (Table 4.4).³ To calculate γ_{\min} , we used a' and b' as defined in Eqs. 3.20 and 3.21. For the rest, a and b are used as defined in Eqs. 3.13 and 3.14.

Figure 4.7 shows in its first row plots of $F'(x)$ against x , and in its second row plots of $x - F(x)$ for different location-scale distributions. The different distributions are indicated using different colour schemes with graphs equated using Normal distributions (N) being red, Cauchy distributions (C) being green, Logistic distributions (L) being blue and Student's t distributions with two degrees of freedom (S) being magenta coloured. In addition, we marked the positions of the fixed points (w_i^* , where $i = [1, 2, 3]$ and $*$ = $[N, C, L, S]$) and the extrema of $x - F(x)$ (x_i^* , where $i = [1, 2]$ and $*$ = $[N, C, L, S]$) using horizontal lines. The parameters a and b are fixed at 2 and 4.5, respectively. For $b = 4.5$, b_c is smaller than b for all distributions.

It becomes clear that for Normal and Student's t distributions, three fixed points occur with $w_1^{N,S}$, $w_3^{N,S}$ being stable fixed points and $w_2^{N,S}$ being an unstable fixed point forming the barrier between $w_1^{N,S}$ and $w_3^{N,S}$. For Cauchy and Logistic distributions, only one fixed point exists: $w_1^{C,S}$, which is a stable fixed point close to one indicating a

³A Student's t distribution with one degree of freedom leads to the Cauchy distribution and if the degree of freedom tends to infinity the Normal distribution is recovered.

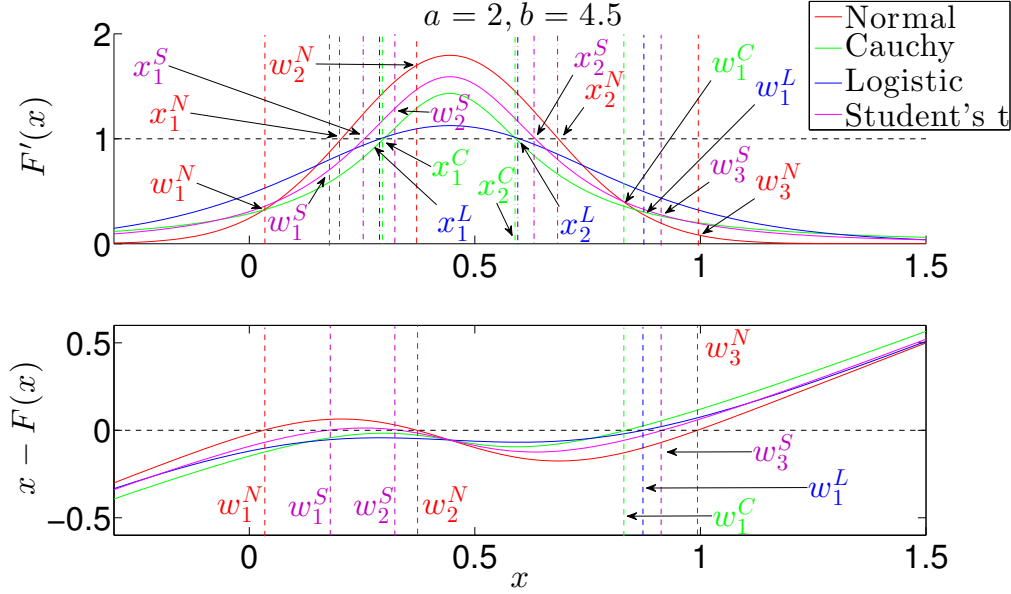


Figure 4.7: The figure shows two subplots. In the first subplot, $F'(x)$ is plotted against x for a Normal distribution (N , red), Cauchy distribution (C , green), Logistic distribution (L , blue) and Student's t distribution (S , magenta). In the second row, $x - F(x)$ is plotted against x for the different distributions using the same colour scheme as in the first row. The parameters $a = 2$ and $b = 4.5$ are fixed. We marked the one (first row) and zero (second row) line, using a black, dotted line. In addition, we indicated the positions of the fixed points (w_i^* , where $i = [1, 2, 3]$ and $* = [N, C, L, S]$) and the extrema of $x - F(x)$ (x_i^* , where $i = [1, 2]$ and $* = [N, C, L, S]$) using horizontal lines.

stable banking system.

Therefore, for a starting value p_0 in $[w_1^{N;S}, w_2^{N;S}]$ or $[0, w_1^{N;S}]$ and L_i, \hat{A}_i drawn from Normal or Student's t distributions, the banking system collapses. Whereas for p_0 in $[w_2^{N;S}, w_3^{N;S}]$ or $[w_3^{N;S}, 1]$ and L_i, \hat{A}_i drawn from Normal or Student's t distributions, the banking system stays stable. For L_i, \hat{A}_i drawn from Cauchy or Logistic distributions, the banking system always reaches $w_1^{C;L}$ given any starting value $p_0 \in [0, 1]$. Because the fixed point, $w_1^{C;L}$, is close to one, the banking system is stable.

Furthermore, note that $x_1^N < x_1^S < x_1^L < x_1^C < x_2^C < x_2^L < x_2^S < x_2^N$ for $a = 2$ and $b = 4.5$. Thus, given $p_0 \in [w_3^*, 1]$, $a = a_2^*$ and $b = 4.5$, the jump from almost all banks surviving to almost all banks insolvent is the largest if L_i, \hat{A}_i are drawn from Normal distributions, and the smallest if L_i, \hat{A}_i are drawn from Cauchy distributions.

In Figure 4.8, we plotted $a_{1,2}$ against b for the different distributions. We have $a_2^{C;L;S} < a_2^N$. This implies that the initial capital needs to be reduced much further if L_i, \hat{A}_i are drawn from Normal distributions in comparison to L_i, \hat{A}_i being drawn

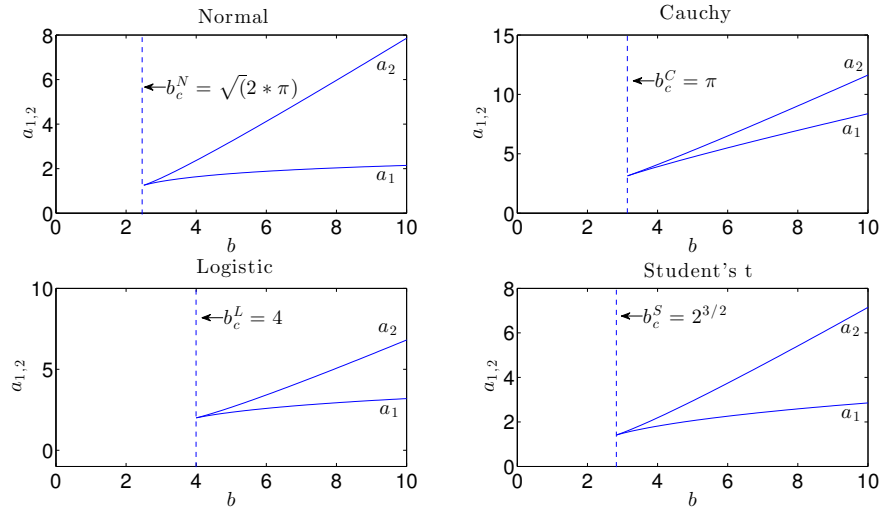


Figure 4.8: The figures show $a_{1,2}$ plotted against b for different distributions as stated in Table 4.1-4.4. In (A), $a_{1,2}$ are plotted using the Normal distributions, in (B) represents $a_{1,2}$ for Cauchy distributions, in (C) the graphs for $a_{1,2}$ are plotted for the Logistic distributions and (D) $a_{1,2}$ are shown for Student's t distributions with two degrees of freedom. In addition, we marked the critical parameter b_c for each distribution using a dotted horizontal line.

from Cauchy, Logistic or Student's t distributions for the jump to occur. Hence, for the latter distributions, the initial shock to the capital can be smaller for the fragile state to occur. That said, the average interbank exposure for banking systems initialized with Cauchy, Logistic or Student's t distributions needs to be greater than the average interbank exposure for banking systems initialized with Normal distributions for the fragile state to become possible.

Figure 4.9 shows the minimum leverage ratio, γ_{\min} , for Normal distributions (red), Cauchy distributions (green), Logistic distributions (blue) and Student's t distributions (red) plotted against the average ratio of interbank exposure to total assets, θ . The recovery rate, q , is set to zero. The location parameter, σ , for each distribution is set to $0.02\mu_A$. The vertical lines indicate θ_c for each distribution. The critical ratio of average interbank exposure to total assets, θ_c , is the smallest for Normal distributions followed by Student's t, Cauchy and Logistic distributions. However, the minimum leverage for Student's t, Cauchy and Logistic distributions increases faster for increasing θ than γ_{\min} calculated for Normal distributions.

Specifically, for $\theta = 0.2$, the minimum leverage to ensure a stable system for Normal distributions is $\gamma_{\min}^N(\theta = 0.2) = 0.0429$, for Cauchy distributions $\gamma_{\min}^C(\theta =$

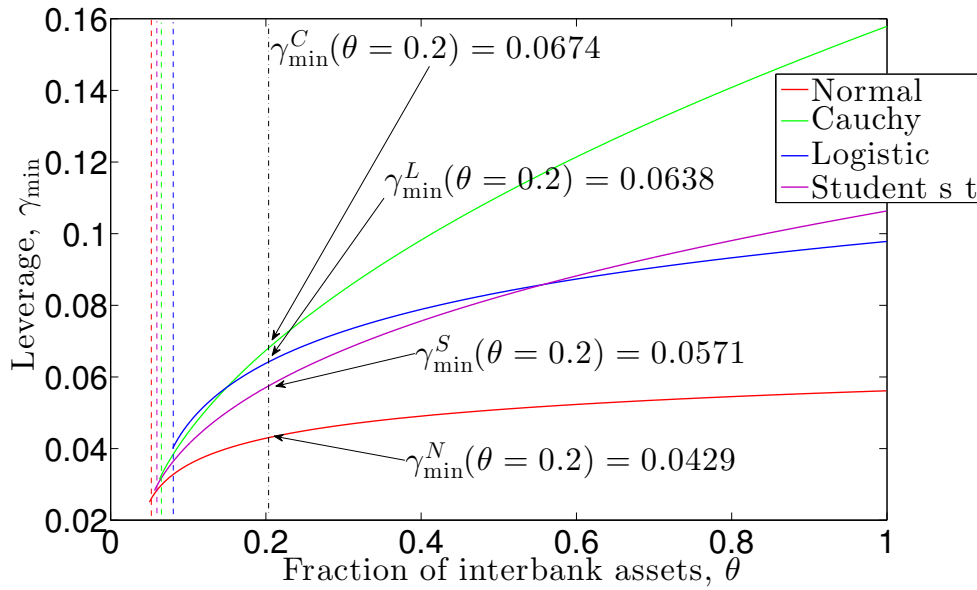


Figure 4.9: The figure shows the minimum leverage for Normal distributions (red), Cauchy distributions (green), Logistic distributions (blue) and Student's t distributions with two degrees of freedom (magenta) plotted against the average ratio of interbank lending, θ . The coloured vertical lines indicate θ_c for each distribution. Furthermore, the minimum leverage when $\theta = 0.2$ is marked ($\gamma_{\min}^*(\theta = 0.2)$, where $*$ $\in [N, C, L, S]$) for each distribution.

0.2) = 0.0674, for Logistic distributions $\gamma_{\min}^L(\theta = 0.2) = 0.0638$, and for the Student's t distribution $\gamma_{\min}^S(\theta = 0.2) = 0.0571$. For increasing θ , γ_{\min} for Student's distribution is about three times larger than γ_{\min} for Normal distributions.

The reason for the difference in the size of the jump, the shock size resulting in the fragile state and varying minimum leverage requirements can be found in the thickness of the tail of the distributions. The tail for standard Cauchy distributions, Logistic distributions and Student's t distributions is wider than the tail of a standard Normal distribution for the same location, μ , and scale, σ , parameter (see Figure 4.7). This implies that the difference between L_i and \hat{A}_i differs more greatly between individual banks if Cauchy distributions, Logistic distributions and Student's t distributions are used to initialize the banking network (in comparison to Normal distributions). Thus, some banks have more capital than others initially when Cauchy distributions, Logistic distributions and Student's t distributions are used. These banks' larger capital reserves stop them from being affected by the collapse of the rest of the banking system. Hence, the difference between x_1 and x_2 , and subsequently, the jump is smaller. Furthermore, banks with large capital reserves form breaking points in the insolvency propagation.

Thus, the probability of solvent banks being connected to insolvent banks is lower. For the fragile state to become possible, the probability of banks being connected to insolvent banks needs to increase. Hence, the critical interbank exposure parameter, b_c , has to increase.

On the other hand, some of the banks initialized with Cauchy distributions, Logistic distributions and Student's t distributions have much less capital, which causes the fragile state to happen at lower values of a_2 . This is also reflected in the minimum leverage requirement, which is larger for Cauchy distributions, Logistic distributions and Student's t distributions than for Normal distributions for the same value of interbank assets to total assets, θ , and scale parameter, σ .

4.8 Analysis of Real Banking Systems Using Balance Sheet Data

Banks report their balance sheet quantities yearly as part of their financial statement in their annual report. We used Bankscope (Bureau Van Dijk, 2014) to collect data for US and UK banks.⁴ The data includes consolidated values for some banks and unconsolidated values for others. Only using the values from consolidated balance sheets would have reduced the list of banks considerably, mostly excluding foreign subsidiaries of foreign banks. We chose the years 2007 and 2012 as reference years, to determine the stability of the UK and US banking system during the recent financial crisis and a non-crisis time. The parameters μ_A and μ_E represent the “true” of the average value of total assets and capital per bank.

We also disregard any seniority of the debt and assume that the recovery rate is set to zero. Hence, we consider the worst case scenario, where a creditor cannot expect any payment for a defaulted loan. Furthermore, Normal CDFs are used for the iteration process. Hence, μ_A and $\mu_L = \mu_A - \mu_E$ are the mean, and σ_A and σ_L represent the standard deviation of the distributions.

Using a' and b' as defined in Eqs. 3.20 and 3.21 and assuming $p_0 = 1$, the two

⁴The query settings were on “Status: Active Banks, Inactive Banks”, “Specialisation: Commercial banks, Savings banks, Cooperative banks, Real Estate & Mortgage banks, Investment banks, Islamic banks, Other non banking credit institutions, Bank holdings & Holding companies, Private banking / Asset management companies” and “Ultimate Owner: Def. of the UO: min. path of 50.01%, known or unknown shareh., closest quoted company in the path leading to the Ultimate Owner (if any); GUO and DUO”

Table 4.5: The table reports the mean value of total assets μ_A and Tier 1 capital of banks μ_E and the standard deviations for the years 2007 and 2012 for the UK and US banking system. The data is from Bankscope. We only considered banks that reported their Tier 1 capital. The table additionally states the number of banks. To compare the Tier 1 capital, we also stated the leverage ratio γ , i.e. Tier 1 capital to total assets.

	UK		USA	
	2007 in GBP	2012 in GBP	2007 in USD	2012 in USD
μ_A	2.0287e+11	1.8307e+11	1.8505e+10	2.0247e+10
STD	4.7503e+11	4.2912e+11	1.3592e+11	1.5234e+11
μ_E	6.3032e+09	8.1836e+09	1.0615e+09	1.5829e+09
STD	1.3785e+10	2.0298e+10	6.6785e+09	1.1102e+10
Leverage, γ	0.0311	0.0447	0.0574	0.0782
No. banks	26	38	666	779

quantities that are decisive for the stability of the banking system in our model are the mean of the total assets μ_A and the mean of loss absorbing capital $\mu_E = \mu_A - \mu_L$. We are using the “Tier 1 Capital” and “Total Assets” as reported in Bankscope. It should be noted that the UK and US use different accounting systems.⁵ This causes different estimations for the value of the same asset and liabilities. Hence, the value of total assets, total liabilities and Tier 1 capital for UK and US banks reported in Bankscope cannot be compared countrywise. However, it is possible to discuss changes in financial stability of the banking systems in a country for different years. To compute the mean values for μ_A and μ_E , we only use banks with Tier 1 capital larger than zero this reduced the list of banks considerably (especially in 2007) as Bankscope does not report the Tier 1 capital value for all banks. The mean values as well as the number of banks used to compute the values can be found in Table 4.5. To compare the values for Tier 1 capital and total assets in the different years, we also included leverage, γ , in the table. It becomes clear that in 2007 the average leverage both in the US and UK was less than it was in 2012 and henceforth already implies a less stable system in 2007.

The parameter σ' is a free model parameter that indicates the uncertainty about the value of asset and liabilities. More precisely σ_A increases if the value for assets is uncertain. Similarly, difficulties in obtaining funding from banks or other funding sources are represented in an increased σ_L . In a way, σ' measures the severity of the

⁵The firms in the UK as the rest of EU countries use *International Financial Reporting Standards* and companies in the US use the *US Generally Accepted Accounting Principles* (Pricewaterhouse Coopers, 2014).

shock, and hence, we tested for different values of σ' . To calibrate σ' , we use a variable $f \in [0, 1]$ and say that σ' is a fraction of the mean value of the Tier 1 capital, μ_E , i.e. $\sigma' = f\mu_E$.

Another parameter that cannot be easily obtained from the annual account data is the average fraction of interbank assets, θ . Banks report their lending to other banks under “Loans and advances to banks” and “Deposits by banks” in their annual reports. However, as it is pointed out in Langfield et al. (2014), loans and advances to banks are not the only exposure banks have to other banks. Thus to monitor the UK interbank market, the BoE collects data about other financial instruments that form part of the interbank market. In particular, Langfield et al. (2014) list: “prime lending (...); holdings of capital and fixed-income securities issued by banks; credit default swaps bought and sold; securities lending and borrowing (...); repo and reverse repo (...); derivatives exposure (...); settlement and clearing lines; asset-backed securities; covered bonds; and short-term lending with respect to other banks and broker dealers”. The balance sheet data reported in the annual reports do not differentiate between the interbank market and products obtained from other financial institutions. Still, using only the values for “Loans and advances to banks” or “Deposits by banks” to calibrate θ would underestimate the average fraction of interbank lending. Henceforth, we use multiple values of θ to test the stability of the system.

Figures 4.10 and 4.12 show various plots of the fraction of surviving banks, p , plotted against the fraction of σ' to the mean Tier 1 capital μ_E , f , for the UK and US system, respectively. The fraction of surviving banks is calculated using the fixed points of Eq. 4.1 and a standard normal CDF as before. The value of the fraction of interbank exposure to total assets, θ , is fixed and given above each subplot. The blue crosses indicate the fraction of surviving banks for a banking system calibrated with the 2007 data and the black circles symbolize the fraction of surviving banks for a banking system calibrated with the 2012 data.

For θ set to zero, the fraction of surviving banks in the UK banking system is almost identical (Figure 4.10). The number of surviving banks declines for a larger f . However, even for f tending to one, more than 85% of banks are operating in both 2007 and 2012. Note that θ equal to zero corresponds to no interbank exposure. The number of insolvent banks is only due to the uncertainty of the value of liabilities and

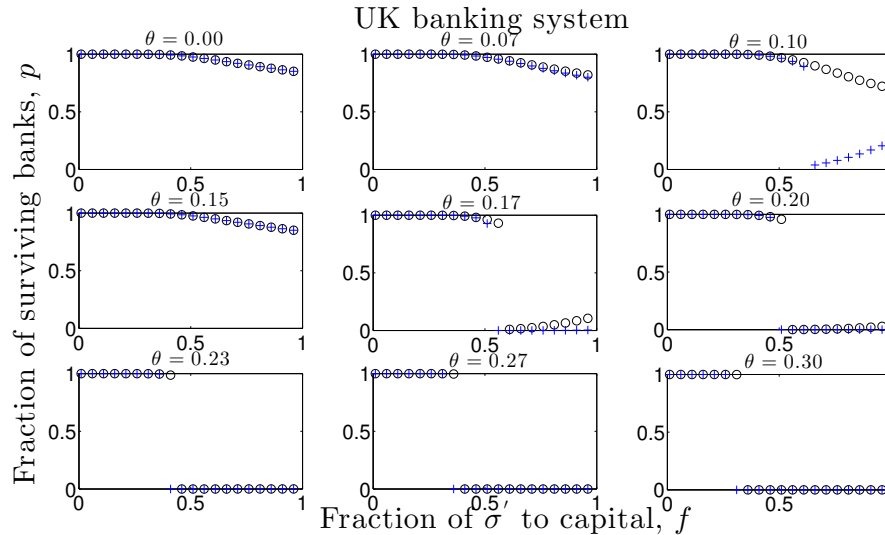


Figure 4.10: The subplots show the fraction of surviving banks for the years 2007 (blue crosses) and 2012 (black circles) against the fraction of σ' to mean value of capital, f , for various values of the fraction of interbank assets to total assets, θ . To calibrate the model, the mean of total assets, μ_A , and the mean of Tier 1 capital, μ_E , was used from banks from the UK banking system ($q = 0$). For $\theta = 0$, banks are not interconnected. In that case, for both years no systemic distress event happens. In order for a system failure to happen, θ needs to be non-zero. The sudden system failure happens for the banking system calibrated with the 2007 UK data for $\theta = 0.07$ at which the banking system calibrated with 2012 UK data is still in a stable state. For $\theta \geq 0.10$, the banking system calibrated with 2012 UK data also becomes unstable for a large enough f . However, f at which the systemic distress happens for the 2007 UK data is smaller than the value for f at which the systemic failure happens when the banking system is calibrated with the 2012 UK data implying that the 2007 system is more prone to failure than the 2012 banking system.

non-interbank assets caused by a large σ' . For the range of σ' from zero to the size of μ_E , no systemic event, i.e. the entire failure of the banking system, becomes possible in both years given that there is only a shock to the value of non-interbank assets or liabilities.

For the next graphs in Figure 4.10, in the first row, θ is increased to 0.03 and 0.07. It becomes clear that the fraction of surviving banks deviates for 2007 and 2012 with p for 2007 being considerable less than p for 2012, implying that the banking system 2007 was much more prone to failure. For $\theta = 0.07$ and the banking system calibrated with the 2007 data set, a jump becomes visible for p for f around 0.5. The banking system calibrated with the 2012 data set remains stable for θ set to either 0.03 or 0.07. This changes when θ is further increased. In the second row of Figure 4.10, θ is set to 0.10, 0.11 and 0.13. The sudden jump for banks calibrated with the 2007 data set

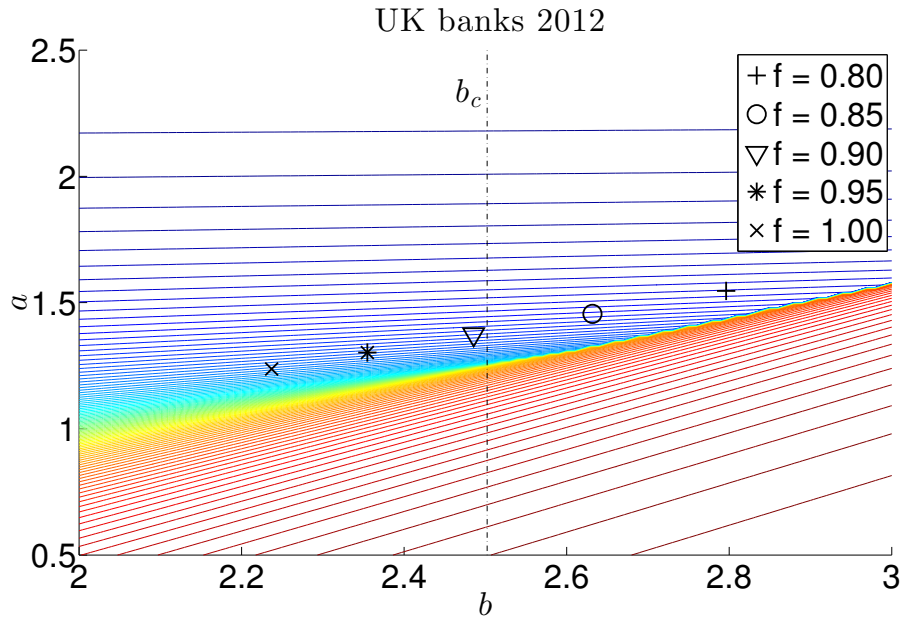


Figure 4.11: The figure is similar to Figure 4.5 showing the fraction of surviving banks for different values of a and b . In addition to the fraction of surviving banks for particular values of a and b , we also plotted the particular values of the fraction of surviving banks calibrated with the 2012 UK data for θ fixed at 0.10 for varying f as indicated. It becomes clear that for increasing f , b decreases such that for $f = 0.90$, b becomes less than b_c . At the same time, p increases, explaining the increase in p observed in Figure 4.10 for $\theta = 0.10$ and $\theta = 0.11$ for increasing f for the 2012 UK data.

happens for f around 0.51 to 0.56 and increases even further in the third row when θ takes the values 0.3, 0.4 and 0.5 with a value of f around 0.31 - 0.46 being sufficient to ensure an unstable banking system. For the banking system calibrated with the 2012 data set, a jump also occurs for values of θ above and including 0.1. For θ equal to 0.10, the jumps happens for f around 0.66. As with the 2007 data set, the jump moves to a lower value of f for a larger θ with θ set to 0.5, f being around 0.36 for the jump to happen.

For θ equal to 0.10 or 0.11, a jump occurs as well in the banking system calibrated with the 2012 UK data set. However, after the jump, p increases for increasing f . This can be explained using Figure 4.11. Figure 4.11 is the same plot of the contour lines of surviving banks as plotted in Figure 4.5. The black symbols indicate the position of p for fixed θ equal to 0.10 and varying f as indicated in the accompanying legend. It becomes obvious that for increasing f , b decreases such that for $f = 0.90$ a jump does not become possible any more and the system is in the reversible region. At the same time, the value of p increases for decreasing b . Hence, we can observe an increase in p

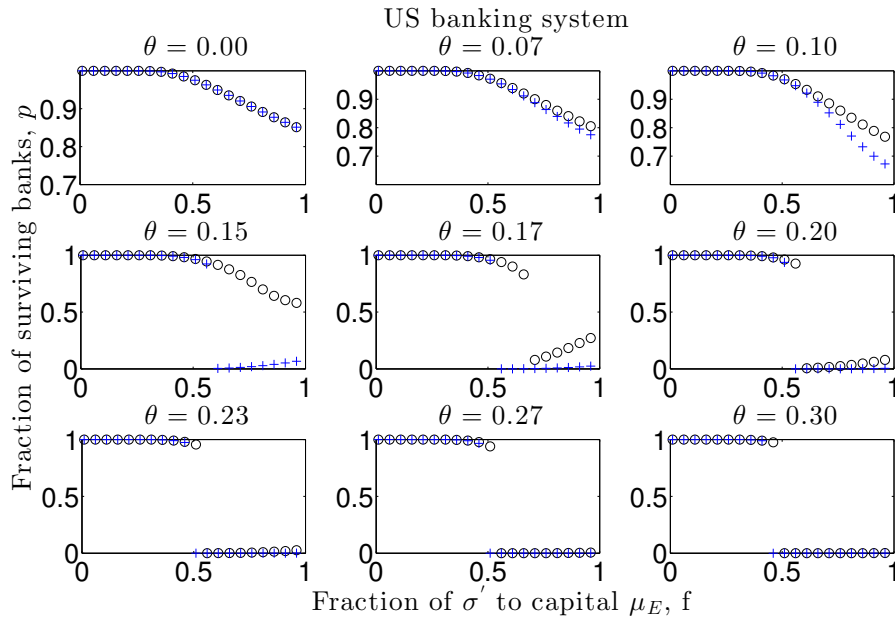


Figure 4.12: The figure is similar to Figure 4.12 except that US balance sheet data for the years 2007 and 2009 were used to calibrate the model with the recovery rate for interbank exposure set to zero. The sub plots show the fraction of surviving banks for the years 2007 (cross) and 2012 (circle) against the fraction of σ' to mean value of capital, f , for various values of the fraction of interbank assets to total assets, θ . To calibrate the model, the mean of total assets, μ_A , and the mean of Tier 1 capital, μ_E , was used from banks from the US banking system. For $\theta = 0$, banks are not interconnected. In that case, for both years, no systemic distress event happens. In fact, even for an increased θ of 0.10 the system is stable with only some losses for large f but no system-wide failure. The sudden system failure happens for the banking system calibrated with the 2007 US data for $\theta = 0.15$. However, we note that for the same value of θ , the banking system calibrated with 2012 US data is still in a stable state. For $\theta \geq 0.17$, the banking system calibrated with 2012 US data also becomes unstable for a large enough f . For both years, σ' needs to be at least half of the size of banks capital in order for the system wide failure to happen.

even though f , and therefore, the uncertainty, σ' , increases.

Figure 4.12 is similar to Figure 4.10 except that we used US banks to calibrate the model with the blue crossed line representing the fraction of surviving banks in 2007 and the black circled line being the fraction of surviving banks in 2012. In Figure 4.12 the difference in the stability of the US banking system in 2007 and 2012 is less visible suggesting that a shock to that similar sized as happened in 2007 would also cause severe damage in 2012 if the ratio of interbank assets to total is also similar.

Figures 4.10 and 4.12 show that exposure to other banks played an important role in the recent financial crisis. As we mentioned before, we cannot be certain about the actual average fraction of interbank loan nor the size of σ' . However, an exposure of

30% of total assets to other banks seems like a valid estimate. A σ' of 25% or 50% of the bank's capital only happens during a period of large uncertainty - which one can argue happened during the 2008 meltdown of the financial sector. In particular, the Financial Services Authority (FSA) stated in their report on "The failure of the Royal Bank of Scotland" FSA (2011) that a mismatch in short-term funding and devaluation of long-term assets, which potentially reduced the capital of RBS by 50%, played part of the failure and eventual bail-out of the Royal Bank of Scotland by the UK government. Hence, it can be assumed that other banks also faced capital losses of similar order that according to our model would result in failure of the entire banking system.

Needless to say, in using the balance sheet test to determine insolvency, a bank failure is always an option as capital is limited. The likelihood of such a large shock happening is not part of this thesis but it can certainly be considered a rare event. Nonetheless, the maximal economically feasible leverage ratio should be used as a minimum to prevent entire system failure and taxpayer intervention.

4.9 Conclusion

In conclusion, simplifying the counterparty risk model using the mean-field assumption allows us to solve the counterparty risk model semi-analytically for a variety of location scale distributions. Additionally, we analysed the balance sheet parameters performing a parameter analysis using the mean-field model to obtain the regions where the banking system is stable or unstable. We showed that the banking system can turn suddenly from a stable system, where most of the banks survive a shock to their loss absorbing capital, to an unstable system, where most of the banks become insolvent. We call this shift in stability the fragile state. In particular, we calculated the size of the shock that induces the fragile state. This allowed us to not only infer the cost of rescuing a banking system but also to compute a restricting minimum leverage ratio that ensures a stable banking system. Another advantage of the mean-field model is that one can obtain data to initialize the model from banks' annual reports. We did so by comparing the stability of the US and UK banking system in 2007 and 2012. We determined that the banking systems in 2012 were more stable than the systems in 2007 for the same level of average counterparty exposure.

Banks in real banking system vary largely in the size of their balance sheets. The

assumptions leading to the mean-field model reduce the banking system to a homogeneous system where only average balance sheet parameters are considered in order to evaluate the stability of the banking system. Furthermore, the interbank network structure is disregarded and banks interbank exposure to other banks is assumed to be the same in the mean-field model. These assumptions are unrealistic as they ignore the heterogeneity of real banking systems. For this reason are we testing in Chapters 5 and 6 the robustness of the mean-field model by comparing the solution of the mean-field model to the solution of more realistic simulation based models of the counterparty risk model.

Chapter 5

Comparison of Simulation and Mean-Field Model of Stylized Banking Systems

Summary: *In this chapter, we use simulation means to test for the robustness of the results deduced from the mean-field model. Different random distributions and standard network topologies are used to initialize banks' balance sheets in a simulation-based model. The equilibrium solution of the simulation model is compared to the fixed point solution of the mean-field model. We find that both solutions are in agreement, which suggests that indeed the results of the mean-field model are robust for different sized banking systems initialized using a variety of random distributions, network topologies and banking system parameters.*

5.1 Initialization of Theoretical, Simulation-based Banking System

In this chapter, we also construct a highly stylized banking system. The intention of this chapter is to show the robustness and limitations of the mean-field model. We do so by comparing the mean-field model to a simulation-based model testing for different random distributions and network topologies to initialize the banking system.

Table 5.1: The table reports the variables and values used for initializing banks' balance sheets and exposure structure in the simulation modelling a stylized banking system. The banking system consists of $N = 500$ banks. The state of each bank is set to operating initially, i.e. $S_i(0) = 1$ for all banks i . Two location scale distributions, the Normal distribution and the Student's t distribution, are used to calibrate the balance sheets of banks with location parameters $\mu_A = 1000$ and $\mu_L \in [700, 1200]$ and scale parameters $\sigma_A = 30$ and $\sigma_L = 50$. To compute the structure of the adjacency matrix $\mathbf{X} = \{\chi_{1 \leq i, j \leq N}\}$, three different network structures are used: Erdős-Rényi networks, Small-World networks and a network structure with core and periphery banks. For the Erdős-Rényi network, a link exists between two banks with probability $\alpha = 0.1$. To construct the Small-World network, we used the algorithm from Watts and Strogatz (1998) with banks having $c = 12$ neighbours and a re-wiring probability of each link of $\beta = 0.1$. To create the core-periphery network, we use the algorithm from Barabási and Albert (1999) with an Erdős-Rényi seed network with 50 banks and connection probability $\alpha = 0.75$ and 450 banks with 15 links added with a preferential attachment to the existing banks. The weight for a loan from bank i to bank j is $\theta A_i g_{ij} / z_i$, where θ is the fraction of interbank assets to total assets. The recovery rate is set to zero. If not explicitly stated otherwise, the values given in this table are used to initialize the simulations.

Variable	Values used for initialization	Description of variables of bank i at time 0
N	500	Number of banks in the stylised banking system.
$\epsilon_i^{A,L}$	$\epsilon_i^{A,L} \sim N(0, 1)$	Standard normal random variables.
$t_i^{A,L}$	$t_i^{A,L} \sim T(\nu)$	Standard Student's t random variables with degree of freedom ν .
ν	2	Degree of freedom for Student's t distribution.
$S_i(t)$	$S_i(0) = 1$	State, all banks are solvent initially.
μ_A	1000	Location parameter for total assets.
σ_A	30	Scale parameter for assets.
μ_L	700 - 1200	Location parameter for liabilities.
σ_L	50	Scale parameter for liabilities.
θ	0.0, 0.1, 0.3	Fraction for interbank assets.
α	0.1	Probability of bank i being connected with bank j , used to generate Erdős-Rényi network and seed network for the core-periphery network.
c	12	Neighbouring banks of all bank i in Small-World network.
β	0.1	Re-wiring probability for a link in the Small-World network .
q_{ij}	0	Recovery rate for exposure from bank i to bank j .

The location-scale distributions tested are Normal and Student’s t distribution. To calibrate total assets and total liabilities with Normal distributions, random variables ϵ_i are drawn from a standard normal distribution; the total assets are $A_i(0) = \mu_A + \sigma_A \epsilon_i^A$ and the total liabilities are $L_i = \mu_L + \sigma_L \epsilon_i^L$. Similarly, if the distribution used to calibrate total assets and total liabilities is the Student’s t distribution, random variables t_i^L, t_i^A are drawn from a standard Student’s t distribution with degree of freedom ν . The total assets and liabilities are given by $A_i(0) = \mu_A + \sigma_A t_i^A$ and $L_i = \mu_L + \sigma_L t_i^L$. Note that the random variables $\epsilon_i^{L,A}$ and $t_i^{L,A}$ are different and independent.

We also use to initialize the balance sheets non-location-scale distributions, namely Log-Normal and Log-Logistic. To calibrate the balance sheets, we start by using the location, μ_A^N, μ_L^N , and scale parameters, σ_A^N, σ_L^N , for Normal distributions. We convert μ_A^N, μ_L^N and σ_A^N, σ_L^N into the input variables of the other distributions such that the arithmetic mean and standard deviation of the samples of banks’ balance sheets constructed using Log-Normal, Logistic and Log-Logistic distributions are μ_A^N, μ_L^N , and σ_A^N, σ_L^N , by using the formulas stated in Table 5.2.

Table 5.2: The table shows the input variables of Normal (N), Log-Normal (LN), Logistic (L) and Log-Logistic distributions (LL) as derived from a Normal distribution’s mean and standard deviation.

Distribution		
Normal	μ^N	σ^N
Log-Normal	$\mu^{LN} = \log\left(\frac{\mu^N}{\sqrt{\sigma^{N^2} + \mu^{N^2}}}\right)$	$\sigma^{LN} = \sqrt{\log\left(\frac{\sigma^{N^2}}{\mu^{N^2}} + 1\right)}$
Logistic	$\mu^L = \mu^N$	$\sigma^L = \frac{\sqrt{3}}{\pi} \sigma^N$
Log-Logistic	$\mu^{LL} = \log\left(\frac{\mu^L}{\sqrt{\sigma^{L^2} + \mu^{L^2}}}\right)$	$\sigma^{LL} = \sqrt{\log\left(\frac{\sigma^{L^2}}{\mu^{L^2}} + 1\right)}$

For constructing the underlying exposure network structure, we use an adjacency matrix \mathbf{X} to represent three different standard network types: the Erdős-Rényi network, the Small-World network (Watts and Strogatz, 1998) and a Barabási-Albert network (Barabási and Albert, 1999), with a tightly connected seed network. For the Erdős-Rényi network, a bank i is connected to a bank j with probability α . For the Small-World network, we used an initial network, where each bank is connected to its c closest neighbours and a probability β is used to re-wire any existing links between the neighbouring banks to other banks creating the small-world effect. We call the

Barabási-Albert network a core-periphery network as we use an Erdős-Rényi seed network of banks with a high connection probability, α , to create the core and add ‘peripheral’ banks individually to the system using the preferential attachment algorithm stated in Barabási and Albert (1999).¹ Constructing a core-periphery network using a Barabási-Albert network has the advantage of producing a network topology quite different to the topology of the Erdős-Rényi and Small-World network. Thus, we test for the influence of quite different network topologies on the stability of the banking system.

We would like to stress that both the network structures as well as the distributions are standard choices, whereas reality might differ greatly. The different structures and distributions are intended to show that predictions of the mean-field model are robust for a variety of assumptions. If not stated otherwise, the parameter values used to initialize the simulation model can be found in Table 5.1.

5.2 Random Distributions

5.2.1 Normal and Student’s t Distributions

The effects of different underlying location-scale distributions are illustrated in Figures 5.1 and 5.2. The underlying network structure of the exposure network is, in both figures, an Erdős-Rényi network.

In Figure 5.1, we report the average simulated fraction of surviving banks against $(\mu_L - \mu_A)/(\sigma_A^2 + \sigma_L^2)^{1/2}$ and the fixed point solution of the iteration map, Eq. 3.15 (black line) against $a' - b'$. For the simulated fraction, we varied μ_L and for the fixed point solution, we changed a' to satisfy $(\mu_L - \mu_A)/(\sigma_A^2 + \sigma_L^2)^{1/2} = a' - b'$. For each μ_L , the simulation was repeated 100 times. In the figure, symbols represent average fractions and vertical error bars are the standard deviations from the 100 simulations. To test the behaviour of the simulation for different fractions of average interbank loans, we changed θ from 0.0 (blue line), to 0.1 (red line) and 0.3 (green line). To compute the equivalent fixed point solution for each value of θ , we use Eqs. 3.20 and 3.21 to compute a' and b' . The critical value for b' for the Normal distribution is $b_c = \sqrt{2\pi}$. For the Student’s t distribution with 2 degrees of freedom, the critical value for b' is reached when $b_c = 2^{3/2}$ (see Tables 4.1 and 4.4). Hence, $\theta = 0.1$ leads to a value of interbank

¹Note that this method is not the core-periphery algorithm as proposed by Craig and Von Peter (2010).

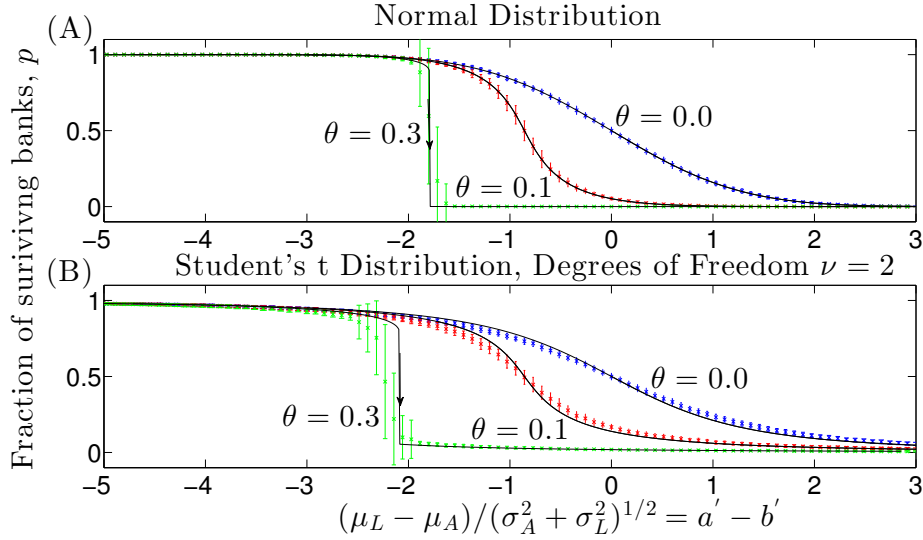


Figure 5.1: The figure shows the fraction of surviving banks, p , evaluated by initializing the liabilities and assets of banks' balance sheets with Normal distributions (A) and Students't distributions with 2 degrees of freedom (B) with varying location, μ_L , and scale parameter, σ_L , for liabilities, fixed location μ_A and scale parameter, σ_A , for assets plotted against $(\mu_L - \mu_A)/(\sigma_A^2 + \sigma_L^2)^{1/2}$. Each symbol is the average of the fraction of surviving banks of 100 simulations. The error bars are the standard deviation of the 100 simulations. To compute the blue line, we set the average fraction of interbank loans to zero, i.e. $\theta = 0.0$, for the red line θ was set to 0.1 and for the green line θ was set to 0.3. The underlying structure of the exposure networks are Erdős-Rényi networks. The black lines accompanying each plot are the fixed points of the iteration map, Eq. 3.15 plotted against $a' - b'$ which is equal to $(\mu_L - \mu_A)/(\sigma_A^2 + \sigma_L^2)^{1/2}$. Note that b' is changed to fit the equivalent θ value. A steep decline in the fraction of surviving banks happens when θ equals to 0.3 in the area of the predicted jump. For θ equal to 0.0 and 0.1 the simulation result for both distributions are close to the fixed point solution of the iteration map, Eq. 3.15. The parameter values used to initialize the system are stated in Table 5.1.

assets of bank i below the critical value and, conversely, setting $\theta = 0.3$ creates a value of interbank assets above the critical value, where a jump becomes visible.

The difference between Figures 4.4 and 5.1 is that in order to compute the fixed point solution in Figure 4.4, the total assets of the banks are varied since the location parameter of non-interbank assets is constant and a change in b' implies that either capital is changed to compensate a decrease or increase in total assets, or q , μ_L , μ_A , σ_L and σ_A change accordingly such that a' is constant. Whereas, in Figure 5.1, the location parameter of the total assets of banks is constant and a change in θ does not effect the size of the balance sheet. Hence, capital stays constant for fixed values of q , μ_L , σ_L and σ_A .

The fractions of surviving banks computed in Figure 5.1 uses Normal distributions

(*A*) and Student's *t* distributions (*B*) to initialize total assets and total liabilities. Similarly, to compute the fixed point solutions, we use a standard Normal CDF in *A* and a standard Student's *t* CDF in *B*. We use Normal and Student's *t* distributions as both distributions are location-scale distributions. Hence, we can compare the simulation results with the solutions of the iteration map, Eq. 3.15.

We note that for $\theta = 0.3$, more banks become insolvent for the same values of $q, \mu_A, \mu_L, \sigma_A$ and σ_L than when $\theta = 0$. The reason is that there exists no counterparty risk when $\theta = 0.0$. For both distributions a sudden decrease in the fraction of surviving banks is observed for $\theta = 0.3$. The jump starts earlier for the banking system with banks initialized with Student's *t* distributions than for banks initialized with Normal distributions. Also, the simulation results for a banking system initialized with Normal distributions are a closer fit to the fixed point solutions of the iteration map, Eq. 3.15, nonetheless the simulated results initialized with the Student's *t* distribution are also close to the fixed points. In the proximity of the jump, the standard deviation of the simulated fractions of surviving banks increases. This indicates that for the values of $q, \mu_A, \mu_L, \sigma_A$ and σ_L , at which the jump occurs, either most of the banks are operating or most of the banks are insolvent with no intermediate state.

To investigate this behaviour for parameter values close to the jump, we plotted the frequency distribution for fixed values of $q, \mu_A, \mu_L, \sigma_A$ and σ_L in proximity of the jump in Figure 5.2. We used different values of μ_L for the simulations when initializing with Normal distributions ($\mu_L = 890$) and Student's *t* distribution ($\mu_L = 870$). This is because of the jump starting earlier for the Student's *t* distribution than for the Normal distribution. The value for θ is set to 0.3 again. To determine the frequency distribution, we repeated the default algorithm for the fixed values of $q, \mu_A, \mu_L, \sigma_A$ and σ_L 10,000 times and sum the occurrence of the same equilibrium fraction of surviving banks. Subplot *A* shows the results for simulations using Normal distributions and subplot *B* shows the results for simulations using Student's *t* distributions.

For both distributions, two peaks occur. The peaks of the frequency distribution for a banking system initialized with Normal distributions occur around p close to zero and for p between 0.9 and 1.0. The first peak for the fraction of surviving banks for a banking system with balance sheets initialized with Student's *t* distributions happen between 0.03 and 0.15 and the second peak for values of p between 0.65 and 0.95.

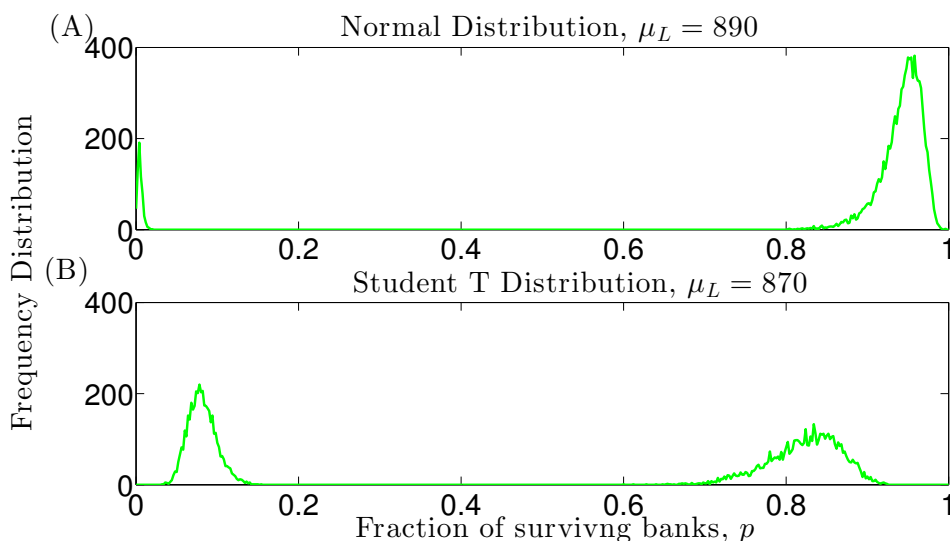


Figure 5.2: This figure shows the frequency distribution of fractions of surviving banks p for banks initialized with Normal (A) and Student's t distribution (B) for fixed values of $q, \mu_L, \mu_A, \sigma_L$ and σ_A . The fraction of interbank loans to total assets, θ , is set to 0.3 and the underlying structure of the exposure network is an Erdős-Rényi network. To observe the behaviour in the proximity of the jump the values for μ_L are set to 890 for the Normal distribution and 870 for the Student's t distribution. To compute the frequency distribution, we repeat the simulation 10,000 times. Two peaks occur because of perturbations of the balance sheet values due to the randomness. The two peaks are visible in both subplots at the end and beginning of the scale of p indicating that most of the banks in the banking system either survive or are insolvent. Intermediate fractions of surviving banks do not occur.

Values of fractions of surviving banks between the two peaks do not occur. The lack of intermediate values is due to the stable and unstable fixed points. The unstable fixed point forms a barrier between the stable fixed points. However, slight perturbations of the values of banks' assets and liabilities caused by the randomness of the simulation either tip the banking system into distress or survival.

The number of banks defaulting before the sudden system failure happens when initialized with Normal distributions and is less than for a banking system initialized with Student's t distributions. The Student's t distribution is a fat tail distribution implying that banks' balance sheets differ more than when the balance sheet values are distributed with a Normal distribution. Thus, after the jump some banks have a greater chance of survival, as they have more capital, than other members of the banking system. However, because of the greater diversity, some banks also have less capital than other banks, causing the system failure to happen for a smaller location parameter for liabilities in comparison to a more homogeneous banking system when initialized

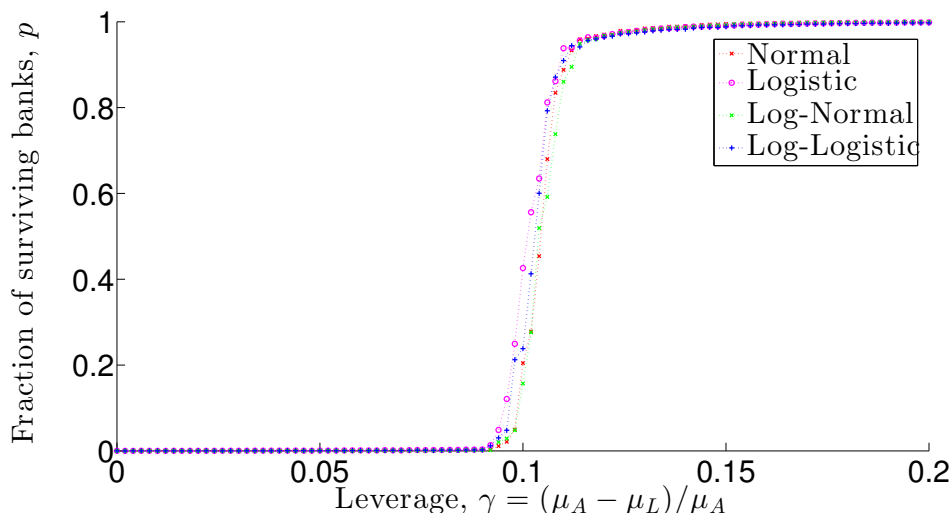


Figure 5.3: The figure shows the average fraction of surviving banks for varying leverage, $\gamma = \frac{\mu_A - \mu_L}{\mu_A}$, for banking systems initialized with Normal (red), Logistic (magenta), Log-Normal (green) and Log-Logistic (blue) distributions. We use 100 simulations to determine the average fraction of surviving banks. The means and standard deviation of the Normal distributions are: $\mu_A^N = 1000$, $\mu_L^N \in [800, 1000]$, $\sigma_A^N = 30$ and $\sigma_L^N = 50$. The ratio of interbank assets to total assets, θ , is set to 0.3 for all simulations. The input variables for the other distributions are calculated as stated in Table 5.2. The leverage, γ , is calculated using the input variables for the individual probability distributions. A steep decline of p occurs for all banking systems around similar leverage values of $\gamma = 0.1$. This indicates that the banking system is in the fragile state for these leverage values.

with Normal distributions. Thus, the more diverse system is more prone to failure but chances of survival of some banks are larger than for a more homogeneous banking system.

5.2.2 Non-Location Scale Distributions

To test the behaviour of a banking system calibrated with non location-scale distributions, we use Log-Normal and Log-Logistic distributions to initialize the balance sheets of banks. In addition to the Log-Normal and Log-Logistic distribution, we also provide the solutions for the fraction of surviving banks for banking systems calibrated with Normal and Logistic distribution. If a random variable X is drawn from a Normal or Logistic distribution, then $\exp(X)$ is the random variable of a Log-Normal or Log-Logistic distribution.

Figure 5.3 shows a plot of the average fraction of surviving banks, p , against leverage, $\gamma = \frac{\mu_A - \mu_L}{\mu_A}$, for Normal (red cross), Logistic (magenta circle), Log-Normal (green star) and Log-Logistic (blue cross) distributions. To produce the graphs in Figure 5.3,

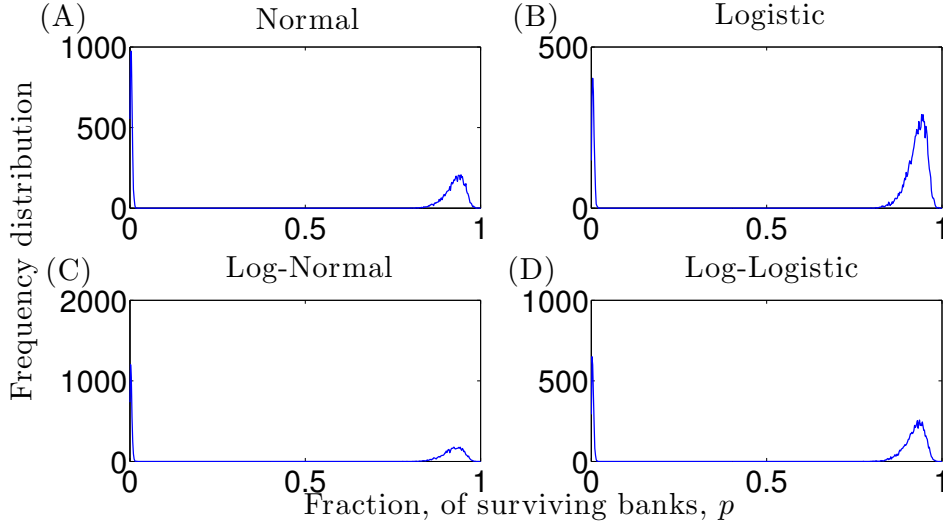


Figure 5.4: The figure shows the frequency distribution for the fraction of surviving banks, p , for banking systems initialized with Normal (A), Logistic (B), Log-Normal (C) and Log-Logistic (D) distributions. The parameters for the Normal distributions were chosen such that all distributions cause the banking system to be in the range of the fragile state. Namely, we fixed $\mu_L^N = 895$ and calculated the other input variables accordingly. As before, we used 10,000 simulations for each distribution to generate the frequency distribution. For each plot, two peaks occur close to $p = 0$ and $p = 0.8$, which shows that indeed the banking system is in the fragile state.

the mean, $\mu_{A,L}^N$, and standard deviation, $\sigma_{A,L}^N$, of Normal distributions are used to calculate the input variables for the other distributions using the formulas as stated in Table 5.2. This has the effect that the samples of banks' balance sheets have the same arithmetic mean and standard deviation for the different random distributions. The average was taken over 100 simulations. The leverage is calculated using the input variables for the specific random distribution used to produce each graph, i.e. for simulations initialized with Log-Normal distribution, the leverage is: $\gamma = \frac{\mu_A^{LL} - \mu_L^{LL}}{\mu_A^{LL}}$.

For the simulations, we set $\mu_A^N = 1000$, $\mu_L^N \in [800, 1000]$, $\sigma_A^N = 30$ and $\sigma_L^N = 50$ and calculated the input variables for the other distributions. The ratio of interbank assets to total assets, θ , is set to 0.3 to ensure that the jump becomes possible. Finally, the underlying network structure is chosen to be an Erdős-Rényi network.

The fragile state in Figure 5.3 occurs for the distributions around a leverage of $\gamma = 0.1$. The banking system initialized with Normal and Log-Normal distributions are the first to default, followed by Logistic and Log-Logistic. That said, the difference between the values is marginal. To ensure that a jump from almost all banks solvent

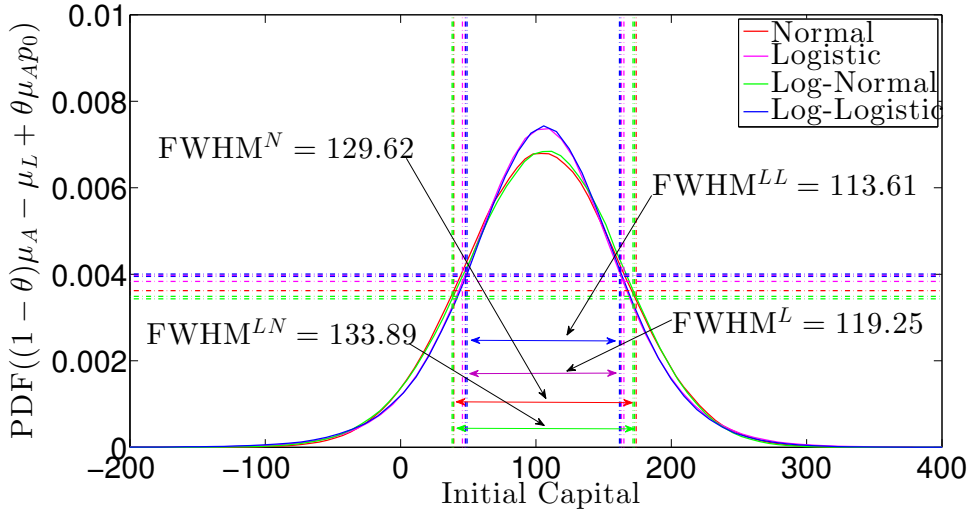


Figure 5.5: The figure shows the PDFs for the average initial capital of a bank given that the banking system is initialized with Normal (red), Logistic (magenta), Log-Normal (green) and Log-Logistic (blue) distributions. For the Normal distribution, the means and standard deviations are $\mu_A^N = 1000$, $\mu_L^N = 895$, $\sigma_A^N = 30$ and $\sigma_L^N = 50$. The input variables for the other distributions are based on the ones for the Normal distribution and calculated using the formulas in Table 5.2. All banks are assumed solvent initially, i.e. $p_0 = 1$. The FWHM for each PDF is also indicated by the vertical and horizontal, dotted lines and the double arrows. The Log-Normal distribution has the largest FWHM with $\text{FWHM}^{LN} = 133.89$, followed by the Normal distribution with $\text{FWHM}^N = 129.62$. The Logistic and Log-Logistic distributions have a FWHM of $\text{FWHM}^L = 119.25$ and $\text{FWHM}^{LL} = 113.61$. This implies that the initial capital for banks initialized with Logistic and Log-Logistic distributions are closer to the arithmetic mean than the initial capital of banks initialized with Normal and Log-Normal distributions.

to almost all banks insolvent happens, the frequency distributions are plotted for fixed $\mu_L^N = 895$ in Figure 5.4.

For all four distributions, two peaks occur close to $p = 0$ and $p = 0.8$ with intermediate values missing. Thus, the fragile state indeed occurs. The graphs suggest that for $\mu_L = 985$, the banking systems calibrated with Log-Normal distributions followed by Normal distributions are more likely to fail than systems calibrated with Logistic and Log-Logistic distributions.

Note that the scale parameters for the Normal ($\sigma = 58.3095$) and Logistic ($\sigma = 32.1477$) distributions differ. This has the effect that the arithmetic standard deviation of the samples of banks' balance sheets is similar and results in a slimmer PDF for the Logistic distribution than for the Normal distribution. The width of the PDFs of each distribution is further described in Figure 5.5. The figure shows the Normal (red),

Logistic (magenta), Log-Normal (green) and Log-Logistic (blue) PDF of $(1 - \theta)\mu_A - \mu_L + \theta\mu_A p_0$ (the initial average capital of a bank). To evaluate the Normal PDF, we fix $\mu_L^N = 895$, and calculate $\mu_{A,L}^{L,LN,LL}$ and $\sigma_{A,L}^{L,LN,LL}$ accordingly to retrieve the input variables for the other PDFs. The initial fraction of surviving banks, p_0 , is set to one.

The horizontal and vertical dotted lines indicate the position of the full width at half maximum (FWHM). The FWHM for the Normal distribution is $\text{FWHM}^N = 129.62$; for the Logistic, FWHM^L equals 119.25; for the Log-Normal, FWHM^{LN} is 133.89, and for the Log-Logistic, FWHM^{LL} equals 113.61. From the figure it becomes clear that the Log-Logistic and Logistic distributions are slimmer than the Normal and Log-Normal distributions. Hence, for a system initialized with Log-Logistic or Logistic distributions, more banks have initial capital closer to the arithmetic mean than in a system initialized with Log-Normal or Normal distributions. In systems initialized with Normal and Log-Normal distributions, there exist more banks with less initial capital that are more prone to failure. These banks start the insolvency at lower leverage values making the total banking system less stable.

5.3 Network Influence

5.3.1 Size of the Banking System, N

Figures 5.6 and 5.7 show the second norm of the difference of the fraction of surviving banks computed using the fixed points of the iteration map, Eq. 3.15 and the average fraction of surviving banks computed using 100 simulations. In the simulation, we use Erdős-Rény networks as underlying structures for the exposure networks, and Normal distributions for liabilities and assets with varying mean liabilities, μ_L . The ratio between interbank assets and total asset, θ , is set to 0.3. For this value of θ , b' is well above its critical value and a jump is predicted. For the fixed point equation a' is varied to balance the changes in μ_L in the simulation. The colour scale in Figures 5.6 and 5.7 reports the error (second norm) between the predicted values and the value achieved using the average from 100 simulations.

In Figure 5.6, the errors for different values of $N \in [11, 1000]$ are plotted. The connection probability α for the Erdős-Rény networks is changed such that the average degree for each N is $\bar{z} = 10^2$. To derive the fixed point solution for the iteration map,

²For an Erdős-Rény network, the average degree is $z = \alpha(N - 1)$.

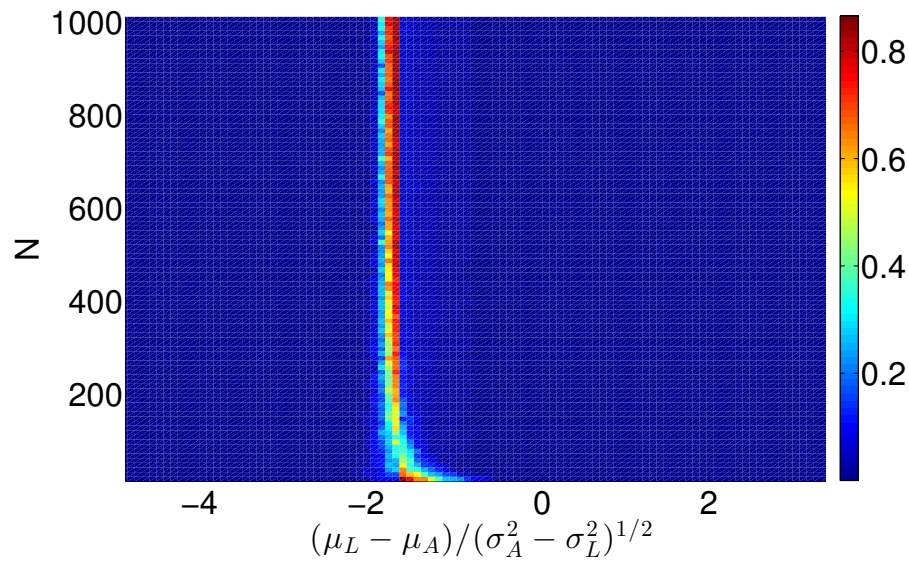


Figure 5.6: The figure shows the average error between the solution of the simulation and iteration map, Eq. 3.15 of the fraction of surviving banks for varying bank population, N . The figure reports the second norms of the difference between the fractions of surviving banks of the fixed point solutions of the iteration map, Eq. 3.15, and the fraction of surviving banks of an average of 100 simulations for fixed values $(\mu_L - \mu_A)/(\sigma_A^2 + \sigma_L^2)^{1/2}$. The exposure network structures are Erdős-Rényi networks. The connection probability for each population size is adjusted such that the average degree of a bank is $\bar{z} = 10$. Banks' balance sheets are calibrated using Normal distributions. An interbank exposure to total exposure $\theta = 0.3$ is used. To test the influence of the size of the banking system, the number of banks N is varied between [11, 1011].

Eq. 3.15, we assume that N tends to infinity. Nonetheless, Figure 5.6 indicates that the number of banks, N , does not affect the outcome of the simulation much. The error close to the jump for $N < 150$ is visible for a wider range of μ_L . For larger N , the error only becomes large close to the jump. For the same amount of average capital in the system, the randomness allows for capital to vary among banks in the simulation model. Close to the jump, this implies that small perturbation in banks' individual capital ensures a stable banking system, whereas in other cases the banking system collapses (see Figures 5.2 and 5.4). Hence, close to the jump predicted in the iteration map, Eq. 3.15, the error is the largest.

5.3.2 The Average Degree, \bar{z}

In Figure 5.7, the errors for different connection probabilities α are plotted for a banking system with $N = 500$. As expected, close to the jump the error is large but becomes

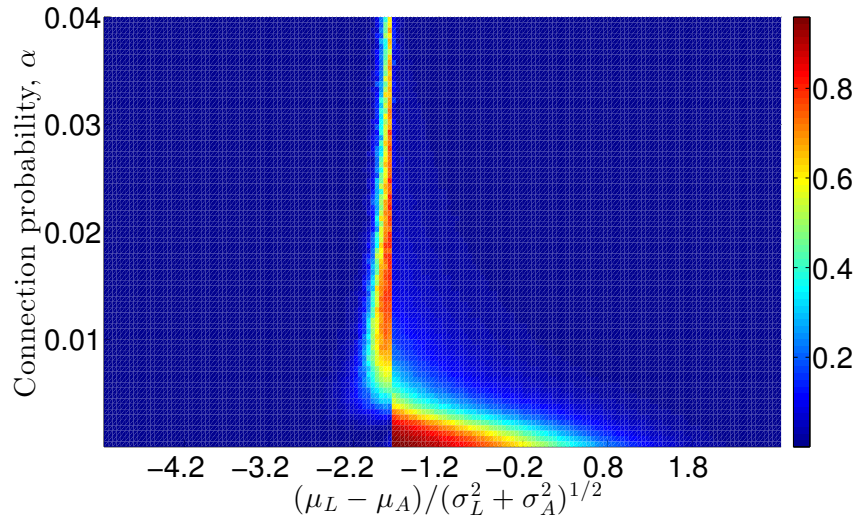


Figure 5.7: The figure shows the average error between the solution of the simulation and the iteration map, Eq. 3.15, of the fraction of surviving banks for varying average degrees of banks in the exposure network. The figure reports the second norm of the difference between the average fraction of surviving banks of the fixed point solutions of iteration map, Eq. 3.15, and the fraction of surviving banks of 100 simulations for fixed values $(\mu_L - \mu_A)/(\sigma_A^2 + \sigma_L^2)^{1/2}$ (changing μ_L for different simulations) and $a' - b'$ (changing a' for different fixed points). The simulation assumes Normal distributions for the balance sheet values, and for the structure of the exposure network, Erdős-Rényi networks with connection probability α and fraction of interbank loans to total assets $\theta = 0.3$ are used. To test the influence of the number of links from one bank to others, α is varied in $(0, 0.1]$.

smaller the larger the average degree \bar{z} in the exposure network. However, for α smaller than 0.03, a large error is also observed. This is because in that region the jump is only marginal or does not occur in the simulation, implying that due to the smaller number of links, the insolvency distribution and subsequent cumulative counterparty losses via the network are not realized.

We note that large errors happen in a range close to the jump for connection probabilities α smaller than $8 \cdot 10^{-3}$. In that region, the average degree \bar{z} of a bank is between 0 and 4 for $N = 500$. For $\alpha < 10^{-3}$, the jump is not observed or it is not very dominant in the simulation testing. The amount loaned from one bank to others is still $\theta A_i(0)$. However, it was shown in Chessa et al. (1998) and Barrat et al. (2008) using simulation means that the upper critical Euclidean dimension for the mean-field assumption of the Ising model is 4. Thus, it becomes clear that the mean-field approximation does not capture the behaviour for average degrees smaller than 4 and further investigation needs to be done into whether an average low number of counterparties in a banking

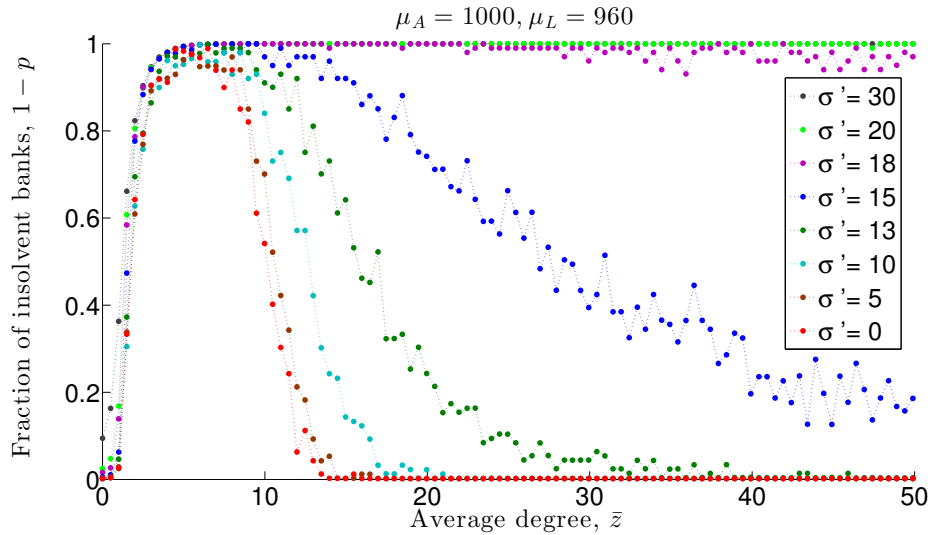


Figure 5.8: The figure shows the average fraction of insolvent banks, $1 - p$, against the average degree, \bar{z} , of the interbank network for different σ . The fraction of insolvent banks is determined using 100 simulations. Banks' balance sheets are initialized using Normal distributions and fixed values of $\mu_L = 960$ and $\theta = 0.3$. The underlying topology of the interbank network is an Erdős-Rényi network. The connection probability α is varied in $[0, 0.5]$. The variance σ is changed for each graph from 0 to 30 ($\sigma_L = 0$ and $\sigma_A = \sigma$). The parameter values used to initialize the banks result in an unstable solution for the mean-field model. However, it can be observed that for decreasing σ , the fraction of insolvent banks decreases for increasing \bar{z} .

system reduces the risk of a systemic stress event.

5.3.3 The Influence of the Variance, σ , on Diversification of Interbank Assets

To test the influence of the variance, σ , we plotted the average fraction of insolvent banks, $1 - p$, against the average degree, \bar{z} , for different values of σ in Figure 5.8. The graphs in Figure 5.8 are the averages of 100 simulations. The topology of the underlying exposure network resembles an Erdős-Rényi network and the random distributions used to initialize the balance sheets are Normal distributions. The simulations are initialized with fixed $\mu_L = 960$ and $\theta = 0.3$. The connection probability, α , is varied in $[0, 0.5]$. The variance, σ , is changed from 0 to 30 for each graph as indicated in the legend. To be more specific, σ_L , is set to zero, and σ_A equals σ .

We use $1 - p$ in this figure to have the same representation as in Gai and Kapadia (2010). In Gai and Kapadia (2010), they test the same contagion algorithm as presented in this thesis. However, in their initialization process, all banks have the same value of total assets, liabilities and capital. They also use Erdős-Rényi networks to initialize

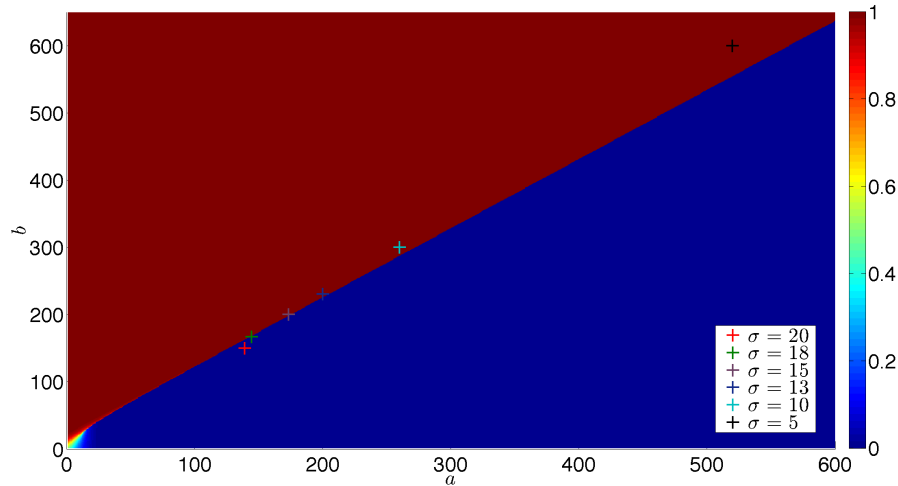


Figure 5.9: The figure is similar to Figure 4.5 showing the fraction of surviving banks, p , for different values of a and b given $p_0 = 1$. In addition, we also plotted the equilibrium solution of the fraction of surviving banks corresponding to the values archived in Figure 5.8 for different values of $\sigma = [20, 18, 15, 13, 10, 5]$. It becomes clear that for σ larger than 15, p is in the stable region, whereas for σ larger smaller than 15, p is in the unstable region.

their exposure networks. The interbank assets in Gai and Kapadia (2010) are, as in this study, a fraction of total assets, and a single weight from a bank i to another bank has the value: $\frac{\theta A_i}{z_i}$. To summarize, in Gai and Kapadia (2010), σ is zero and the balance sheets of banks are identical except the exposure from one bank to another, which depends on the out-degree of each individual bank.

The increased fragility of the banking system for increasing σ can be explained using Figure 5.9. Figure 5.9 shows a plot similar to Figure 4.5. It depicts the fraction of surviving banks for given a and b . Additionally, we plotted p for a and b using the same parameters as used to created the graphs in Figure 5.8 as indicated by the legend. For σ larger than 15 the equilibrium fraction of surviving banks is above a_2 . However, for σ below 18, the equilibrium fraction of surviving banks is below a_2 in the stable region.

For \bar{z} increasing and small σ , the fraction of insolvent banks decreases as well. Reducing σ causes the balance sheets of banks to be more alike. If $\sigma = 0$, each bank has the same amount of capital initially. The randomness in the system is caused by the distribution of the degree of the underlying exposure network. In the simulation model for $\sigma = 0$, the exposure leaving bank i to any loaner bank j is given as $\theta A_i(0)/z_i$. Thus,

for bank i to be vulnerable in round r (assuming that bank i withstands insolvency until round r) at least one counterparty of bank i needs to be insolvent. Additionally, given that bank i is only connected to one insolvent bank, the capital of bank i in round r , $E_i(r) = A_i(r) - L_i$, needs to be less than $\theta A_i(0)/z_i$ for bank i to become insolvent.

Let us consider the parameter values used to initialize the simulation in Figure 5.8 and set $\sigma = 0$. That implies that all banks have the same amount of total assets, initially, namely $A_i(0) = 1000$. The capital in round $r = 0$ of a solvent bank i is 40 and the single weight of exposure from bank i to bank j is: $300/z_i$. Thus, for $z_i = 7$, an insolvent counterparty bank j will cause insolvency to bank i since the exposure of bank i to bank j is 42.9, greater than bank i 's capital. However, for $z_i = 8$, bank i needs to be connected to more than one insolvent bank to become insolvent itself.

Hence, assuming all banks i have the same amount of balance sheet quantities, this implies that the larger the degree of a bank i , the more secure bank i is from counterparty failure. Furthermore, any cascades will eventually stop, since only banks with small out-degrees are affected by counterparty default and the network effects can be disregarded. This is in accordance with the results in Gai and Kapadia (2010).

If the balance sheet parameters are also random variables, then the amount of capital distributed among banks also differs. This causes the variance of loss-absorbing capital for banks to be greater with some being more prone to failure than others. Therefore, the cumulative losses increase as the likelihood of banks being connected to an insolvent bank increases (and even more so the larger the number of counterparties). This result is in accordance with Battiston et al. (2012a) and Battiston et al. (2012b), where they tested the banking cascade model in Gai and Kapadia (2010) using random variables for the balance sheet parameters. They also observe that for an increase in σ , counterparty insolvency continues to propagate through the network with large average degree.

Thus, it can be argued that for a highly homogeneous banking system counterparty risk can be lowered by diversifying interbank exposure. Whereas, for a more heterogeneous system, where banks have different levels of loss absorbing capital, diversification does not necessary make the system more stable.

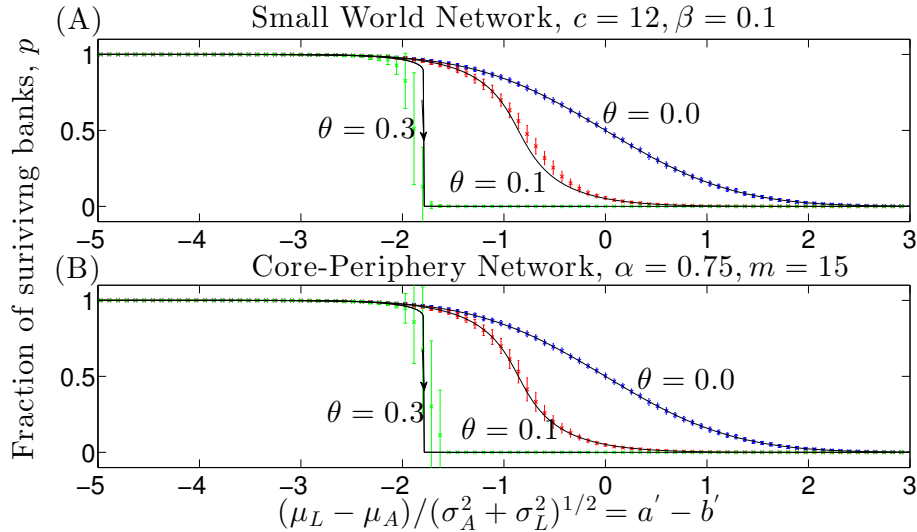


Figure 5.10: The figure shows the average fraction of surviving banks, p , computed using 100 simulations plotted against $(\mu_L - \mu_A)/(\sigma_A^2 + \sigma_L^2)^{1/2}$. The balance sheet values are normally distributed. The underlying structure of the exposure networks are Small-World with neighbouring nodes $c = 12$ and a re-wiring probability β set to 0.1 (A) and core-periphery networks with a strongly connected core created using Erdős-Rényi networks with connection probability $\alpha = 0.75$ and 50 banks, and 450 periphery banks that are added one by one and joined to the 50 already existing banks using the preferential attachment algorithm. As in Figure 5.1, for a fraction of interbank assets to total assets, $\theta = 0.3$, p is plotted using green symbols; for $\theta = 0.1$, we used red symbols; and for 0.0, blue symbols were used. The error bar is the standard deviation of the results of 100 trials. The black line represents the fixed points of the iteration map, Eq. 3.15, plotted against $a' - b'$ for changing θ as used in the simulation. The values of p for the simulation and the iteration map, Eq. 3.15, are for both network structures close and the steep decrease in the proximity of the jump are for both network structures observable.

5.3.4 Network Topology

Interbank networks of various countries (Austria (Boss et al., 2004), Brazil (Cont et al., 2010), UK (Langfield et al., 2014), Italy (Iori et al., 2008), etc.) have been studied with the outcome that the networks do not resemble Erdős-Rényi networks. Instead, they consist of “low clustering coefficients with short average path length” (Boss et al., 2004) and the links in the interbank networks resembling the exposure from one bank to others are distributed with tails exhibiting “a linear decay in log-scale, suggesting a heavy Pareto tail” (Cont et al., 2010) indicating a core-periphery structure with banks in the centre being highly connected and periphery banks being connected to core banks (Viegas et al., 2013).

In Figure 5.10, we test the influence of other exposure network structures than the Erdős-Rényi network. The distributions used to initialize the balance sheets for

both subplots are Normal distributions. The structure of the outline of Figure 5.10 is similar to the one in Figure 5.1. Again, we plotted the average fraction of 100 trials of surviving banks for a θ of 0.3 (green line), 0.1 (red line) and 0.0 (blue line) against $(\mu_L - \mu_a)/(\sigma_A^2 + \sigma_L^2)^{1/2}$ varying μ_L . The black lines are the solution of the fixed points of Eq. 3.15 for changing b' to match the equivalent value of θ . Plot *A* shows the results given that the underlying exposure network has a Small-World structure and in plot *B*, the underlying exposure network structure uses the preferential attachment algorithm to create a core-periphery structure. To tightly connected core banks, we used Erdős-Rényi core networks made out of 50 banks with a connection probability α of 0.75. The remaining 450 periphery banks are added one-by-one connecting to 15 banks using the preferential attachment algorithm.

As shown in Figure 5.10, the simulation results using both network structures are close to the fixed point solutions of the iteration map, Eq. 3.15, with a steep decline in surviving banks for $\theta = 0.3$. The steep decline of p , when the Small-World network is used, starts a bit earlier than the predicted jump in the mean-field model. Before the rewiring process, the Small-World network is an ordered lattice. The Ising model on an ordered lattice can be approximated using the mean-field solution as long as the number of close neighbours is larger than 4. The re-wiring creates long-distance links between banks, distributes the shock quicker through the network.

Thus, it can be said that the network influence is marginal given that the number of lending banks is large enough. This can be explained using the results in Section 4.2. There, we showed that when $p_r = x_1$ (and assuming a small change from p_r to p_{r-1}) and $a = a_2$, the average number of banks failing as a result of one insolvent bank is one again. Therefore, this implies that when capital is low the insolvency of one bank causes a chain of insolvencies in connected banks resulting in distress throughout the entire system. This implies that the network structure is secondary in the distribution of insolvencies. However, it has been reported that in the real world networks, periphery banks are of smaller size than core banks, which we did not account for and might lead to a different result.

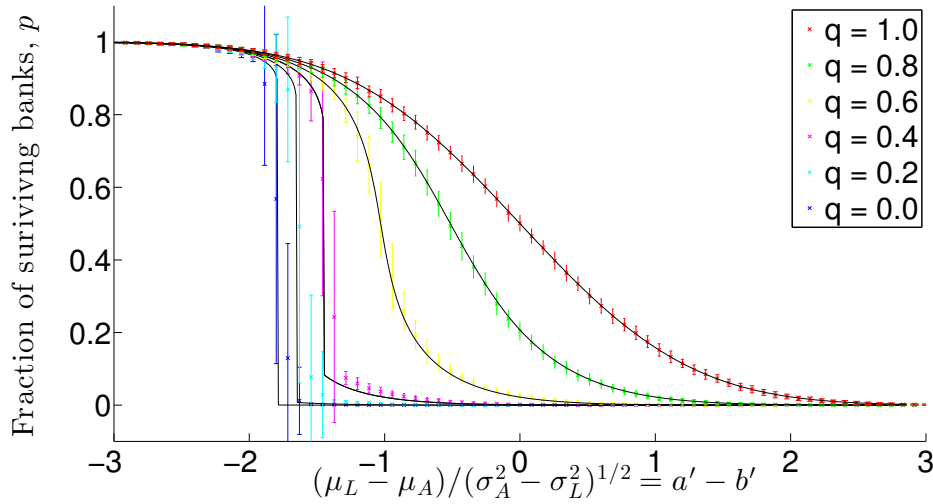


Figure 5.11: The figure shows the average fraction of surviving banks p computed using 100 simulations plotted against $(\mu_L - \mu_A)/(\sigma_A^2 + \sigma_L^2)^{1/2}$. The balance sheet values are normally distributed. The underlying structure of the exposure network is an Erdős-Rény network. A collateral term, a recovery rate q , was added when the total assets were computed during simulation modelling. The collateral on loans becomes active after the counterparty becomes insolvent. The black line represents the fixed points of the iteration map, Eq. 3.15. The fixed points are plotted against $a' - b'$ ($\theta = 0.3$ was used in the simulation). The different coloured lines represent varying fractions $q \in [0, 1]$. The value of the collateral for any loan from bank i to bank j is $q\theta A_i g_{ij}$. For increasing q , the interbank interaction is reduced such that for $q = 1$ the interbank loans can be disregarded.

5.4 Recovery Rate

Figure 5.11 is a plot of the fraction of surviving banks, p , using simulation testing including the recovery rate and the fixed point solution of the iteration map, Eq. 3.15. The average fraction of surviving banks was plotted for 100 trials along with the error bars (coloured lines) for fixed $\theta = 0.3$. As in the plots before, μ_L is varied in the simulation and a' is changed accordingly in the mean-field model. The black lines are the fixed point solutions of the iteration map, Eq. 3.15. The different colours represent varying fractions of $q \in [0, 1]$. For increasing q , the interaction in form of interbank loans between banks can be disregarded. However, for lower values of q , the jump can still be observed. This can be explained using the critical value of the ratio of interbank assets to total assets, θ_c , which increases for increasing q . In fact, if q tends to one, banks do not have any losses to compensate when counterparties fail. Thus, unsurprisingly, a large q diminishes the importance of counterparty risk.

In the literature on recovery rates (Bruche and González-Aguado, 2010), it has

been observed that the value of recovery rates fluctuates with economic cycles. During a downturn the recovery rates are usually lower than when the economic cycle is in an upturn. According to Bruche and González-Aguado (2010), the recovery rates for bonds of US companies range between 0.15 to 0.80.³ In Fleming and Sarkar (2014), it is stated that the recovery rate of Lehman Brothers was estimated to be 0.28. They further say: “The settlement of OTC [Annot.: over the counter] derivatives was a long and complex process...” and that “the Lehman estate was able to make the first distribution to creditors [Annot.: OTC derivatives contracts with big bank counterparties] on April 17, 2012.” Thus, it is fair to assume that the instantaneous recovery rate is much lower. Hence, a jump in a real economic setting with positive recover rates is still feasible. However, the economic conditions need to be dire, allowing for low recovery rates, and a considerable loss in the value of assets or increase in the cost of funding.

5.5 Changes in Liabilities and Assets During the Insolvency Propagation

To investigate the impact of changes in liabilities and assets during the insolvency propagation, we apply Eqs. 3.23 ($\hat{A}_i(r+1) = \exp(-\kappa(1-p_r))\hat{A}_i(r)$) and 3.24 ($L_i(r+1) = (1-\kappa)L_i(r)$) to the simulation model. We use Normal distributions to initialize the balance sheet quantities and say the underlying network structure resembles an Erdős-Rényi network with $\theta = 0.3$.

To investigate the effects of reducing the value on non-interbank assets proportional to the fraction of insolvent banks, $1 - p_r$, in round r , we adopted the insolvency algorithm from Chapter 3 slightly. In particular, Eq. 3.23 is applied after the third step in the insolvency algorithm. That is, in round r we have:

- The current value of interbank assets, $A_i(r)$, is calculated for each bank i using Eq. 3.22.
- For all banks i with $A_i(r) - L_i < 0$, the state, $S_i(r)$, of bank i set to zero.
- The number of solvent banks is counted and divided by N to obtain the fraction of solvent banks, p_r , in round r .

³They used the Altman-NYU Salomon Center Corporate Bond Default Master Database to extract the recovery rates.

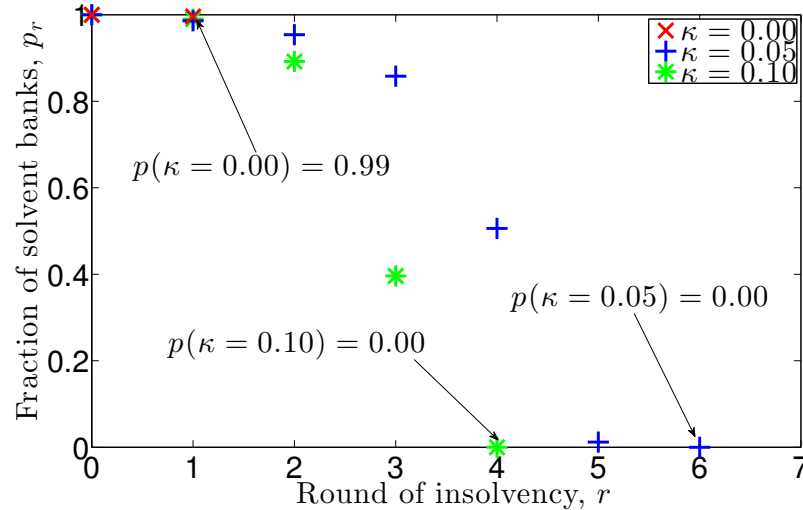


Figure 5.12: The figure shows the fraction of solvent banks, p_r , against r for one simulation run given that in each round r , the non-interbank assets, $A_i(r)$, are reduced by $\exp(-\kappa(1 - p_r))$ as outlined in Eq. 3.23. The parameters to initialize the balance sheets are chosen such that only a small number of banks become insolvent initially but the overall system stays stable ($\mu_L = 860$). For each graph the constant, κ , is changed from zero (magenta x), to 0.05 (blue cross), to 0.10 (green star). For $\kappa = 0.00$, as expected, the equilibrium solution of surviving banks is $p = 0.99$. However, for $\kappa = 0.05$ and $\kappa = 0.10$, the system defaults with $p = 0$.

- The value of non-interbank assets, $\hat{A}_i(r)$, is calculated for each bank i according to Eq. 3.23.
- The iteration is repeated until no further bank becomes insolvent.

Figure 5.12 shows the fraction of solvent banks, p_r , in round r plotted against round r . To create the plot, the location parameter of the liabilities is chosen such that the banking system is stable when disregarding a reduction in the value of assets, i.e. $\mu_L = 860$. To be more precise, only a few banks become insolvent and the majority of banks stay stable. The ratio of interbank assets to total assets is set to $\theta = 0.3$. Figure 5.12 consist of three graphs representing the fraction of solvent banks, p_r , in round r computed using one simulation run. For each graph the constant, κ , is changed from zero (magenta x), to 0.05 (blue cross), to 0.10 (green star). For $\kappa = 0$, non-interbank assets do not lose in value and most banks in the banking system survive with the equilibrium fraction of surviving banks being $p(\kappa = 0) = 0.99$ in round $r = 1$. Increasing κ to 0.05 and 0.10 results in a reduction of the value of interbank assets. This causes the banking system to become unstable with the equilibrium fraction of surviving banks for $\kappa = 0.05$ and $\kappa = 0.10$ being $p(\kappa = 0.05, \kappa = 0.01) = 0.00$.

The reduction in non-interbank assets results in a greater loss in capital and moves the system into the unstable region eventually.

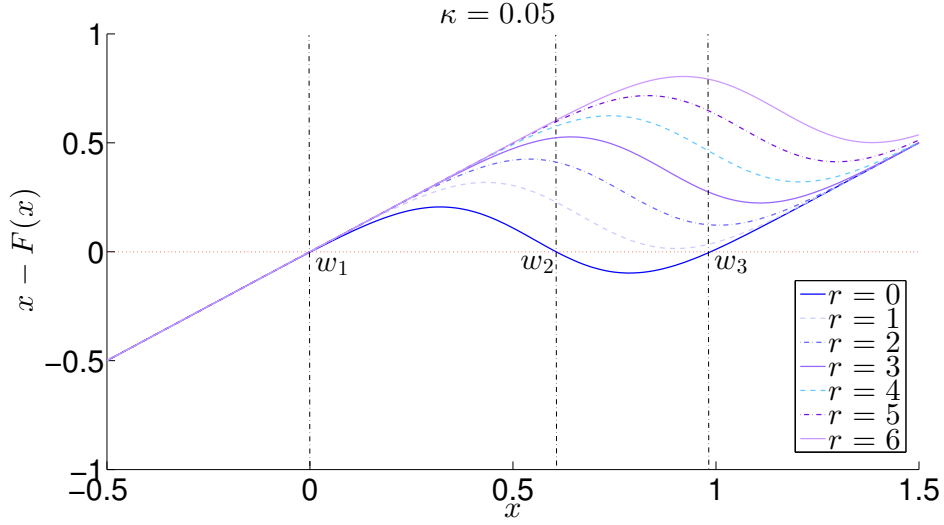


Figure 5.13: The figure shows multiple plots of $x - F(x)$ against x . The values for $a''(r)$ and b' are calculated using Eqs. 3.21 and 5.1. Because of the reduction term, $\exp(-\kappa(1 - p_r)) \frac{\sum_{i=1}^N \hat{A}_i(r)}{N}$, in Eq. 5.1 the value for $a''(r)$ changes for each insolvency round, r . This causes $x - F(x)$ to shift upwards for each r . For $r = 0$, $x - F(x|a''(0))$ has three roots, w_1, w_2 and w_3 , which are the fixed points of $p_{r+1} = F(p_r|a''(0))$. For $r \leq 1$, $p_{r+1} = F(p_r|a''(r))$ has only one fixed point close to zero. Hence, a reduction in non-interbank assets resulted in an unstable banking system.

We visualized in Figure 5.13 the change of the system from a stable to an unstable system conditional on the reduction. Figure 5.13 shows multiple plots of $x - F(x)$ against x . To calculate b' , we used Eq 3.21. However, because of the asset reduction function, Eq. 3.23, we adopted the formula for a' , Eq. 3.20, to (assuming $q = 0$):

$$a''(r) = \frac{-\exp(-\kappa(1 - p_r)) \frac{\sum_{i=1}^N \hat{A}_i(r)}{N} + \mu_L}{\sqrt{\sigma_A^2 + \sigma_L^2}}, \quad (5.1)$$

i.e. we changed the term $(1 - \theta)\mu_A$ to $\exp(-\kappa(1 - p_r)) \frac{\sum_{i=1}^N \hat{A}_i(r)}{N}$. Note that $\frac{\sum_{i=1}^N \hat{A}_i(r)}{N}$ is the arithmetic mean of the non-interbank assets, $\hat{A}_i(r)$, for all banks i in round r . Thus, we say $a''(r)$ changes in time. It should be noted that the value for the non-interbank assets, $\hat{A}_i(0)$, for a bank i is specific for each simulation and changes for each simulation run. To produce the graphs in Figure 5.13, we used the same values for $\hat{A}_i(0)$ as were used in the banking system to produce the fractions of solvent banks, p_r , in Figure 5.12 for $\kappa = 0.05$. Hence, $a''(r)$ differs for each graph in Figure 5.13

resulting in an upwards shift of the graphs of $x - F(x|a''(r))$. The legend indicates the round of insolvency for each graph.

For $r = 0$ (dark blue line), $x - F(x|a''(r))$ has three roots. Hence, the iteration map, $p_r = F(p_{r-1}|a''(0))$ has three fixed points, w_1, w_2 and w_3 . For reasons outlined in Chapter 4, w_1 and w_3 are stable fixed points and w_2 is an unstable fixed point forming a barrier between the two stable fixed points. Note also that w_1 is slightly smaller than one. Thus, for all banks solvent initially ($p_0 = 1$), some banks become insolvent in the initial round ($r = 0$). This has the effect that the non-interbank assets are reduced and $a''(1)$ increases. The increase in $a''(1)$ causes $x - F(x|a''(1))$ to shift upwards. Because of the shift, $x - F(x|a''(1))$ only has one root, namely w_1 , which is the stable fixed point of $p_r = F(p_{r-1}|a''(1))$. In fact, for any $a''(r)$ for $r \leq 1$, $p_r = F(p_{r-1}|a''(r))$ has only one fixed point. The fixed point w_1 is zero for all $a''(r)$ with $r \leq 1$. This implies that for any $r \leq 1$, the reduction in non-interbank assets results in system failure for $\kappa = 0.05$.

In Figure 5.14, we test for the influence of a capital injection into an unstable system. Because of that, the parameters are chosen such that the banking system collapses given $\kappa = 0$, i.e. $\mu_L = 890$ and $\theta = 0.3$. To be more precise, we adopt the insolvency algorithm stated in Chapter 3 and reduce the liabilities in a particular round r by applying Eq. 3.24 to the liability side of banks' balance sheet. That is, for each bank i , $L_i(r+1)$ is a fraction $(1 - \kappa)$ of $L_i(r)$. Figure 5.14 shows the fraction of solvent banks, p_r , against round r . For each graph, we reduced the value of liabilities in round r as specified in the accompanying legend. For example, for the graph represented by the magenta triangles, the liabilities were reduced in round $r = 7$. Additionally, we marked the fraction of solvent banks at the point right before the liabilities are reduced. To be more precise, for a reduction in liabilities at $r = 7$, the fraction of solvent bank before the reduction is $p_{r=7} = 0.05$.

The graphs show that if a reduction of 5% in the value of liabilities takes place before the 6th iteration step, the banking system returns to almost all banks solvent again. However, if the reduction in liabilities takes place after the 6th iteration step, all banks become insolvent. Note that we did not plot average solutions but only the solution of a single simulation. Hence, depending on the initial distribution of balance sheet quantities and the underlying network structure, a system might be rescuable after the 6th iteration or doomed to default before the 6th iteration step. Nonetheless,

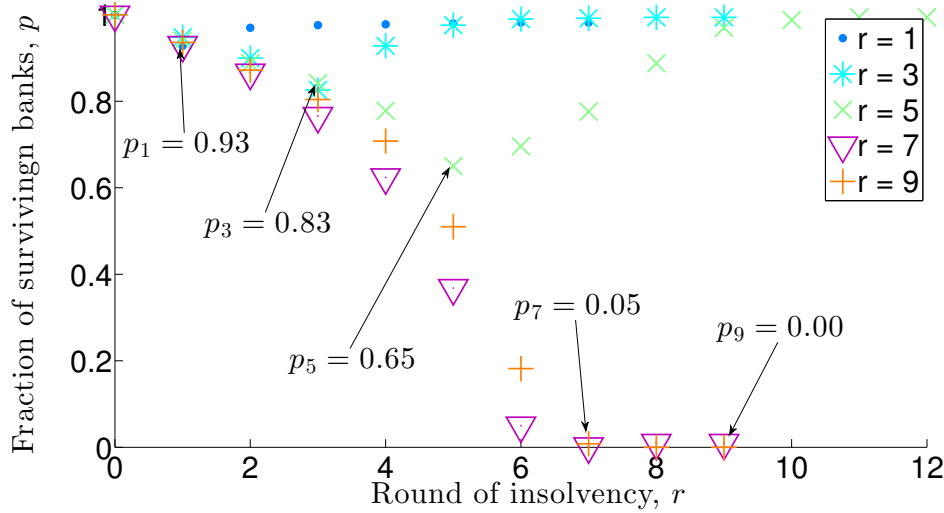


Figure 5.14: The figure shows the fraction of solvent banks, p_r , against round r . To produce the graphs, the liabilities, $L_i(r)$, of each bank i are reduced by a fraction $1 - \kappa$ in round r . The legend indicates the specific round, r , in which liabilities are reduced. Additionally, we marked p_r for each simulation before reduction in liabilities takes place. For liability reductions in round $r = 1, \dots, 5$, the banks in the banking system return to normally operating. For $r = 7, 9$, all banks become insolvent.

it can be deduced from Figure 5.14 that there exists a point in the iterative process, at which a capital injection does not save the banking system even though the same capital injection could have rescued the banking system in earlier iteration steps.

This can be explained using Figure 5.15. In Figure 5.15, the function $x - F(x|a')$ is plotted twice against x . The difference in the two graphs is the parameter a' . For both graphs, the parameter b' is calculated using the values used to initialize the simulation model. However, for the solid line, we used the initial value of μ_L to calculate $a'_1 = 3.60$. For the dotted graph, $(1 - \kappa)\mu_L$ was used to calculate $a'_2 = 2.82$. The parameter $b' = 5.1$ is the same for both graphs. The vertical lines indicate x corresponding to the values of p_r before the reduction in liabilities. For example, the vertical magenta line ($x = 0.05$) corresponds to the fraction of solvent banks in round $r = 7$ for the magenta coloured triangle graph in Figure 5.14, i.e. $p_7 = 0.05$. The vertical black lines mark the position of the fixed points, w_1, w_2 and w_3 , of the iteration map $p_r = F(p_{r-1}|a'_2)$, which are the roots of $x - F(x|a'_2)$.

As can be deduced from the graphs in Figure 5.15, the reduction in capital causes the iteration map, $p_r = F(p_{r-1}|a')$, to change from one fixed point solution (for $a' = a'_1$) to three fixed point solutions ($a' = a'_2$). The fixed point, w_1 , for $a'_1 = 3.60$ is close

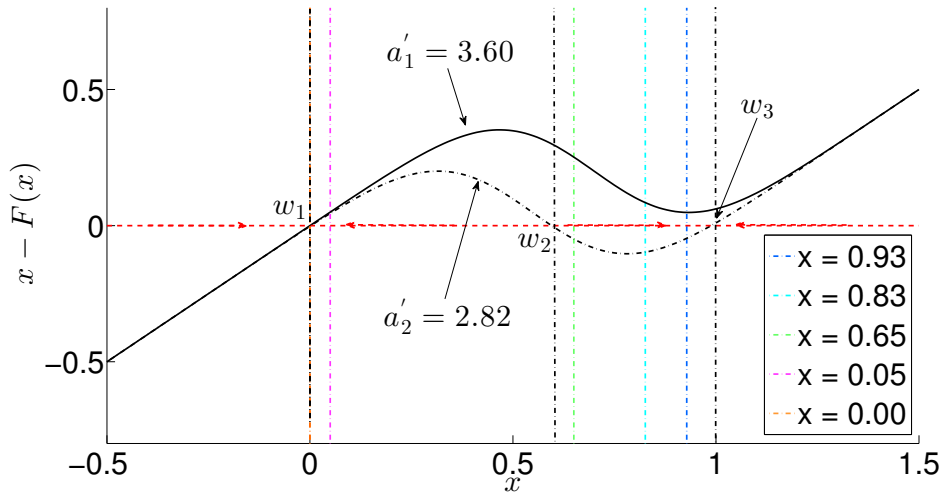


Figure 5.15: The figure shows two plots of $x - F(x|a')$ against x . The parameter b' equals 5.1. The parameter a' varies for the two graphs. For the solid black line we used $a'_1 = 3.60$. Whereas for the dotted black line a'_2 equals 2.82. The parameters a'_1 and b' are calculated using the values $q, \mu_A, \mu_L, \sigma_A, \sigma_L$ and θ to initialize the simulation model before the reduction in liabilities takes place. For the dotted black graph, b' stays the same. However, a'_2 varies because we used $(1 - \kappa)\mu_L$ for the average liabilities to represent the reduction in liabilities instead of μ_L . The black vertical lines represent the roots of $x - F(x|a_2)$, w_1, w_2 and w_3 . The coloured vertical lines are specific x values corresponding to p_r in Figure 5.14 before the liabilities are reduced.

to zero. The stable fixed points, w_1, w_3 , for $a'_2 = 2.82$ are close to zero and one. The unstable fixed point, w_2 , forms a barrier between the two stable fixed points around 0.6.

Therefore, without the reduction in liabilities, all banks in the banking system will become insolvent. However, if the liabilities are reduced in round r , instead of one orbit, the new iteration process has two orbits. For any starting value p_r in $[w_1, w_2]$, the fixed point reached is going to be w_1 ; and for any p_r in $[w_2, w_3]$, the fixed point reached is going to be w_3 . For example, for $p_{r=7} = 0.05$ the iteration process will stop at zero. Whereas, for $p_{r=6} = 0.65$, the system returns to normally operating again.

5.6 Conclusion

We conclude that the results of the mean-field model can be replicated using a simulation-based model for a variety of random distributions and banking system parameters. We determine that interbank networks are crucial to the distribution of counterparty failure, but the network structure is secondary for the onset of the insolvency propagation. We also show that diversification of interbank assets does not necessarily

reduce the risk of failure. Hence, monitoring precise exposure from one bank to another is not necessary. Instead, ratios of interbank assets to total assets should be monitored to guarantee financial stability. This is of interest as interbank exposure from one bank to another is not published by regulators. This is because the information contained in reports on interbank exposures collected by regulators is considered market changing. The conclusions of this chapter suggest that publishing information on the ratio of interbank assets to total assets is sufficient to monitor financial stability. It would allow other participants to obtain a better picture about banks' solvency. That said, we did not incorporate the importance of recovery rates other than using the same value for all banks or how maturity times for different financial products influence the solvency of banks. These should be checked before solely relying on the ratio of interbank assets to total assets as a measure of how counterparty failure influences financial stability.

Finally, we incorporate functions changing the time value of assets and liabilities in the simulation model and explain the observations in the setting of the mean-field model. The functions used are not realistic to model actual processes during a real financial crisis. The intention of using these functions was to show that value changes of assets and liabilities can be incorporated into the mean-field setting.⁴ Depending on the balance sheet values, the equilibrium solution of the counterparty risk model shifts. This potentially causes a seemingly stable system to move into an unstable region given reductions in banks' capital during the insolvency iteration. Furthermore, we find that because the equilibrium solution is history dependent, capital injections during the insolvency propagation might not have the desired effect of rescuing the banking system, even so the same amount of external capital would have caused the system to return to stability again at earlier iteration rounds.

⁴One assumption to derive the mean-field model is to keep the value of non-interbank assets and liabilities constant after the initial round of insolvency.

Chapter 6

Empirical Analysis of Counterparty Failure in the UK Banking System

Summary of the chapter: *In this chapter, we investigate the simulation-based model and the mean-field model using banking systems initialized with UK regulatory data. In the first part of this chapter, we conduct an analysis of bilateral exposure and balance sheet data of the UK banking system. We construct interbank exposure networks from the bilateral exposure data and apply network measures to obtain a better understanding of the topology of the banking networks. We observe that the UK banking system consists of banks varying greatly in the size of their balance sheets. Furthermore, large UK banks that operate globally can be found in the core of the interbank network with smaller regional operating banks in the periphery. In the second part of this chapter, the solutions of both the mean-field and simulation models are compared. We conclude that the simulation-based model of a highly heterogeneous banking system and the mean-field model, where we assume a homogeneous banking system, behave similar. To be more specific, we observe the occurrence of the fragile state in both models for similar sized shocks. We conclude the chapter by calculating the leverage requirements using the regulatory data.*

6.1 Data Analysis

6.1.1 Description of Regulatory Datasets

The dataset presented in this thesis consist of regulatory reports of UK banks to the BoE. In particular, we use regulatory reports on bilateral exposure data and balance sheet information to calibrate a simulation-based and mean-field model. The data was

collected at the end of 2011 (2011 H2), the end of 2012 (2012 H2) and the first half of 2013 (2013 H1). The exposure data are supplemented by balance sheet information obtained from the BoE for UK regulated banks. The balance sheet quantities relevant for calibrating the counterparty risk models are “total assets” and “Tier 1 capital”.

The datasets are classified due to their market changing nature. The results of the network and balance sheet analysis in Section 6.1.3 and 6.1.2, and simulations results presented in Section 6.3 were initialized and run by our collaborator at the BoE. We need permission from the BoE for publishing any information related to the two datasets. For this reason, we limit the data analysis to measures relevant to calibrate the counterparty risk models and to understand the cascade process.

The BoE supervises 176 UK consolidated banking groups. Each bank reports exposures by instrument to their top 20 bank and broker-dealer counterparties. If the top 20 do not have at least six UK-based counterparties, firms are asked to report exposures to up to six UK-based counterparties in addition to the top 20. Branches of foreign banking groups in the UK are not included in the data collection as their supervisory authority is not situated in the UK.¹ UK banks disclose their exposures to other banks and broker dealers by financial instruments. The financial instruments² reported include:

- Lending, unsecured, secured³ and undrawn;
- Holdings of equity and fixed-income securities issued by banks;
- Credit default swap, bought and sold;
- Securities lending and borrowing (net of collateral);

¹Because the 176 UK banks report their exposures to other global consolidated banking groups, there are 314 non-UK banks recorded in the dataset. These 314 non-UK banks do not submit their own exposures to the BoE and are only listed as counterparties of the UK banks. In this study, we consider the 176 UK regulated banks only and disregard the 314 non-UK banks when constructing the network since we do not have enough information on the exposure of non-regulated banks to UK regulated banks.

²Moreover, banks state exposures with breakdown by the maturity of the instrument. Categories of maturities are: open; less than three months; between three months and one year; between one year and five years; and more than five years. Derivatives are not reported with a maturity breakdown. Banks’ internal risk management limits, with respect to counterparties and instruments, are also supplied. However, for this study, we disregard any differences in maturity time and debt structure.

³Secured loans do not include reverse repurchase agreements, which have a different contractual nature. Secured loans are collateralised by various assets such as buildings, lands and other physical assets.

Table 6.1: The table reports the number of banks in the system. The first line indicates the total number of banks regulated by the BoE, which is the same for all years. Only banks are used for calibrating the counterparty risk models that belong to the largest connected component of the interbank network, have total assets larger than total liabilities, and banks where interbank assets and liabilities are larger than the recorded total assets and liabilities.

Year	Total No.	LB	BS	IB	OB	CB
All banks recorded	176	8	47	14	67	40
2011 H2	158	8	45	14	54	37
2012 H2	154	8	44	14	50	38
2013 H1	147	8	46	14	44	35

- Repurchase agreements and reverse repurchase agreements (net of collateral); and
- Derivatives exposures: The breakdown covers interest rate derivatives; credit derivatives; equity derivatives; foreign-currency derivatives; commodities derivatives; and other derivatives.

Finally, we use the BoE’s classification of banks into “Large Banks” (LB), “Building Societies” (BS), “Investment Banks” (IB), “Oversea Banks” (OB) and “Other Commercial Banks” (CB). The BoE’s classification groups banks into particular bank types with similar sized banks, or banks with similar business models belonging to the same bank type. The number of banks for each bank type are reported in Table 6.1, first row.

For the counterparty risk model, we only use banks that belong to the largest connected component of the network (see Section 6.1.3). Further, we restrict our investigation to banks, where the difference between assets and liabilities is positive. A negative difference can be a result of restructuring, insolvencies and other organisational events. Finally, we include only banks, where the value of interbank assets and interbank liabilities is smaller than the banks value for total assets and total liabilities. The reason for the discrepancy between interbank assets and liabilities, and total assets and liabilities is a result of combining the two datasets. When constructing the interbank network, we assume that any exposure to an international banking group is the exposure to the UK subsidiary. For example, any exposure to Santander Group is assumed to belong to Santander UK when the interbank network is constructed. In some cases the exposure reported to the international banking group exceeds the value of the total assets or liabilities reported by the UK subsidiary to the BoE. Hence, for some banks, OB in

particular, the interbank exposure exceeds the balance sheet values, and consequently, we exclude these banks from the model calibration. The total number of banks in the dataset and the number of banks used for model calibration, can be found in Table 6.1.

We must stress that combining the data for international banking groups and UK subsidiaries together with limiting the number of counterparties during reporting to the BoE results in a distorted replication of the real UK banking system.

6.1.2 Data Analysis of Balance Sheets

The balance sheet parameters needed to calibrate the counterparty risk model are: total assets and loss absorbing capital. In this thesis, we assume that Tier 1 capital is equivalent to loss absorbing capital.⁴ Liabilities of a bank, are computed as the difference between the value of total assets and Tier 1 capital.

Table 6.2: The table reports the average value of assets of banks of a particular bank type for the years 2011 H2, 2012 H2 and 2013 H1 in Mil. GBP. The STD is reported below in brackets. The STD are of the same order or larger than the mean values indicating that banks grouped in one bank type have balance sheets varying greatly in size.

Year	LB	BS	IB	OB	CB	Total
2011 H2	675855 (576078)	2707 (6487)	183337 (219105)	2695 (6752)	4901 (10528)	53305 (205547)
2012 H2	642503 (522503)	2881 (6949)	189115 (213583)	2594 (6199)	5371 (11667)	53560 (195977)
2013 H1	646177 (522810)	2809 (6881)	189152 (214470)	2928 (6766)	5529 (11317)	56252 (200985)

The majority of banks in the system are BS, OB and CB. LB and IB are the minority, but as we can see in Table 6.2, they have the largest balance sheets. Table 6.2 reports the mean values of total assets per bank type and standard deviations (STD) of assets (in Mil. GBP) as used in the model calibration. In terms of balance sheet size, the UK banking system is very heterogeneous. Balance sheets of LB and IB are about ten times larger than the average value of all banks. BS, OB and CB are on average about 10 times smaller than the average. The average size of all banks' balance sheets remains similar for the three years. However, the mean value of total assets of LB decreases. This is because major UK banks conducted some restructuring of balance sheets to decrease the overall financial risk.

⁴There is still an on-going discussion as to what counts as loss absorbing capital. For example, the UK government states that beside equity "potentially loss-absorbing liabilities" (UK parliament, 2013) should be included.

Table 6.3: The table reports the mean value of Tier 1 capital of banks of different bank types in the years 2011 H2, 2012 H2 and 2013 H1 in Mil. Pounds. The values in brackets are the STD. Analogous to the STD of the assets values reported in Table 6.2, the STD for Tier 1 capital is also of the same order or larger than the mean values. Tier 1 capital can be considered to be the loss absorbing capital buffer. From 2011 H2 to 2013 H1, an increase of the average Tier 1 capital in banks of all bank types can be observed. In recent years, banks increased their capital to meet the capital requirements as outlined in Basel III.

Year	LB	BS	IB	OB	CB	Total
2011 H2	29619 (24088)	124 (266)	4630 (5426)	265 (502)	358 (574)	2120 (8405)
2012 H2	32835 (25583)	155 (331)	7966 (8574)	315 (564)	380 (750)	2670 (9568)
2013 H1	33113 (25453)	151 (328)	7990 (8565)	336 (611)	416 (766)	2810 (9809)

The mean Tier 1 capital of all banks and banks aggregated to their bank type is reported in Table 6.3 together with the STD. We observe that the total average Tier 1 capital increases over the years. This is due to regulatory requirements in the UK for banks to increase their capital reserves following the guidelines in Basel III (BIS, 2011).

Table 6.4: The table reports the leverage ratios (ratio of the average Tier 1 capital to the average total assets) for the years 2011 H2, 2012 H2 and 2013 H1 for the different bank types. The leverage ratio increases for LB, BS, IB and OB. The ratio for CB stays almost constant. Further, the leverage ratio for OB and CB is considerably higher than the leverage ratio of LB, IB and OB.

Year	LB	BS	IB	OB	CB	Total
2011 H2	0.044	0.046	0.025	0.098	0.073	0.040
2012 H2	0.051	0.054	0.042	0.121	0.071	0.050
2013 H1	0.051	0.054	0.042	0.115	0.075	0.050

Table 6.4 denotes the leverage ratio, which in this case is the ratio of Tier 1 capital to total assets. We note that the leverage ratio increases over time from 0.04 (2011 H2) to 0.05 (2012 H2 and 2013 H1). This implies that the rate of accumulation of Tier 1 capital is greater than the rate of growth of the value of banks' balance sheets showing the regulatory efforts to increase overall capital reserves. The lowest leverage ratio is achieved by IB in 2011 H2 with 0.025. OB have the largest leverage ratio (0.1213) in 2012 H2. The leverage ratios of LB and BS are similar in all years increasing slightly from around 0.04 to 0.05. CB have leverage ratios around 0.07 for all years. The reason

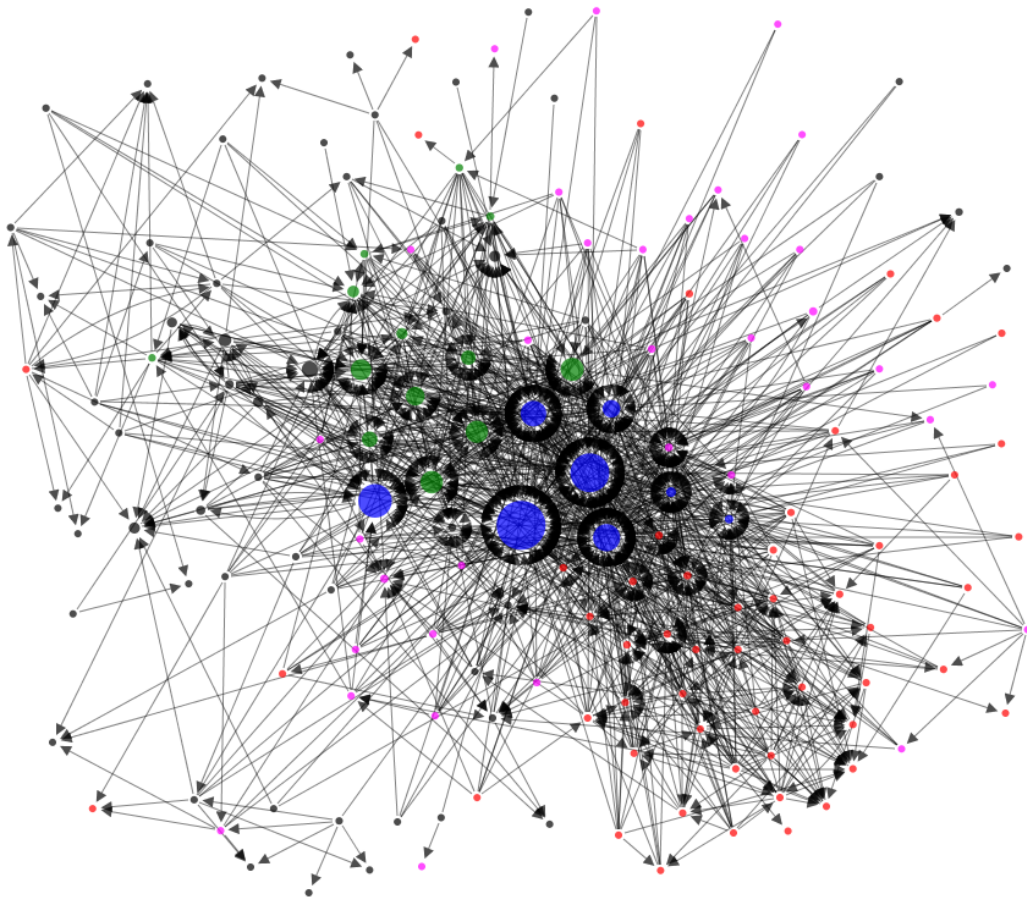


Figure 6.1: The figure shows the exposure network 2013 H1 as used in model calibration. The nodes of the exposure network are the banks, with the links depicting the exposure from one bank to another creating a directed network. The size of the nodes varies relatively to the size of banks balance sheets. The nodes are also coloured according to bank type with blue for LB, red for BS, green for IB, black for OB and magenta for CB.

for the larger leverage ratios of OB and CB as well as some BS is that small banks typically do not have the skills and resources to apply advanced approaches to calculate Risk Weighted Assets (RWA). So small banks tend to use the standardised approach, which leads to higher RWA, and hence, higher risk-based capital requirements.

6.1.3 Topology of the UK Interbank Network

The interbank exposure network from the 2013 H1 data as used in model calibration is shown in the Figure 6.1. A node in the interbank network represents a bank $i \in [1, N]$ in the banking system. The size of the nodes in Figure 6.1 are proportionate to the size of banks' balance sheets. Furthermore, the nodes are coloured according to their bank type with blue for LB, red for BS, green for IB, black for OB and magenta for CB.

The interbank network is a directed graph, i.e. the links in the network have a direction associated with them. In particular, a link from a bank i to another bank j indicates the exposure g_{ij} from bank i to bank j . While creating the interbank network from the exposure data, we do not differentiate between different financial instruments and disregard variations in maturity time.

The network measures used in this study to calibrate the models and to understand the insolvency process are a connected component analysis, out-degree, in-degree, weights and assortativity coefficient (Newman, 2010). We measure the averages of these quantities over the whole network and the averages aggregated by bank type.

6.1.3.1 Connected Component Analysis

The component analysis reveals that most of the banks belong to the largest connected component; meaning that, disregarding the directedness of a link, there exist at least one path between any two nodes. The banks that do not belong to the largest connected component are isolated.⁵ Compositions of the largest connected components per bank type are reported in Table 6.1 (second to fourth row). For the stability analysis of the UK banking system, we only use banks in the largest connected component. The insolvency of banks that are not members of the largest component is not influenced by counterparties. This is because banks not included in the largest connected component do not have any counterparties and form a component on their own. If there exists more than one network component of connected banks then all components need to be considered for calibration that contain more than one bank.

6.1.3.2 Degree Analysis

The average in- and out-degree states the average number of links leaving or directed to a bank in the interbank network. To compute the average in- and out-degree of a bank of a specific bank type to other bank types, we only use banks belonging to the specific bank type. To be more specific, the in- and out-degree of a bank i of type $\tau \in \{LB, BS, IB, OB, CB\}$ are given as:

$$z_{i\tau}^{\text{in}} = \sum_{j \in \mathcal{V}^{\tau*}} \{1\}_{(g_{ji} > 1)}, \quad z_{i\tau}^{\text{out}} = \sum_{j \in \mathcal{V}^{\tau*}} \{1\}_{(g_{ij} > 1)}, \quad (6.1)$$

⁵In 2011 H2 and 2012 H2, four banks are not part of the largest connected component (2011 H2: 2 BS, 1 OB, 1CB, and 2012 H2: 1 OB, 3 BS). In 2013 H1, 8 banks do not belong to the main component with 1 being a CB and 7 being OB.

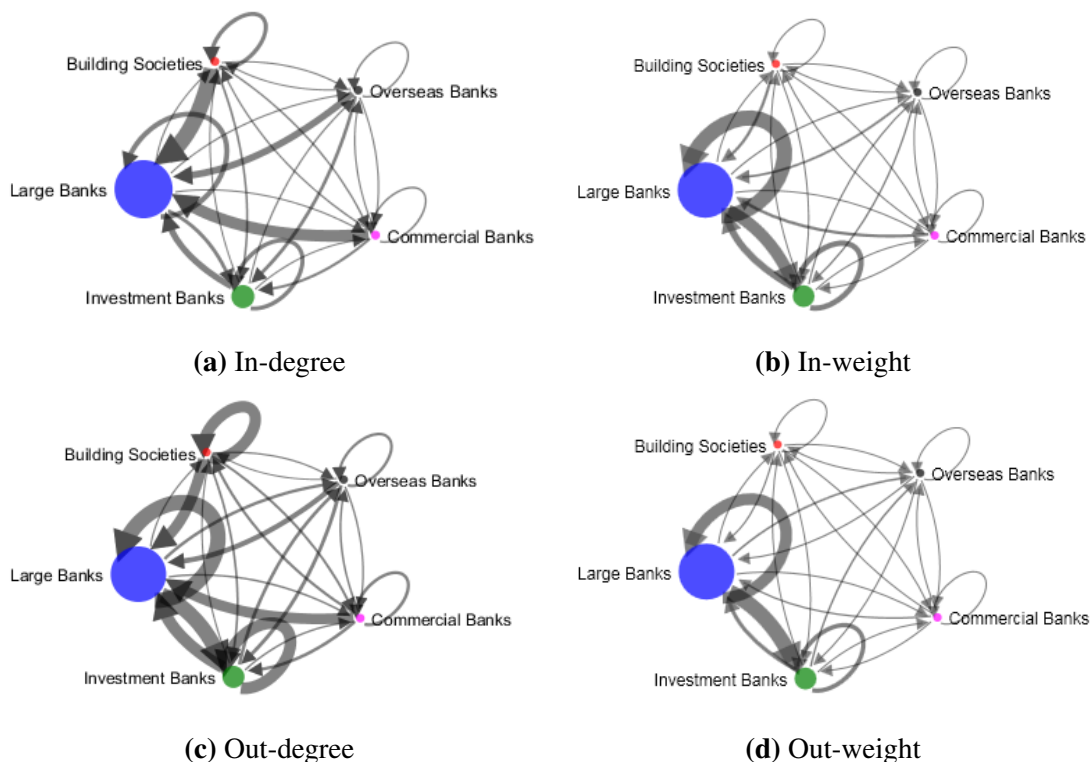


Figure 6.2: The networks represent the average in- and out-degree (subplots (a) and (b), respectively), and the average in- and out-weight (subplots (c) and (d)) to and from a bank of a particular bank type to banks of other bank types of the exposure network 2013 H1. The graphs are visualizations of the information contained in Tables B.3, B.4, B.1 and B.2. It becomes clear that LB and IB form a central role in the exposure network with the majority of BS, OB and CB situated in the periphery.

where \mathcal{V}^{τ^*} is the sets of banks belonging to bank type $\tau^* \in \{LB, BS, IB, OB, CB\}$.

The average in- and out-degree of a bank of type τ to banks in the set \mathcal{V}^{τ^*} are:

$$\bar{z}_{\tau^*}^{\text{in}} = \frac{1}{N_{\tau^*}} \sum_{i \in \mathcal{V}^{\tau^*}} z_{i \tau}^{\text{in}}, \quad \bar{z}_{\tau}^{\text{out}} = \frac{1}{N_{\tau}} \sum_{i \in \mathcal{V}^{\tau^*}} z_{i \tau^*}^{\text{out}}. \quad (6.2)$$

Tables B.3 and B.4⁶ report the average and STD of in- and out-degree from one bank type (columns) to another (rows), or vice versa. The information from the tables is visualized in Figures 6.2a⁷ and 6.2c. Figures 6.2a and 6.2c show the average in-degree from bank types to a particular bank type and the out-degree from a bank type to other bank types for the exposure network in 2013 H1.

The degree analysis is to a certain extent limited by the number of links banks have to report to the BoE. This is also reflected in the small STD of average number of

⁶Because of the size of the tables they are placed in the Appendix, Chapter B.

⁷The transpose of Table B.3 for 2013 H1 is used to produce the directed links in the graph in Figure 6.2a.

out-degrees. Thus, it should be kept in mind that without the threshold, the potential number of counterparties from one bank type to others might differ greatly.

We can note that the average in-degrees have high STD, which is mostly due to the high number of in-coming links LB and IB receive and low number of links directed to BS, CB and OB. The largest number of links to LB are directed from BS, OB and CB. However, the number of banks belonging to BS, OB and CB is larger than the number of banks belonging to LB and IB. Thus, in relative terms LB and IB are also almost entirely exposed to other LB. Similarly, most of the links directed to IB are coming from LB, IB and OB. BS, CB and OB have on average very low incoming links. The STD for both OB and CB are also close to the average values. Thus, the majority of OB and CB only receive little exposure from other bank types.

The degree analysis indicates that LB in all three years as well as IB in 2012 H2 and 2013 H1 form the centre of the interbank network with BS, OB and CB mostly interacting with LB or IB. Hence, BS, OB and CB are forming the periphery with LB and IB being in the centre of the interbank network.

6.1.3.3 Weight Analysis

To evaluate the importance of the different bank types towards counterparty risk, the weights of the links are also of importance. The in- and out-weight of states the size of the exposure of a bank of a particular bank type to and from banks of other bank types. That is

$$w_{i\tau}^{\text{in}} = \sum_{j \in \mathcal{V}^{\tau*}} g_{ji}, \quad w_{i\tau}^{\text{out}} = \sum_{j \in \mathcal{V}^{\tau*}} g_{ij}. \quad (6.3)$$

The average in- and out-weights of a bank of type τ to banks in the set $\mathcal{V}^{\tau*}$ are:

$$\bar{w}_{\tau}^{\text{in}} = \frac{1}{N_{\tau}} \sum_{i \in \mathcal{V}^{\tau*}} w_{i\tau}^{\text{in}}, \quad \bar{w}_{\tau*}^{\text{out}} = \frac{1}{N_{\tau}} \sum_{i \in \mathcal{V}^{\tau*}} w_{i\tau}^{\text{out}}. \quad (6.4)$$

Tables B.1 and B.2⁸ report the average total in- and out-weights in GBP Mil. leading to or direct from a specific bank type (rows) from or to banks of another bank type (columns), as well as the total averages for the entire network. The average total weights are the sum of the single weights directed to or leaving a bank. To obtain the

⁸Because of the size of the tables, they are placed in the Appendix, Chapter B.

single average weight directed to or leaving a bank of a specific bank type, the total average weight needs to be divided by the average link as stated in Tables B.3 and B.4. In Figures 6.2b⁹ and 6.2d, the in- and out-weights for 2013 H1 to and from a bank of a particular bank type from or to other bank types are plotted visualizing the data stated in Tables B.1 and B.2.

The break down into different bank types reveals that total exposure varies by orders of magnitude for different bank types with the mean in- and out-weight of LB being around GBP Mil. 10,000, IB weights being about a tenth smaller than LB, and BS, OB and CB again being a tenth smaller than IB. This is not too surprising as the sizes of the balance sheets also vary by orders of magnitude (see Table 6.2). The average in- or out-weight for BS, OB and CB does not vary much over time. However, the exposure of LB and IB to IB increases considerably from 2011 H2 to 2012 H2 and 2013 H2. The average out-weight of LB to LB decreases from 2011 H2 to 2012 H2.

Table 6.5: The table reports the ratio of the average values of interbank assets to total assets, θ_{out} , aggregated to different bank type levels and the entire banking system. The values θ , used in the mean-field model, are the total over all banks types.

Year	LB	BS	IB	OB	CB	Total θ
2011 H2	0.0162	0.0351	0.0097	0.0634	0.038	0.0158
2012 H2	0.0162	0.0217	0.0126	0.0538	0.0231	0.0159
2013 H1	0.0156	0.0329	0.0126	0.0312	0.0328	0.0159

The relative out-weight, θ_{out} , is calculated using the average out-weights as given in Table B.2 and the mean values for total assets as reported in Table 6.2 and Table 6.5. That is

$$\theta_{\text{out}\tau} = \frac{\bar{w}_{\tau}^{\text{out}}}{\mu_{A_{\tau}}}, \quad (6.5)$$

where $\mu_{A_{\tau}}$ states the mean value of assets of banks of type τ . The value of θ_{out} for all bank types is used to calibrate the parameter θ , the ratio of interbank assets to total assets in the mean-field model (see Chapter 4).

The average value of θ_{out} for all bank types averaging around 1.6% is relatively low. In comparison, in Müller (2006) and Upper (2011), the average interbank lending in the second half of the 2000s is between 10% to 20%, which indicates that the

⁹The transpose of Table B.1 for 2013 H1 is used to produce the directed links in the graph in Figure 6.2b.

recorded interbank network is incomplete. This is partly due to the data structure used in other studies, where interbank exposures is measured on a gross-of-collateral basis. In this thesis, exposure is measured on a net-of-collateral basis. Another reason why the interbank exposure of banks is lower than observed in other studies is the limited number of twenty counterparties UK regulated banks have to report as well as the restriction made to only investigate UK regulated banks, which makes the dataset incomplete. Because of this, we test the effects of increased exposure in Section 6.3.3.

6.1.3.4 Associativity Coefficients Analysis

Finally, the associativity coefficients of the interbank exposure networks also indicate a core-periphery structure. The associativity coefficient is the ratio of the covariance of nodes over edges to the value of perfect mixing and can take values between one and minus one (Newman, 2010). It states whether nodes with a large (small) number of links are connected to nodes with a large (small) number of links, in which case the associativity coefficient is closer to one and the network is associative. If nodes with a large (small) number of links are connected to nodes with a small (large) number of links, the associative coefficient is closer to minus one and the network is said to be disassociative. We used the algorithm from the *Brain Connectivity Toolbox* (Brain Connectivity Toolbox, 2010) to compute the associativity coefficient. The algorithm is described in Rubinov and Sporns (2010). The associativity coefficient of the exposure networks are: -0.32 (2011 H2), -0.27 (2012 H2) and -0.28 (2013 H1). The negative associativity coefficients indicate that banks with a small number of degrees are mostly connected to banks with a large number of degrees.

Overall, the network analysis shows that the topology of the interbank networks in 2011 H2, 2012 H2 and 2013 H1 resembles a core-periphery structure with LB and IB in the core and BS, OB and CB in the periphery. The core-periphery structure has been observed in other studies on interbank network topology (Boss et al., 2004; Fricke and Lux, 2015; van Lelyveld et al., 2012). The core-periphery structure suggests that LB and IB are financial intermediaries, i.e. these banks provide links between banks with money surplus to banks with liquidity or hedging needs.

6.2 Model Calibration

6.2.1 Calibration of Homogeneous Mean-Field Model

The mean-field model requires the calibration of 6 parameters for each historic period: $\mu_A(t_0)$, $\mu_L(t_0)$, $\theta(t_0)$, $\sigma_A(t_0)$, $\sigma_L(t_0)$, and $q(t_0)$, where $t_0 = 2011$ H2, 2012 H2 and 2013 H1.

The random distribution to initialize the balance sheets is chosen to be a Normal distribution. The parameters $\mu_A(t_0)$ and $\mu_L(t_0)$ can be traced from the balance sheet data. In particular, $\mu_A(t_0)$ is the average of total assets, reported in Table 6.2. For $\mu_L(t_0)$, we use the difference between the mean value of total assets and Tier 1 capital for the entire banking system as reported in Tables 6.2 and 6.3. In addition, we multiply $\mu_L(t_0)$ by a parameter f_L . We introduced f_L in Section 4.6. The parameter f_L is used to stress the system by increasing (or decreasing) average liabilities with respect to the empirically measured ones. Thus, we are testing stability over different average loss absorbing capital.

Note that we could have chosen to multiply $\mu_A(t_0)$ by a fraction, increasing or decreasing the mean value of the total assets, creating a positive or negative shock to the price value of assets. In both cases, the loss absorbing capital is increased or reduced. The more the loss absorbing capital is reduced initially, the more stressed is the banking system.

The values for $\theta(t_0)$ are reported in Table 6.5. For the purpose of this model, we set the instantaneous recovery rate $q(t_0)$ equal to zero for all t . In the event of a bank becoming insolvent, any loaner banks cannot expect any repayment. Thus, we consider the worst case scenario only.

The free-model parameter is σ . We set σ to be equal to $\sqrt{2}f_A\mu_A(t_0)$, i.e. $\sigma_A(t_0) = f_A\mu_A(t_0) = \sigma_L(t_0)$; in this way making θ_c independent of μ_A .

As in Chapter 5, we assume all banks solvent initially. Hence, the initial fraction of solvent banks, p_0 , equals one.

6.2.2 Calibration of the Heterogeneous Simulation

The number of banks, N , used in the simulation are reported in Table 6.1. The initial values for banks' total assets and total liabilities are drawn from Normal distributions. The mean value $\mu_{A_i}(t_0)$ is taken from the raw data. Hence, $\mu_{A_i}(t_0)$ differs for each

bank i . The STD is assumed to be a fraction of the mean of the total assets, $\mu_{A_i}(t)f_A$. Thus, the total assets of bank i are initially: $A_i(0) \sim \mathcal{N}(\mu_{A_i}(t_0), f_A\mu_{A_i}(t_0))$, where $\mathcal{N}(\cdot, \cdot)$ is the normal distribution.

The liabilities of each bank i , are initialized by computing $\mu_{L_i}(t_0)$ as the difference of a bank i 's total assets and Tier 1 capital. In the simulation, values are then drawn from a Normal distribution with mean $f_L\mu_{L_i}(t_0)$. The STD is $f_A\mu_{A_i}(t_0)$, causing $\sigma_i = \sqrt{\sigma_{A_i(t_0)}^2 + \sigma_{L_i(t_0)}^2} = \sqrt{2}f_A\mu_{A_i}(t_0)$, which is consistent with the homogeneous model. Thus, the liabilities of bank i are: $L_i(0) \sim \mathcal{N}(f_L\mu_{L_i}(t_0), f_A\mu_{A_i}(t_0))$.

For each simulation, the interbank network is the real network for the respective year. That is g_{ij} is the exposure as recorded in the data. The recovery rate of any exposure is assumed to be zero.

Furthermore, we consider all banks solvent initially, i.e. $S_i(0) = 1$ for all banks i .

Because of the incompleteness of the exposure data, any result calculated with the mean-field model or achieved with the heterogeneous simulation model should still be considered with caution as these might differ greatly with the values calculated when the complete exposure network is used.

6.3 Stress Simulation Results and Comparison with Homogeneous Solutions

6.3.1 Inducing System Stress by Increasing Average Liabilities

We perform 1,000 simulations by using the simulation-based model calibrated with UK regulatory data setting $f_A = 0.001$ and varying the factor f_L between 0.8 and 1.3. Let us first observe that when $f_L \leq 1$ and $f_A = 0.001$, the banking system is in a stable state with all banks operating normally. When the system is stressed by increasing liabilities and reducing loss absorbing capital, we observe the occurrence of a jump in the number of normally operating banks with the system becoming distressed.

Figure 6.3 shows in the upper subplot the fraction of surviving banks, p , against the fraction of the mean liabilities, f_L , for banking systems calibrated with the 2013 H1 data. The same plots for banking systems initialized with 2011 H2 and 2012 H2 data can be found in the Appendix, Figure C.1. There are three graphs in each figure: 1) p_S is the mean value of the fraction of surviving banks over 1,000 simulations; 2)

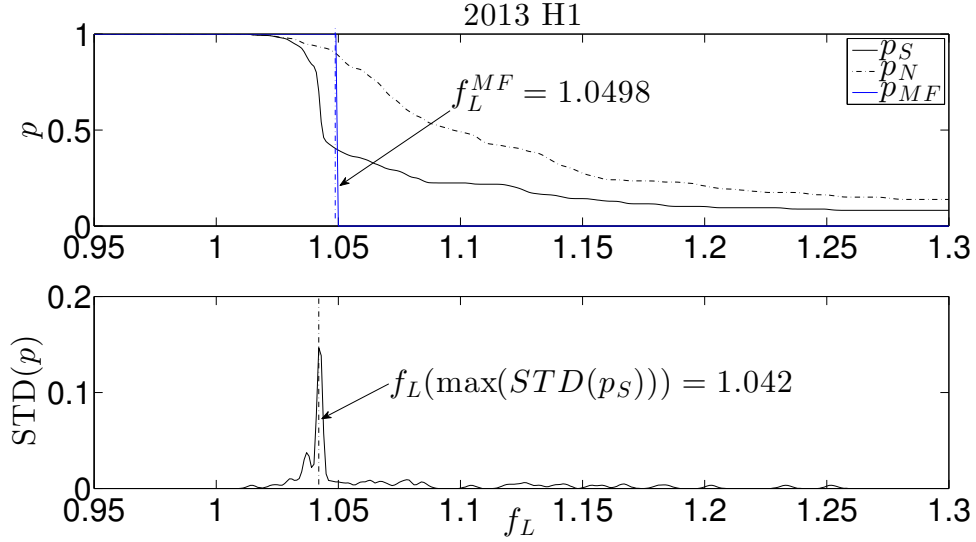


Figure 6.3: The figure shows in its first row the fraction of surviving banks, p , against the mean liabilities, f_L , for models calibrated with the 2013 H1 data. We set $f_A = 0.001$. The solid black line shows the average fraction of surviving banks, p_S , from 1,000 simulations. The dotted black line shows the average fraction p_N of surviving banks from 1,000 simulations when g_{ij} is set to zero for all banks i, j . This solution, p_N , is the null model as it shows the stability of the banking system when direct contagion is excluded. The blue line shows the solution of Eq. 3.15, p_{MF} , when $p_0 = 1$. The second row shows the STD of p_S . In the upper row, we indicated the position of f_L , at which p_{MF} jumps from almost all banks solvent to almost all banks insolvent. In the second row, we indicated the value of f_L , at which the STD of p_S is maximal. It becomes clear that, for a given f_L , the exposure network causes significantly more losses with respect to the case when the exposure network is disregarded. Also, close to the value of f_L , at which the jump occurs in the mean-field model, the STD is at maximum, suggesting that in that region, p_S also experiences a jump. The figures calibrated with 2011 H2 and 2012 H2 data can be found in the Appendix (Figure C.1).

p_{MF} is the fixed point solution of Eq. 3.15 when $p_0 = 1$; 3) p_N is the ‘null hypothesis’ mean value of the fraction of surviving banks. In the null hypothesis solution, all links of the underlying exposure network are set to zero ($g_{ij} = 0$). Thus, bank failure is only caused by changes to the value of liabilities and non-interbank assets. We note that p_S decreases in value first, followed by a sharp decline in the value of p_{MF} , followed finally by p_N at larger values of f_L . The second row of each plot shows the STD of the simulation solution, p_S , plotted against the fraction of the mean liabilities, f_L .

There is a considerable difference between p_N and p_S . The decline of p_N is much smoother because banks become insolvent when their capital becomes negative, which happens independently for each bank. When the exposure network is incorporated into the simulation, in the first iteration round, the same number of banks become

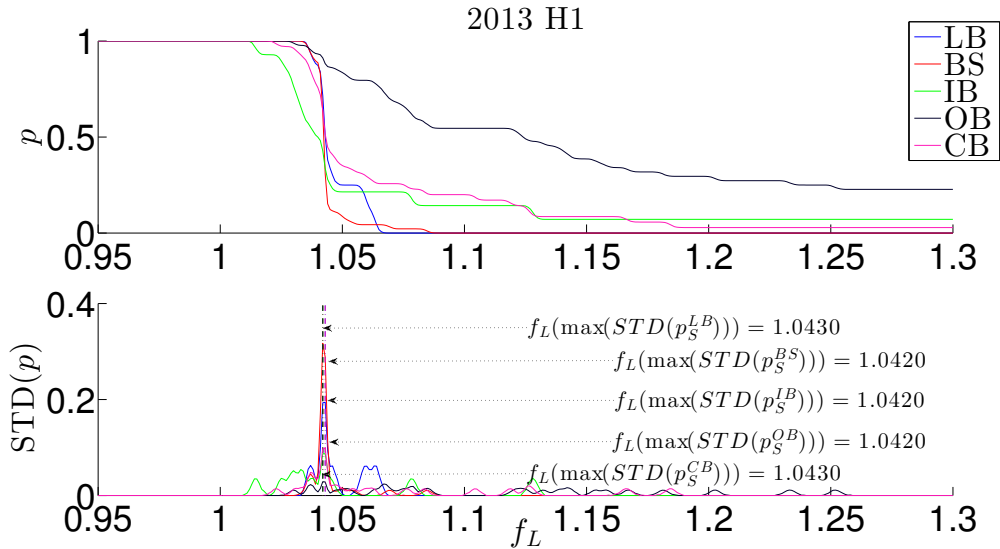


Figure 6.4: The figure shows the mean fraction of surviving banks of 1,000 simulations of particular bank types plotted against the fraction of mean liabilities, f_L , in the upper subplots for banking systems calibrated with 2013 H1 data. The parameter f_A was fixed at 0.001. The different bank types are indicated using the colours blue for LB, red for BS, green for IB, black for OB and magenta for CB. In the lower plot, the STD of the mean fractions of surviving banks of particular banks is plotted against f_L . The figure showing the corresponding graphs for banking systems calibrated with 2012 H2 and 2012 H2 data can be found in the Appendix (Figure C.2).

insolvent as in the null model (for fixed f_L). In later insolvency rounds, the insolvent banks reduce the total asset value of healthy banks, potentially flipping these (formerly healthy) banks into insolvency. This process continues until a stable fixed point is reached, at which point all surviving banks have enough capital to withstand the losses caused by direct exposure.

The homogeneous mean-field model behaves as predicted in Chapter 4 and a sudden jump happens from almost all banks operating to almost all banks insolvent. The value of f_L^{MF} , at which the mean-field model predicts the jump, is calculated using Eq. 4.6. We obtain: $f_L^{MF} = 1.0383$ (2011 H2), $f_L^{MF} = 1.0495$ (2012 H2) and $f_L^{MF} = 1.0498$.

In the second row of each figure, the STD of p_S , $STD(p_S)$, is plotted against f_L . It becomes clear that around the value of f_L , at which the steeper decline in p_S starts, $STD(p_S)$ has a sharp peak. This indicates that this is a region, where small fluctuations can bring most of the system down; and for the same set of average parameters, simulations can produce very different results leading to large values of $STD(p_S)$.

In Figures 6.4 and C.2 (Appendix), we plotted the mean fraction of surviving banks aggregated to bank type level against f_L (upper rows) and the STD for each bank type (second row). The banking systems in Figure 6.4 are initialized with 2013 H1 data and the banking system used to produce Figure C.2 are initialized with 2011 H2 (a) and 2012 H2 (b) data. Again, averages are over 1,000 simulations. The average fraction of LB is the blue line, BS are represented by the red line, the fraction of surviving IB banks is green, OB are the black line and CB are represented by the magenta line.

Splitting the fraction of surviving banks into the different bank types reveals a bit more detail about the loss dynamic. For instance, we observe that in 2011 H2 (Figure C.2 (a)), IB default much earlier than the other bank types. Further, the losses of IB do not cause a system failure. The earlier insolvencies happen because the capital reserves of IB are much smaller than the capital reserves of the other bank types in 2011 H2 (see Section 6.1.2). In Table B.2 and B.4, we see that in 2011 H2 bank types were not as much exposed to IB as in 2012 H2 and 2013 H1. The low average capital explains the earlier insolvencies of IB; and the less-central position of IB in the interbank network accounts for the smaller influence of IB to the stability of other bank types.

A steep decline in the fraction of surviving banks for all bank types (except for IB in 2011 H2) happens around the same value of f_L in each single year. The value of the fraction of surviving banks for specific bank types, at which the steep decline stops, varies for the individual bank types, such that for LB and BS, the shock causes the majority of banks to suddenly become insolvent. CB and OB lose during the steep decline about half to a third of banks. The reason why OB and CB are less effected by the shock is that most of these banks have only a small number of outgoing links with the average out-degree being between 3 to 4 (see Table B.4). Furthermore, the capital reserves of OB and CB are larger (See Section 6.1.2). Thus, the stability of these bank types are only minimally effected by counterparty risk.

The STD is plotted in the second row. The graphs of the STD also indicate that the largest bank failure happens for all banks around the same value of f_L . Again, we marked the value of f_L , at which the STD is at maximum for all different bank types. We observe that in 2011 H2, the values of f_L vary slightly, but in 2012 H2 and 2013 H1 the largest STD for all bank types happen almost at the same value of f_L . From

this value of f_L , the direct exposure of banks has a significant influence, causing the majority of banks in the banking system to become insolvent independent of the bank type.

The simulation results reveal that in 2012 H2, LB, OB and IB form a platform after f_L equals 1.0420 with 2 LB surviving. Again a steep decline of banks happens around f_L equal to 1.0670. This suggests that an in-between stable state occurs for values of f_L close to 1.0670, which cannot be explained by the result of the mean-field model. We hypothesize that the heterogeneity of the simulation-based model causes multiple fixed points for various values of f_L . This, however, still needs to be verified.

Overall, let us observe that the sudden decline happens earlier in 2011 H2 than in 2012 H2 and 2013 H2. In Section 6.1.2, we argued that the leverage ratio increases for LB, BS, IB and OB. This shows that to a certain extent, larger capital reserves can make the banking system more stable, making the system capable of absorbing losses of individual banks. However, if the cumulative losses caused by direct exposure in an interbank network create a system failure, then banks with larger leverage ratios are also at risk of insolvency.

6.3.2 Frequency Distribution for Fixed f_L

To further show that at specific values of $f_L(\max(\text{STD}(p_S)))$, the simulation indeed experiences a jump, in Figures 6.5 and C.3 (in the Appendix), we plotted the frequency distribution of p_S . Again, banking systems in Figure 6.5 are initialized with the 2013 H1 data, and the banking systems in Figure C.3 are initialized with 2011 H2 (a) and 2012 H2 (b) data. To obtain these frequency distributions, we fixed f_L at 1.038 (2011 H2) and 1.042 (2012 H2 and 2013 H1). Again, f_A was set to 0.001. We then repeated the simulation 10,000 times and recorded the occurrence of each value of p_S . It becomes visible that in all three years multiple peaks occur. In 2011 H2, the most dominant peaks materialise around 0.4 and 0.65 with an island formed in between these peaks. The picture in 2012 H2 is similar with the two dominant peaks occurring around 0.5 and 0.85 and smaller islands in between. In 2013 H1, there are three peaks. The first one occurs around 0.45, a second one occurs around 0.55 and a third one is formed around 0.8. This means that for most simulations, about 80% or about 40-50% banks of the banking system survive.

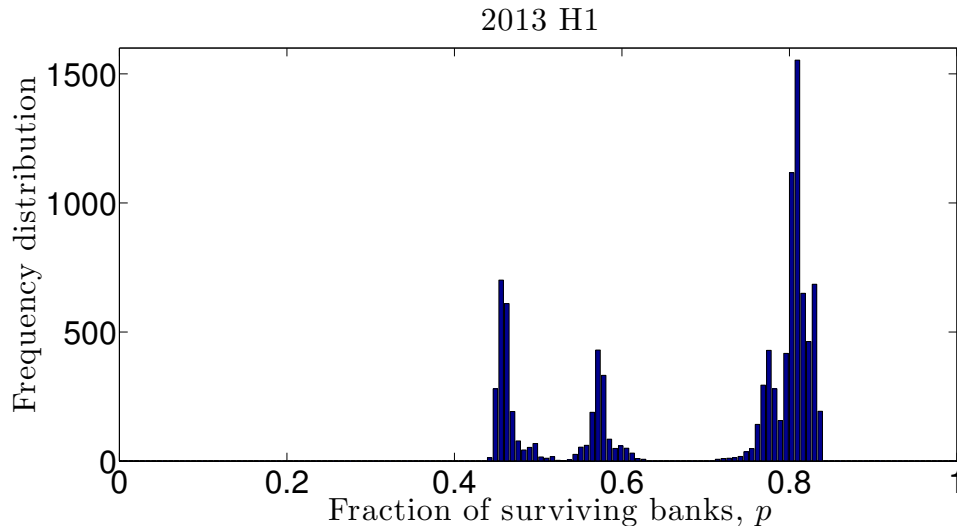


Figure 6.5: The figure shows the frequency distribution of the fraction of surviving banks, p_S . The simulation was repeated 10,000 times at fixed values of f_L at 1.042 for the 2013 H1 data. The parameter f_A was set to 0.001. Distinct peaks occur around 0.45, 0.57 and 0.8 in 2013 H1. This indicates that small perturbations in liabilities and assets cause p_S to jump from around 0.8 to 0.57 or 0.45 confirming the existence of the discontinuity predicted in the mean-field model. The figure showing the corresponding graphs for banking systems calibrated with 2011 H2 and 2012 H2 data can be found in the Appendix (Figure C.3).

Figure 5.2 in Chapter 5 also shows the frequency distribution of a simulation-based risk model, where two distinct peaks occur close to either end of the interval $[0, 1]$. The simulations of the heterogeneous banking system initialized with UK data do not lead to such a clean picture as in Figure 5.2. That is, in the simulations in Chapter 5, the banking system is assumed to consist of banks with similar sized balance sheets with similar ratios of interbank assets to total assets. Thus, banks behave more similarly. Nonetheless, a discontinuity in the fraction of surviving banks instead of a steady decline can be observed in Figures 6.5 and C.3. This suggests that indeed jumps occur caused by the direct exposure of banks to other banks.

Note that the middle peak in Figure 6.5 can not be explained by the mean-field model. The mean-field model homogenises the system and we expect that the third peak is a result of the diverse UK banking system. This needs to be further investigated by, for example, extending the one-tier mean-field model into a more realistic multi-tier mean-field model including banks with different sized balance sheets.

We can conclude that the main feature of the mean-field model, namely, the jump from almost all banks operating to almost all banks insolvent, is also observed in the

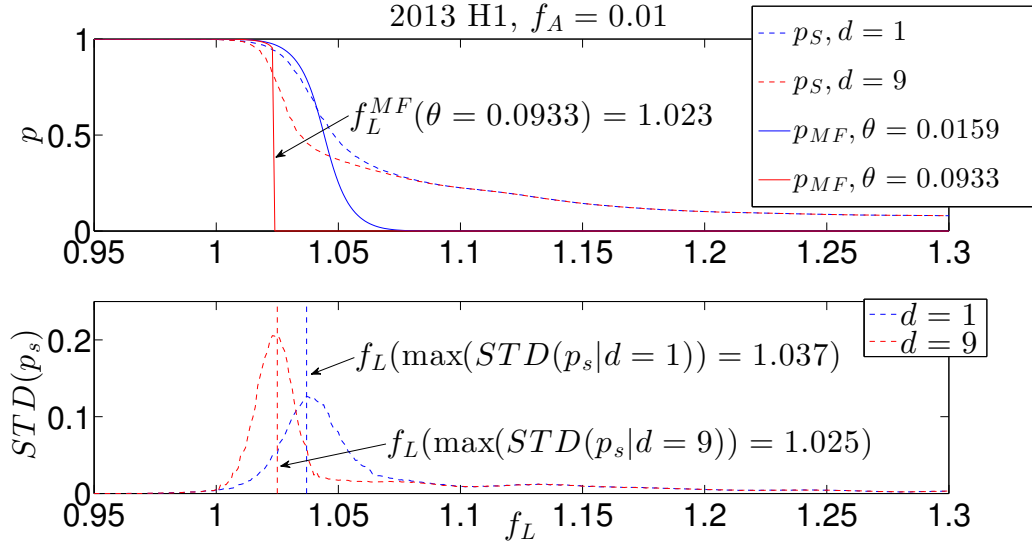


Figure 6.6: As in Figure 6.3, the first row of each subplot shows the fraction of surviving banks, p , plotted against the fraction of the mean liabilities, f_L . The second row shows the STD of p_S plotted against f_L . The models are initialized with the 2013 H1 data. The dotted lines are the average of 1,000 simulations and the solid lines indicate the solution of Eq. 3.15 given $p_0 = 1$. The green lines use the original interbank network for each year. Whereas for the red line, the exposure of LB was multiplied by $d = 9$. Multiplying the exposure of LB by 9 increased θ from 0.0159 to 0.0933 in 2013 H1. The parameter f_A for both simulation models as well as the mean-field model is set to 0.01. This causes θ for the original network to be smaller than θ_c , and for the network with increased exposure to be larger than θ_c . As a result, for the green lines we are not able to observe a jump but a smooth decline in p for increasing f_L , whereas for the red line a jump can be observed. The figure showing the corresponding graphs for banking systems calibrated with 2012 H2 and 2012 H2 data can be found in the Appendix (Figure C.4).

simulation model of the heterogeneous banking system. In addition, the mean liabilities, f_L^{MF} , at which the jump occurs in the mean-field model is relatively close to f_L where the fragile state is induced in the simulation model. This implies that the parameter analysis of the highly homogeneous banking system in Chapter 4 can be used for stability evaluation of a heterogeneous banking system. However, the heterogeneity of the banking system most likely allows for more than two stable states at the point of the jump such that intermediate states can reduce the size of the jump for some scenarios. Further, more than just one jump seems to occur when f_L is increased.

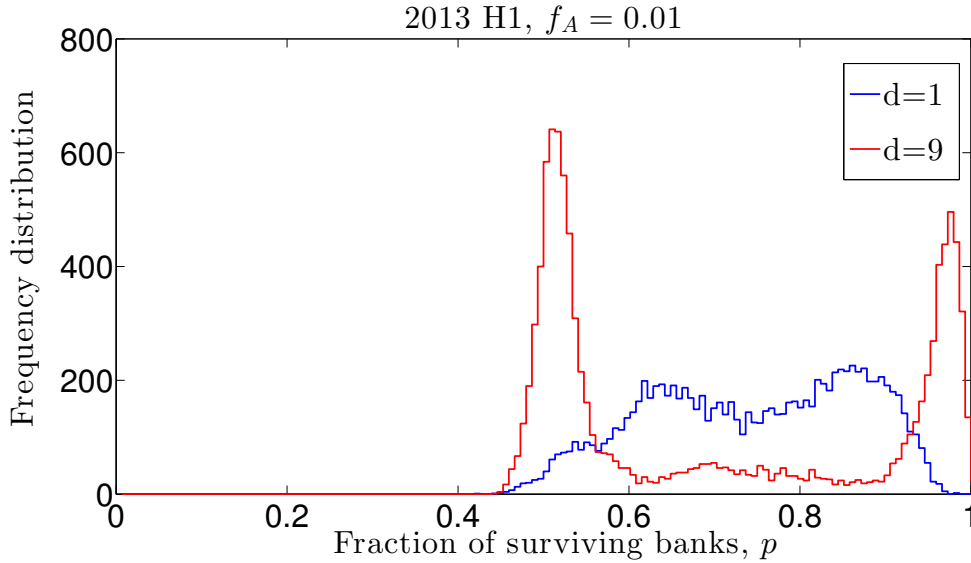


Figure 6.7: The figure shows the frequency distribution of the fraction of surviving banks, p , of 10,000 simulations for banking systems calibrated with 2013 H1 data. The parameter f_A is set to 0.01. For the blue line f_L is fixed at 1.037 for 2013 H1 and the original interbank networks have been used during the simulations. For the red line, the exposure of LB was multiplied by a factor $d = 9$, and f_L is fixed at 1.025. For $d = 1$ (blue line), θ for the 2013 H1 (and 2011 H2, 2012 H2) network is below θ_c , and henceforth, no jump is visible. Instead the frequency distribution is almost bell shaped. For $d = 9$ (red line), θ is larger than θ_c , and peaks become visible around p approximately 0.5 and 0.95 confirming that the banking system can be in two states, where either most banks are operative or half of the banks are insolvent. These peaks cannot be observed for the frequency distribution when the original interbank network is used. The figure showing the corresponding graphs for banking systems calibrated with 2012 H2 and 2012 H2 data can be found in the Appendix (Figure C.4).

6.3.3 Inducing Stress by Increasing Direct Exposure of Large Banks

In Section 4.6, we discuss that the fragile state can only be observed for f_A ($\sigma = \sqrt{2}f_A\mu_A$) being smaller than or equal to $\frac{(1-q)\theta}{\sqrt{2}b_c}$. For f_A larger than $\frac{1-q}{\sqrt{2}\theta b_c}$, some banks have enough capital to withstand the shock and form a barrier preventing the insolvency to propagate through the entire network. For θ as recorded in Table 6.5, this implies f_A needs to be smaller than 0.0044 for the fragile state to become possible. This restriction on f_A results in a small minimum leverage requirement (see the next section, Section 6.4). In that section, we calculated the minimum leverage requirements using Eq. 4.5 for θ as recorded in Table 6.5. Because of the small value of f_A and θ , the minimum leverage value ensuring a stable system is also relatively small with 0.0031 in 2011 H2, and 0.0041 in 2012 H2 and 2013 H1. That is, if θ is indeed of similar order

as recorded in the regulatory data, the UK banking system could be considered stable if banks set their leverage requirements to 0.3%.

However, as mentioned before, the values of θ recorded in Table 6.5, are relatively small in comparison to other studies, where interbank assets to total assets are estimated to be 10% to 20% (Müller, 2006; Upper, 2011). Another example illustrating the inaccuracy of the values in Table 6.5 can be found in banks' annual reports. The financial statement in banks' annual reports lists, among others, "Loans and advances to banks" in addition to "Total assets". The ratio of "Loans and advances to banks" to "Total assets" of the Royal Bank of Scotland in their annual report of 2013 is 0.05 (RBS, 2014). Values for other banks are similar. The section "Loans and advances to banks" lists reverse repos, and loans and receivables to banks, excluding other obligations. If repos, derivatives and other assets to banks would be included, then it can be assumed that the ratio of interbank assets to total assets for the Royal Bank of Scotland is even higher than 5%.

To test the effects of increased exposure, we increase the exposure of LB by multiplying a factor $d = 9$. This increase has the effect to change θ_c to 0.035. We chose to increase the exposure of LB only as the exposure of some banks of other bank types exceeded their total assets when their exposure is increased by $d = 9$. This changes θ from 0.0158 to 0.0991 in 2011 H2, from 0.0159 to 0.0966 in 2012 H2 and from 0.0159 to 0.0933 in 2013 H1. Hence, the observed θ s are now below the critical value θ_c and the homogeneous model predicts no jumps. However, when for the network with increased exposure, θ is above θ_c , a jump becomes possible. We induce the system into the fragile state by setting f_A equal to 0.01.

In the upper row of Figures 6.6 and C.4, the fraction of surviving banks for the mean-field solution, p_{MF} , for θ equal to 0.0158 (blue line) and to 0.0991 (red line) in 2011 H2 (Figure C.4 (a)); 0.0159 (blue line) and to 0.0996 (red line) in 2012 H2 (Figure C.4 (b)); and 0.0159 (blue line) and to 0.0933 (red line) in 2013 H1 (Figure 6.6) are plotted against the fraction of the mean liabilities, f_L . Additionally, the fraction of surviving banks evaluated using the simulation, p_S , is computed for the original network (blue dotted line) and when the exposure of LB is multiplied by d equal to 9 (red dotted line). It should be noted that changing d does not change the network structure nor the average mean value of total assets of a bank i . The second row of each

subfigure shows the STD of the simulation solution when $d = 1$ (blue dotted line) and when $d = 9$ (red dotted line).

We observe that, when $d = 1$, the homogeneous mean-field solution does not experience a jump. Instead, the decline is smooth in all years. The simulation solution for $d = 1$ starts a decline at similar f_L to the mean-field solution, but eventually diverging from the mean-field solution. When $d = 9$, the mean-field solution jumps from almost all banks operating to almost all banks defaulted. Furthermore, the value of f_L , at which the jump is predicted, is fairly similar to the value of f_L , at which the STD is the largest. This suggests that a jump occurs.

To verify this, we again plotted the frequency distribution of each simulation for fixed values of f_L in Figures 6.7 and C.4 for 10,000 simulations. Figures 6.7 and C.4 show the frequency distribution for the years 2011 H2 (Figure C.4 (a)), 2012 H2 (Figure C.4 (b)) and 2013 H1 (Figures 6.7). For $d = 1$, f_L was fixed respectively at 1.032 for 2011 H2, at 1.037 for 2012 H2 and 2013 H1. Whereas, for $d = 9$, f_L was fixed respectively at 1.013 for 2011 H2, 1.037 for 2012 H2 and 1.025 for 2013 H1. The blue line indicates the frequency distribution for $d = 1$ and the red line is used for the frequency distribution when $d = 9$.

Peaks are not visible in the frequency distributions for $d = 1$ for all years. Instead one bump occurs between p equal to 0.4 and 1.0. The bump is most dominant in 2011 H2. In Figure C.5 (b) and 6.7 the bump has a dent around 0.7 for both years. The dent indicates the beginning of the peak formation. However, values of p within the dent are still likely since θ for $d = 1$ is below θ_c . Hence, the decline in p for increasing f_L is still smooth. This clearly shows that no jump occurs in the simulation when $d = 1$; instead, small perturbations in the values of assets and liabilities cause a smooth decline. For $d = 9$, the shape of the frequency distribution looks quite different. Peaks occur around 0.5 and 0.95 in 2011 H2; 0.55, 0.7 and close to one in 2012 H2 and 0.5 and close to one in 2013 H1 suggesting that small perturbations in the value of assets and liabilities cause the system to jump from a fairly stable state, where most banks are operative, to an unstable state, where half the banks are insolvent. Thus, a jump occurs.

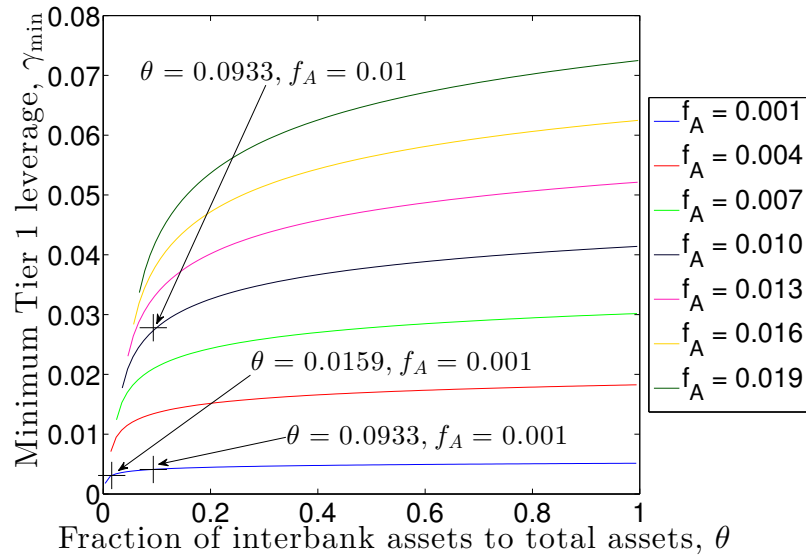


Figure 6.8: The figure shows the minimal leverage ratio, γ_{\min} that is needed for a banking system to be stable plotted against the fraction of interbank asset to total assets, θ , for a fixed $\sigma = \sqrt{2}f_A\mu_A$. The different curves correspond to different values of f_A . In addition, the crosses indicate the minimum leverage ratio for a banking system for some given θ and f_A , where the parameter θ correspond to the values calculated from the interbank data from 2013 H1.

6.4 Minimum Leverage Ratio

We have shown that the system failure in a model of a heterogeneous banking system happens around similar values as the jump predicted in the mean-field model of a homogeneous banking system. This implies that we can use Eq. 4.5 to calculate the minimum leverage requirement for more heterogeneous banking systems.

Eq. 4.5 allows us to calculate the minimal leverage ratio needed to ensure a stable system when θ is greater than θ_c . If $d = 1$, then θ in 2011 H2 is 0.0158; and in 2012 H2 and 2013 H1 θ is 0.0159. These values are very close and result in a minimum leverage ratio of 0.0031 (2011 H2) and 0.0041 (2012 H2 and 2013 H1), if f_A equals 0.01. When increasing θ to 0.0991 in 2011 H2, to 0.0996 in 2012 H2 and to 0.0933 in 2013 H2, the minimum leverage ratio changes to 0.0278 for f_A equal to 0.01.

Figure 6.8 shows the minimum leverage ratio, γ_{\min} , plotted against the fraction of interbank assets to total assets, θ , for different values of f_A as stated. The crosses indicate the position of the minimum leverage ratio, γ_{\min} , for θ and f_A as indicated. These θ values correspond to θ as calculated using the 2013 H1 data. It becomes clear that the larger f_A , the larger γ_{\min} has to be in order to ensure a stable system.

In Bank for International Settlement (2014), it is stated that the recommended non-risk based leverage ratio for banks is 3%. The minimum leverage ratios ensuring a stable system calculated for $d = 1$ and $d = 9$ are below the recommended leverage ratio. That said, the incompleteness of the bilateral exposure data implies that the calculated leverage ratios are most likely underestimating the actual leverage ratios.

6.5 Conclusion

The chapter is divided into two parts. In the first part, we introduce the dataset used to calibrate the mean-field and simulation-based models discussed in the second part of the chapter. The two regulatory datasets are studied recording balance sheet and exposure information of banks in the UK banking system for three different years. Our analysis reveals that banks in the UK vary largely in the size of their balance sheets. Additionally, we showed that banks' capital reserves increased over the years following regulatory requirements set by the BoE.

The dataset containing the exposure data is limited by the number of counterparties banks have to report to the BoE. Because of that, the exposure networks constructed from the data only provide limited representation of the real UK interbank networks. Nonetheless, we can deduce from the network analysis that LB and IB form the centre of the interbank network with BS, OB and CB being positioned in the periphery. This result is in line with the outcomes of other studies. Obtaining data for this thesis was one of the biggest obstacles, not only because access to exposure data is limited but also because regulators (with a few exceptions) started only recently, following the financial crisis, collecting interbank exposure data. For future studies, the quality of exposure data needs to improve in order to investigate further how financial stability is influenced by counterparty exposure. In particular, more data on exposure between international banks needs to be collected because via international banks a banking crisis can propagate from one country to another.

In the second part of the chapter, we calibrate the mean-field and simulation models with the datasets. The banking system in the simulation-based model is highly heterogeneous with banks varying in size, position in the interbank network, links directed towards them and value of exposure to other banks. Nonetheless, we observed that the fragile state in the simulations occurs for a similar sized shock to banks' capital

as is predicted in the mean-field model. Hence, we mapped the results of the mean-field model of a simple banking system to a simulation-based model of a more complicated banking system. This suggests that the minimum capital requirements deduced from the mean-field model can be applied to real world banking systems to create a more stable financial system given more accurate data on interbank exposure.

Chapter 7

Conclusions

This study set out to explore the influence of counterparty failure on the financial stability of a banking system. For this reason, we studied a counterparty cascade model, where banks' stability depends on their balance sheet quantities and the solvency of their counterparties. In our model, the balance sheet parameters are random variables. The model was solved in two ways: semi-analytically by applying a mean-field assumption homogenizing the banking system, and by constructing a simulation model to test counterparty failure in more complex banking systems.

The mean-field assumption allowed us to conduct a parameter analysis of the balance sheet quantities to determine the ratios of assets, liabilities and capital that ensure a stable banking system. We showed that the results extracted from the mean-field solution can be mapped to the simulation-based model of a more complex banking system, where banks vary in size, have different leverage ratios, and exposure to other banks. Because of that we can conclude that a simple model of counterparty failure of a homogeneous banking system predicts the propagation of counterparty failure in banking systems dynamics before, during and after a crisis. Therefore, the results of this thesis can be used to set restricting guidelines on leverage ratios and interbank exposure that also ensures financial stability for more complex real-world financial systems.

By applying the mean-field assumption in Chapter 4, we were able to reduce a multi-parameter counterparty risk model into a two-parameter iteration map. The iteration map states the average fraction of surviving banks in an iteration round r . The two parameters, a and b , represent the influence on the stability of banks of external factors changing balance sheet parameters (a), and the average exposure between banks (b). A fixed point analysis of the iteration map revealed that for fixed b above a critical

value and changing a , the solution of the iteration map has a hysteresis cycle. This is because the iteration map has at least one and at most three fixed points depending on the values of the parameters a and b . This implies that the solution of the iteration map is history dependent. That is, depending on the initial value of solvent banks, the solution of the iteration map for the same parameters can differ. This result allowed us to draw conclusions about the cost of rescuing a defaulted banking system. Furthermore, the hysteresis cycle explains a discontinuity in the fraction of surviving banks also observed in other studies (Gai and Kapadia, 2010; Amini et al., 2012; Hurd and Gleeson, 2011). In this thesis, we calculated the values of a , namely a_1 and a_2 , where the fraction of surviving banks changes for slight perturbations from almost all banks solvent to almost all banks insolvent and vice versa. We determined a_1 and a_2 for different location-scale distributions, which allowed us to draw conclusions on restricting leverage ratios to ensure a stable banking system. Additionally, we showed that in the proximity of the jump, the failure of one bank is sufficient to induce system failure.

Finding exposure data for calibrating the counterparty risk model was one of the major challenges of this thesis. Balance sheet data is published each year by banks in their annual report and are publicly accessible. However, exposure data between banks is, in most cases, only collected by regulators. For this reason, we calibrated the mean-field model in Section 6.1 with balance sheet data only. We used balance sheet data of UK and US banks from the years 2007 and 2012 to demonstrate the stability of the banking systems in the individual years. We showed that interbank lending made both the US and UK systems more prone to failure in 2007 such that small fluctuations in assets and liabilities could have caused catastrophic events. In 2012, for the same fluctuations, both banking systems are more stable with much larger fluctuations needed to create a system-wide bank failure.

In Chapter 5, we tested the robustness of the mean-field model comparing the solution of the mean-field model to the solution of a more complex simulation-based model. The assumptions used to find the solution of the mean-field model create an overly simplistic banking system of banks of similar size and with the same value of interbank exposure to other banks. We showed using the simulation model that the predicted fragile state in the mean-field model occurs for different distributions and various network structures used to initialize the simulation model. In particular, we were able

to show that the discontinuity occurs when banks initial capital is shocked for location-scale and non-location scale distributions. We further explained how the mean and full width at half maximum (FWHM) of random distributions used to initialize the balance sheets affected the size of the jump, and the size of the shock to banks' initial capital needed to induced the fragile state. When banking systems are initialized with different random distributions with the same mean but different FWHM, banks in the banking systems with small FWHM have more similar levels of initial loss-absorbing capital than banks in banking systems with larger FWHM. In systems with similar levels of initial capital, the size of the jump is more severe. Whereas, in banking systems with differing levels of capital, the size of the jump is smaller but the fragile state occurs at larger mean values of initial capital. This is because some banks have less capital than others. These banks induce the fragile state at higher levels of average capital in comparison to a more homogeneous system. However, some banks in a system with diverse capital levels also have more initial loss absorbing capital and therefore are able to withstand the shock. Eventually, these banks form a barrier in the distribution of insolvency on the interbank network, and they stop the insolvency induced by a small number of initially failing banks. This suggest that for a homogeneous banking system, a two-tier leverage system as suggested in in the Basel III (Basel Committee on Banking Supervision, 2010)), where systemically important banks have larger capital requirements, could have a positive effect on financial stability. However, more research needs to be conducted to provide a definitive answer. An analysis of a multi-tier model with banks of different size and exposure towards other banks using the mean-field method presented in Chapter 4 could potentially answer some of these questions in more detail.

Standard network topologies were used in the simulation model to compare the simulation solution with the solution of the mean-field model in Chapter 5. The results indicate that network topology and the size of the banking system do not influence the solvency propagation through interbank networks in a homogeneous banking system. Furthermore, diversification only reduces the risk of spreading insolvency if banks in the banking system have very similar balance sheets. If the distribution of initial capital varies a lot in the banking system, then diversification does not necessary reduce the risk of insolvencies caused by counterparties. This is because the probability of being

connected to an insolvent bank also increases when a bank increases the number of counterparties. Previous studies (Allen and Gale, 2000; Freixas et al., 2000; Gai and Kapadia, 2010) suggested that diversification lowers the risk of failure of a banking system. We repeated in our model-setting the results in Gai and Kapadia (2010) and explained that stochastic effects causing slight changes in banks' initial capital result in banks to become insolvent regardless of the number of counterparties.

We conclude Chapter 5 by relaxing the assumption that banks' balance sheet quantities do not change in time during the insolvency propagation. It is much more reasonable to assume that due to the announcement of a bank failure asset prices change, than to consider that no correlation between changes in asset values and bank failure exist. Similarly, QE programs and government bail-outs can prevent the failure of a banking system by providing external capital, and reducing the debt of banks. To address this short-coming of the mean-field model, we changed the values of non-interbank assets and liabilities in the simulation model using functions that change the value of assets proportional to the fraction of insolvent banks and induce capital into the banking system at a particular round in the insolvency process. We explained how the changes in the balance sheet values influenced the equilibrium solution of the mean-field model and how the mean-field model can still be used to calculate the fraction of surviving banks. By doing so, we showed that asset price devaluation can move the banking system into an unstable (from a formerly healthy) region and can induce the fragile state. Furthermore, we showed that capital injections into a failing system do not necessarily cause the system to return to a stable state. Our model suggests that if external capital is provided too late, the system still fails, even though earlier rescue attempts would have saved the banking system for the same cost of external capital. We wish to stress that the functions used to stress balance sheet quantities were chosen arbitrarily. This was done mainly to affirm that time changing variables can also be incorporated into our model set-up. Nonetheless, it would be of interest to incorporate more realistic functions that imitate the process of price changes or cost of borrowing in a better way. In addition, functions modelling more complex interactions between banks such as derivatives that depend on the solvency of multiple parties or repayment agreements can be added in future research.

The analysis in Chapters 4 and 5 was done on highly stylized banking system.

Banks' balance sheet parameters and weights of the interbank network are, by construction of the banking system, fairly similar. The real world banking system consists of banks of various sizes. This issue is addressed in Chapter 6, where we used real-world exposure and balance sheet data obtained from the BoE for three different years to calibrate the mean-field and a simulation-based model. We constructed the banking system in the simulation-based model such that, for each bank, the recorded values of banks' balance sheets in the respective years form the means of the random distributions used to initialize the assets and liabilities. Furthermore, we use real-world exposure data to construct the exposure networks. From the data analysis in Section 6.1, we can conclude that the UK banking system is highly heterogeneous with banks vary in size of their balance sheets by orders of magnitude. The banking system constructed using the balance sheet data is therefore heterogeneous as well.

In that section, we group banks into different banktypes: LB, BS, IB, OB and CB¹. We find that LB are the largest, and BS and OB are the smallest banks on average. Nonetheless, the leverage ratios between the bank types vary only marginally, with OB having the largest leverage ratio and IB the smallest. We were also able to observe that leverage ratios increased between 2011 to 2013 for most bank types due to regulatory requirements set by the BoE. Hence, we can conclude that even though the sizes of UK banks' balance sheets vary by orders of magnitude, the ratio of capital to total assets (i.e. the leverage ratio) is of similar value across most bank types. The explanation for this can be found in the regulatory framework. The required leverage ratio in the UK was set according to Basel II guidelines using the same leverage value for all banks. Note that with the introduction of Basel III, this changes because systemically important banks have to satisfy higher leverage requirements.

The degree, weight, component and assortative analysis of the interbank networks show that LB and IB are in the center of the exposure network with most links directed towards these bank types. Hence, we can state that the structure of the interbank network resembles a core-periphery network with LB and IB in the centre of the network and BS, OB and CB in the periphery. The core-periphery structure has been observed in other studies and confirms that LB and IB form intermediaries that provide financial

¹LB = large bank, BS = building society, IB = investment bank, OB = oversea bank, and CB = other commercial bank.

services and access to international markets for regionally operating banks. The relative out-weight, namely the average interbank assets to total assets, for LB, BS, IB and CB are fairly similar. However, we argued that the values observed in Section 6.1.3 are lower than the values observed in other studies since the exposure is measured net of collateral and the number of counterparties that banks have to report to the BoE is restricted.

In Section 6.3, we found that the model of the more realistic heterogeneous banking system reproduces the main feature of the mean-field model: We observe the occurrence of a fragile state in both models, where a large portion of banks in the banking system can become suddenly insolvent as a consequence of an external shock to the banks' non-interbank asset or liabilities, and the interconnectedness of banks via direct exposure.

We showed that the capital in both the homogeneous and heterogeneous model has to be reduced to similar levels for a sudden system failure to occur. This effect is surprising and can be explained by the cumulative losses that the majority of banks experience in later rounds of insolvency. We showed that the loss in the fraction of surviving banks in the simulation-based heterogeneous system was not as severe as for the mean-field model. For the heterogeneous system, about 50% of banks become insolvent, whereas for the mean-field model almost the entire banking system defaults. The banks surviving the shock are mostly OB and CB in the periphery with little exposure to the rest of the banking system.

Nonetheless, in the heterogeneous banking model, the sudden insolvency occurs for most failing banks of all bank types at the same fraction of mean liabilities, independent of balance sheet size. Variations in the capital reserves of banks in the simulation-based model lead to smaller jumps occurring for the rest of the banks that survived the first jump at lower capital values. These are heterogeneous effects that cannot be explained by the mean-field model. These are probably the consequence of the onset of multiple fixed points caused by the heterogeneity and can be explained by extending the one-tier mean field model into a multi-tier model.

Finally, we addressed the low values of out-weight, θ , in the dataset by artificially increasing the exposure of LB such that the average ratio of interbank assets to total assets are closer to 10%. We find that for larger exposure the minimum leverage re-

quirements increase. This is because it is more likely that large shocks to banks' capital can propagate through the interbank network for larger values of average exposure.

We should note that we disregarded any additional information about the interbank exposure such as maturity time, risk weights and variations in financial products. We did so because of the low number of data points. Similarly, we only briefly discussed the effects of collateral and recovery rates due to a lack of data. However, variations in exposure clearly do have an effect on counterparty risk and should be part of future research projects. In general, the quality of the data needs to improve. Without actual data on interbank exposure, the precise risk imposed via counterparty failure can not be quantified.

In conclusion, we used a simple cascade counterparty risk model to explain the propagation of distress in a connected banking system and explained the mechanism and conditions under which a system failure occurs. The simple model of banking failure demonstrates the risk that counterparty failure imposes in a highly connected banking system and can be used to create a more stable banking system.

Appendix A

Propositions and Lemmas Needed for Fixed Point Analysis

The section states the propositions and lemmas used in the fixed point analysis here. Propositions, lemmas and proofs from textbooks are in italics. We adapted the notation of the propositions, lemmas and proofs to fit the notation of this thesis.

In general, a fixed point of an iteration map, $f_n(x)$ (where n indicates the n th iteration step), is defined as the point where $p = f(p)$ (Devaney et al., 2003). Fixed points can be repellent or attracting. The two following propositions can be found in Devaney et al. (2003) (Propositions 4.4 and 4.6) and help to determine whether a fixed point is repellent or attracting:

Proposition A.4.1 [Proposition 4.4 in Devaney et al. (2003)] *Let $f_n(x)$ be an iteration map at the n th iteration step and $f'(\cdot)$ be continuous. Let p be a fixed point of $f_n(x)$ with $|f'(p)| < 1$. Then there exists an open interval U about p such that if $x \in U$, then*

$$\lim_{n \rightarrow \infty} f_n(x) = p. \quad (\text{A.1})$$

Proof *Since $f'(x)$ is continuous, there exists $\epsilon > 0$ such that $|f'(x)| < A < 1$ for $x \in [p - \epsilon, p + \epsilon]$. By the Mean Value Theorem*

$$|f(x) - p| = |f(x) - f(p)| \leq A|x - p| < |x - p| \leq \epsilon. \quad (\text{A.2})$$

Hence $f(x)$ is contained in $[p - \epsilon, p + \epsilon]$ and, in fact, is closer to p than x is. Via the same argument

$$|f^n(x) - p| \leq A^n|x - p| \quad (\text{A.3})$$

so that $f^n(x) \rightarrow p$ as $n \rightarrow \infty$.

Proposition A.4.2 [Propositions 4.6 in Devaney et al. (2003)] *Let $f_n(x)$ be an iteration map at the n th iteration step and $f'(\cdot)$ be continuous. Let p be a fixed point of $f_n(x)$ with $|f'(p)| > 1$. Then there is an open interval U of p such that, if $x \in U$, $x \neq p$, then there exists $n > 0$ such that $f_n(x) \notin U$.*

Proof Since $f'(\cdot)$ is continuous, there exists $\epsilon > 0$ such that $|f'(x)| > A > 1$ for $x \in (p - \epsilon, p + \epsilon)$. Using the Mean Value Theorem, we have

$$\epsilon < |p - x| < A|p - x| = |f(p) - f(x)| = |p - f(x)|. \quad (\text{A.4})$$

Hence, the distance to ϵ increases if f is applied to x . Thus,

$$|p - f^k(x)| > \epsilon, \quad (\text{A.5})$$

for any k .

Thus, for $|f'(p)| < 1$, p is a stable fixed point and $|f'(p)| > 1$, p is an unstable fixed point.

Furthermore, note that the iteration map in Eq. ?? is a monotone decreasing one-dimensional map on a compact set. In Smith (2008), Lemma 1.2 (and proof) can be found. It states:

Lemma A.4.1 [Lemma 1.2 in Smith (2008)] *A monotone sequence contained in a compact subset of X converges in X .*

Proof Suppose x_n is a sequence satisfying $x_n \leq x_{n+1}$ and $x_n \in A$ for $n \geq 1$ where A is a compact subset of X ; the case for a decreasing subsequence is treated similarly. It follows that the sequence x_n has convergent subsequences. The Lemma will be proved by showing that there exists a unique $p \in X$ which is the limit of every convergent subsequence. If x_{n_k} and x_{m_k} are two subsequences of x_n and if $x_{n_k} \rightarrow p$ and $x_{m_k} \rightarrow q$ as $k \rightarrow \infty$ then, by monotonicity of x_n , for each k there exists $l(k)$ such that $x_{n_k} \leq x_{m_{l(k)}}$. Passing to the limit as $k \rightarrow \infty$, $p \leq q$. A similar argument shows that $q \leq p$. [Thus,] ... $q = p$. Hence, Lemma 4.1 ensures that the iteration map in Eq. ?? has at least one stable fixed point.

The following lemma states the extrema of $x - F(x)$. The function $x - F(x)$ is important

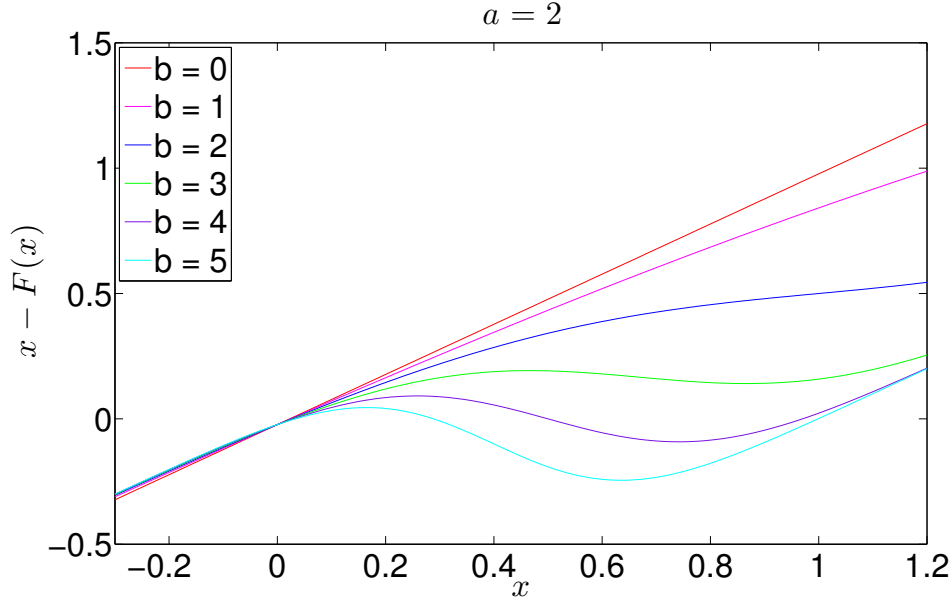


Figure A.1: The figure shows the function $x - F(x)$ plotted against x for fixed $a = 2$ and various values of b as indicated in the legend. For $b = 0, 1, 2$, $x - F(x)$ is monotone increasing. Whereas, for $b = 3, 4, 5$, $x - F(x)$ has a maximum and a minimum.

as its roots are equal to the fixed points of the iteration map $p_r = F(p_{r-1})$.

Lemma A.4.2 Assume $P(\cdot)$ in Eq. ?? is a standard normal CDF. Given $b > b_c = \sqrt{2\pi}$, $x - F(x)$ has extrema $x_{1,2} = b^{-1}(a \mp \sqrt{2 \ln \frac{b}{b_c}})$, where x_1 is a maximum and x_2 is a minimum.

Proof The derivatives of $x - F(x)$ relevant for the extrema analysis are

$$\frac{d(x - F(x))}{dx} = 1 + \frac{b}{b_c} \exp\left(-\frac{(a - bx)^2}{2}\right), \quad (\text{A.6})$$

and

$$\frac{d^2(x - F(x))}{dx dx} = \frac{b^2}{2b_c} (a - bx) \exp\left(-\frac{(a - bx)^2}{2}\right). \quad (\text{A.7})$$

For $f \frac{d(x - F(x))}{dx} = 0$, two solution exist if $b \geq b_c$, namely, $x_{1,2}$ as defined above. Furthermore, $\frac{d^2(x - F(x))}{dx dx}(x_1) = -2\sqrt{\ln(\frac{b}{b_c})} \leq 0$ and $\frac{d^2(x - F(x))}{dx dx}(x_2) = 2\sqrt{\ln(\frac{b}{b_c})} \geq 0$. Hence, x_1 is a maximum and x_2 is a minimum of $x - F(x)$.

Figure A.1 illustrates the behaviour of $x - F(x)$ for changing b . The function $x - F(x)$ is plotted against x for fixed $a = 2$. To plot the graphs, we used a standard Normal CDF for $P(\cdot)$ in $F(\cdot)$. The parameter b is changed for each plot as indicated in the legend. For $b = 0, 1, 2 < b_c$, $x - F(x)$ is monotonically increasing. Whereas, for $b = 3, 4, 5 > b_c$, $x - F(x)$ has a maximum (x_1) and a minimum (x_2).

Appendix B

Emperical Information on Interbank Network

The exposures among banks of different kinds are reported in Table B.1. In Table B.2, we report the empirical values for interbank exposures. The interbank network average out-degree and in-degree are reported in Tables B.3 and B.4.

Table B.1: The table shows the average value of exposure in Mil. GBP to a bank of a particular bank type (row) from banks of another bank type (column) (the total in-weight) for 2011 H2, 2012 H2 and 2013 H1. The brackets below each mean value indicates the STD. The STD of the mean values are of the same order or larger than mean values indicating that the size of funding a bank of a particular bank type differs largely from the size of funding other banks of the same bank type receive.

2011 H2	LB	BS	IB	OB	CB	Total
LB	6645.09 (5259.03)	378.66 (297.83)	1263.91 (1070.73)	658.52 (514.38)	726.48 (680.33)	9672.66 (7204.10)
BS	0.87 (4.32)	14.58 (28.49)	0.33 (2.02)	0.11 (0.75)	3.09 (13.74)	18.98 (41.43)
IB	2335.04 (2579.48)	4.45 (8.49)	804.70 (817.13)	198.22 (166.78)	23.76 (32.24)	3366.18 (3421.39)
OB	12.61 (56.30)	1.39 (10.22)	51.19 (276.59)	14.27 (33.51)	2.32 (11.28)	81.77 (290.05)
CB	30.90 (150.68)	12.39 (38.23)	22.45 (66.46)	10.89 (44.50)	14.61 (52.27)	91.25 (297.74)
Total	555.16 (2053.47)	27.10 (105.95)	158.15 (498.23)	58.36 (192.88)	43.98 (215.63)	842.75 (2898.26)
2012 H2	LB	BS	IB	OB	CB	Total
LB	4153.29 (3418.68)	251.51 (207.29)	1567.65 (1355.99)	441.00 (350.40)	474.43 (504.83)	6887.88 (5010.34)
BS	3.21 (14.80)	12.55 (19.75)	0.00 (0.00)	0.36 (2.41)	5.12 (21.94)	21.25 (44.72)
IB	3452.42 (3590.70)	6.47 (18.82)	1279.51 (1221.12)	186.45 (178.93)	21.53 (21.29)	4946.38 (4778.66)
OB	27.17 (192.12)	0.00 (0.00)	53.09 (324.64)	14.29 (29.84)	0.45 (2.47)	95.00 (533.05)
CB	5.04 (30.85)	2.68 (13.13)	4.54 (19.43)	2.97 (15.29)	10.01 (40.31)	25.25 (116.32)
Total	540.59 (1827.85)	17.90 (72.00)	216.11 (690.57)	45.34 (141.53)	30.68 (152.07)	850.63 (2679.19)
2013 H1	LB	BS	IB	OB	CB	Total
LB	4158.68 (3556.12)	420.08 (332.13)	1678.31 (1474.11)	266.77 (311.03)	486.48 (456.85)	7010.32 (5528.95)
BS	1.24 (8.40)	11.73 (23.30)	0.35 (2.36)	0.22 (1.47)	6.24 (29.43)	19.78 (53.18)
IB	3221.71 (3225.70)	12.35 (20.68)	1220.62 (1336.57)	111.55 (160.77)	27.01 (27.67)	4593.24 (4602.72)
OB	43.30 (254.48)	0.54 (2.56)	61.20 (353.01)	5.33 (10.11)	4.22 (18.51)	114.60 (607.31)
CB	1.71 (7.92)	4.48 (21.41)	3.82 (18.78)	2.16 (9.11)	45.56 (253.94)	57.72 (309.97)
Total	546.91 (1787.25)	28.94 (120.38)	226.92 (739.28)	27.32 (106.49)	43.11 (192.72)	873.20 (2727.08)

Table B.2: The table reports the total average amount in Mil. GBP of interbank exposure of banks belonging to a particular bank type (row) to banks of other bank types (columns), i.e. the total out-weight. The amount in the brackets is the STD. The values can be thought of as the total in-weight of banks in the interbank system. The STD are of the same order or larger than the mean values suggesting that even banks in the same bank type have highly varying exposure to other banks.

2011 H2	LB	BS	IB	OB	CB	Total
LB	6645.09 (5953.31)	4.90 (9.39)	4086.32 (4483.17)	85.09 (88.69)	142.92 (223.11)	10964.32 (8245.12)
BS	67.32 (114.01)	14.58 (28.74)	1.39 (4.36)	1.67 (6.92)	10.19 (33.23)	95.14 (161.91)
IB	722.23 (869.15)	1.06 (3.60)	804.70 (807.09)	197.46 (340.39)	59.34 (134.02)	1784.80 (1675.86)
OB	97.56 (175.18)	0.09 (0.68)	51.39 (133.84)	14.27 (29.76)	7.46 (22.94)	170.77 (315.73)
CB	157.08 (204.28)	3.76 (12.01)	8.99 (15.54)	3.38 (7.49)	14.61 (25.57)	187.82 (217.02)
Total	489.75 (1931.81)	5.41 (17.49)	298.27 (1332.73)	27.95 (115.77)	21.37 (73.06)	842.75 (3005.22)
2012 H2	LB	BS	IB	OB	CB	Total
LB	4153.29 (3782.40)	17.65 (32.48)	6041.74 (7329.54)	169.81 (435.75)	23.94 (44.85)	10406.43 (10989.00)
BS	45.73 (61.45)	12.55 (16.89)	2.06 (11.00)	0.00 (0.00)	2.31 (5.92)	62.65 (79.21)
IB	895.80 (892.90)	0.00 (0.00)	1279.51 (1458.27)	189.61 (349.11)	12.33 (29.48)	2377.30 (2489.23)
OB	70.56 (108.63)	0.32 (1.63)	52.20 (133.55)	14.29 (23.35)	2.26 (5.78)	139.63 (241.96)
CB	99.88 (176.06)	5.93 (17.76)	7.93 (17.96)	0.59 (2.82)	10.01 (20.67)	124.34 (191.97)
Total	357.81 (1259.30)	6.07 (15.46)	449.67 (2121.37)	30.84 (152.07)	6.23 (17.96)	850.63 (3397.48)
2013 H1	LB	BS	IB	OB	CB	Total
LB	4158.68 (3956.45)	7.12 (20.14)	5637.99 (6574.11)	238.16 (445.99)	7.47 (15.98)	10049.41 (10261.69)
BS	73.06 (86.26)	11.73 (15.54)	3.76 (12.17)	0.52 (1.71)	3.41 (7.65)	92.47 (108.98)
IB	959.04 (1049.12)	1.14 (4.28)	1220.62 (1281.65)	192.34 (252.25)	9.54 (29.38)	2382.69 (2466.63)
OB	48.50 (112.96)	0.23 (1.51)	35.49 (126.04)	5.33 (10.81)	1.72 (4.68)	91.28 (219.47)
CB	111.20 (189.47)	8.21 (17.22)	10.80 (23.89)	5.31 (12.11)	45.56 (210.14)	181.07 (305.91)
Total	381.51 (1325.74)	6.19 (13.75)	437.45 (1978.79)	34.30 (144.08)	13.74 (103.54)	873.20 (3309.62)

Table B.3: The table shows the average number of links to a bank of a particular bank type (rows) from banks of another bank type (columns), i.e. the average in-degree, for 2011 H1, 2012 H2 and 2013 H3. The number in the brackets is the STD of each value. It becomes clear that LB and IB receive the largest number of in-coming links from other banks. OB, CB and BS hardly receive any, indicating that LB and IB form the core, and BS, OB and CB the periphery of the interbank network.

2011 H2	LB	BS	IB	OB	CB	Total
LB	4.63 (1.92)	17.88 (8.32)	7.80 (4.19)	18.64 (11.27)	18.21 (8.85)	67.14 (28.82)
BS	0.07 (0.33)	2.51 (3.63)	0.04 (0.21)	0.02 (0.15)	0.32 (0.74)	2.97 (4.31)
IB	2.36 (2.34)	0.64 (0.84)	4.32 (2.96)	5.67 (4.38)	2.16 (1.98)	15.15 (10.82)
OB	0.13 (0.44)	0.06 (0.41)	0.23 (0.67)	1.03 (1.52)	0.22 (0.84)	1.66 (2.55)
CB	0.19 (0.52)	0.65 (1.89)	0.16 (0.37)	0.58 (1.50)	0.66 (2.33)	2.24 (6.00)
Total	0.55 (1.44)	1.85 (4.74)	0.91 (2.38)	1.94 (5.08)	1.43 (4.57)	6.68 (16.50)
2012 H2	LB	BS	IB	OB	CB	Total
LB	5.25 (2.25)	17.26 (9.35)	8.47 (5.09)	16.37 (9.93)	16.77 (8.73)	64.12 (29.04)
BS	0.07 (0.25)	4.57 (4.69)	0.00 (0.00)	0.05 (0.30)	0.31 (0.96)	5.00 (5.21)
IB	3.36 (3.15)	0.41 (0.75)	5.00 (3.68)	6.28 (4.54)	1.58 (1.32)	16.63 (11.17)
OB	0.06 (0.42)	0.00 (0.00)	0.18 (0.66)	1.11 (1.61)	0.07 (0.26)	1.41 (2.46)
CB	0.08 (0.36)	0.36 (1.61)	0.13 (0.40)	0.28 (1.04)	0.46 (1.96)	1.31 (5.12)
Total	0.64 (1.80)	2.33 (5.20)	0.98 (2.76)	1.86 (4.68)	1.24 (4.28)	7.05 (16.24)
2013 H1	LB	BS	IB	OB	CB	Total
LB	5.63 (2.07)	23.63 (12.46)	8.08 (4.38)	8.94 (6.98)	17.06 (9.46)	63.33 (32.48)
BS	0.021 (0.15)	4.34 (4.93)	0.02 (0.15)	0.02 (0.15)	0.46 (1.34)	4.86 (5.68)
IB	3.64 (3.30)	1.29 (1.66)	4.50 (3.68)	3.27 (2.24)	2.01 (1.54)	14.71 (10.56)
OB	0.14 (0.63)	0.14 (0.55)	0.27 (1.09)	0.62 (0.98)	0.23 (0.75)	1.40 (2.48)
CB	0.06 (0.24)	0.64 (2.46)	0.09 (0.28)	0.23 (0.77)	0.77 (2.72)	1.78 (6.06)
Total	0.71 (1.95)	2.96 (6.68)	0.98 (2.66)	1.05 (2.76)	1.51 (4.60)	7.21 (16.67)

Table B.4: The table shows the average number of links from one a bank of a particular bank type (rows) to banks of another bank type (columns), i.e. the average out-degree, for 2011 H1, 2012 H2 and 2013 H3. The number in the brackets is the STD of each value. It becomes clear that LB and IB have the largest number of links to other banks. OB, CB and BS are mostly exposed to LB and IB. This is another indication for the core-periphery structure.

2011 H2	LB	BS	IB	OB	CB	Total
LB	4.63 (0.92)	0.38 (0.74)	4.13 (2.03)	0.88 (0.64)	0.88 (1.13)	10.88 (2.36)
BS	3.18 (2.45)	2.51 (3.67)	0.20 (0.46)	0.07 (0.25)	0.53 (0.99)	6.49 (5.84)
IB	4.46 (1.85)	0.14 (0.36)	4.42 (2.72)	0.89 (1.21)	0.43 (0.65)	10.24 (3.82)
OB	2.76 (1.73)	0.02 (0.14)	1.47 (1.60)	1.03 (1.12)	0.40 (0.73)	5.68 (3.36)
CB	3.93 (1.77)	0.39 (1.02)	0.82 (0.88)	0.32 (0.53)	0.66 (0.88)	6.13 (3.20)
Total	3.40 (2.04)	0.85 (2.28)	1.34 (1.88)	0.57 (0.90)	0.52 (0.86)	6.68 (4.43)
2012 H2	LB	BS	IB	OB	CB	Total
LB	5.25 (0.71)	0.38 (0.52)	5.88 (1.96)	0.38 (0.52)	0.37 (0.52)	12.25 (2.25)
BS	3.14 (2.13)	4.57 (5.06)	0.13 (0.46)	0.00 (0.00)	0.31 (0.59)	8.15 (6.88)
IB	4.84 (1.35)	0.00 (0.00)	5.00 (3.21)	0.64 (0.84)	0.36 (0.71)	10.83 (3.78)
OB	2.61 (1.68)	0.04 (0.20)	1.76 (2.00)	1.10 (1.27)	0.21 (0.45)	5.74 (3.57)
CB	3.53 (2.04)	0.36 (0.80)	0.58 (0.87)	0.09 (0.27)	0.46 (0.63)	5.03 (3.27)
Total	3.33 (1.99)	1.43 (3.37)	1.51 (2.34)	0.46 (0.92)	0.32 (0.57)	7.05 (5.11)
2013 H1	LB	BS	IB	OB	CB	Total
LB	5.63 (0.74)	0.13 (0.35)	6.38 (1.41)	0.75 (0.46)	0.25 (0.46)	13.13 (1.73)
BS	4.11 (1.54)	4.34 (4.62)	0.39 (1.29)	0.13 (0.34)	0.49 (0.86)	9.46 (5.69)
IB	4.62 (1.60)	0.07 (0.27)	4.50 (2.93)	0.86 (1.10)	0.21 (0.43)	10.26 (3.96)
OB	1.63 (1.83)	0.02 (0.14)	1.04 (1.77)	0.62 (1.13)	0.18 (0.37)	3.49 (3.59)
CB	3.90 (1.87)	0.60 (1.86)	0.80 (1.55)	0.29 (0.77)	0.76 (0.76)	6.36 (3.15)
Total	3.45 (2.09)	1.52 (3.18)	1.40 (2.27)	0.42 (0.80)	0.42 (0.65)	7.21 (5.13)

Appendix C

Additional Figures of Empirical Counterparty Risk Analysis of the UK Banking System

For readability, we placed the figures of the results for the simulation and the mean-field models calibrated with 2011 H1 and 2012 H2 data in this chapter.

In particular, the figure corresponding to Figure 6.3 is Figure C.1, to Figure 6.5 is Figure C.3, to Figure 6.6 is Figure C.4, and to Figure 6.7 is Figure C.5. The datasets used to produce subplot (a) of each figure are 2011 H2. For the initialization of subplot (b) of each figure, we used the 2012 H2 datasets.

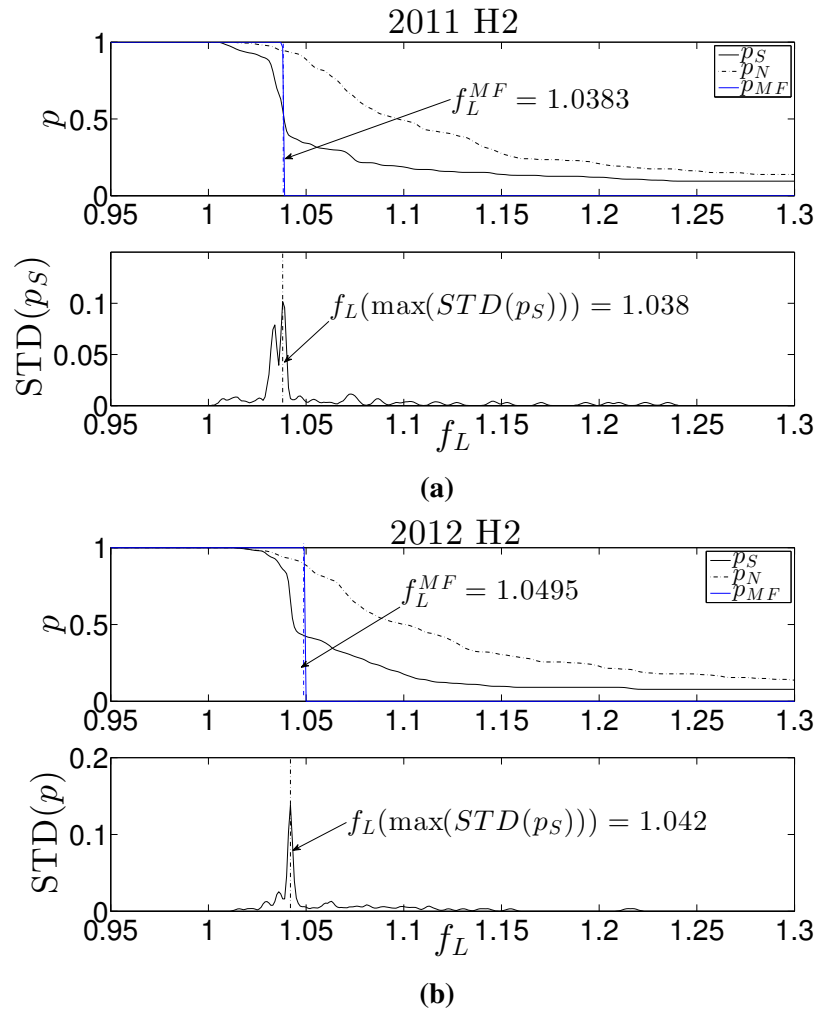


Figure C.1: To produce the plots in this figure, we use the same simulation set-up as was used to produce Figure 6.3. However, for the initialization of the models, we apply the 2011 H2 (a) and 2012 H2 (b) datasets for UK banks' balance sheets and interbank exposure data. The plot in the upper row shows the fraction of surviving banks, p , against the mean liabilities, f_L , evaluated using the average of 1'000 simulation (black solid line, p_S); the mean-field model (blue solid line, p_{MF}); and the solution of a null-model (black dotted line, p_N), where all links in the interbank network are set to zero. The second row is a plot of the STD of the simulation solution, p_S , against the mean liabilities, f_L . Additionally, we marked the position at which the jump occurs in the mean-field model, f_L^{MF} , and the maximum STD of p_S .

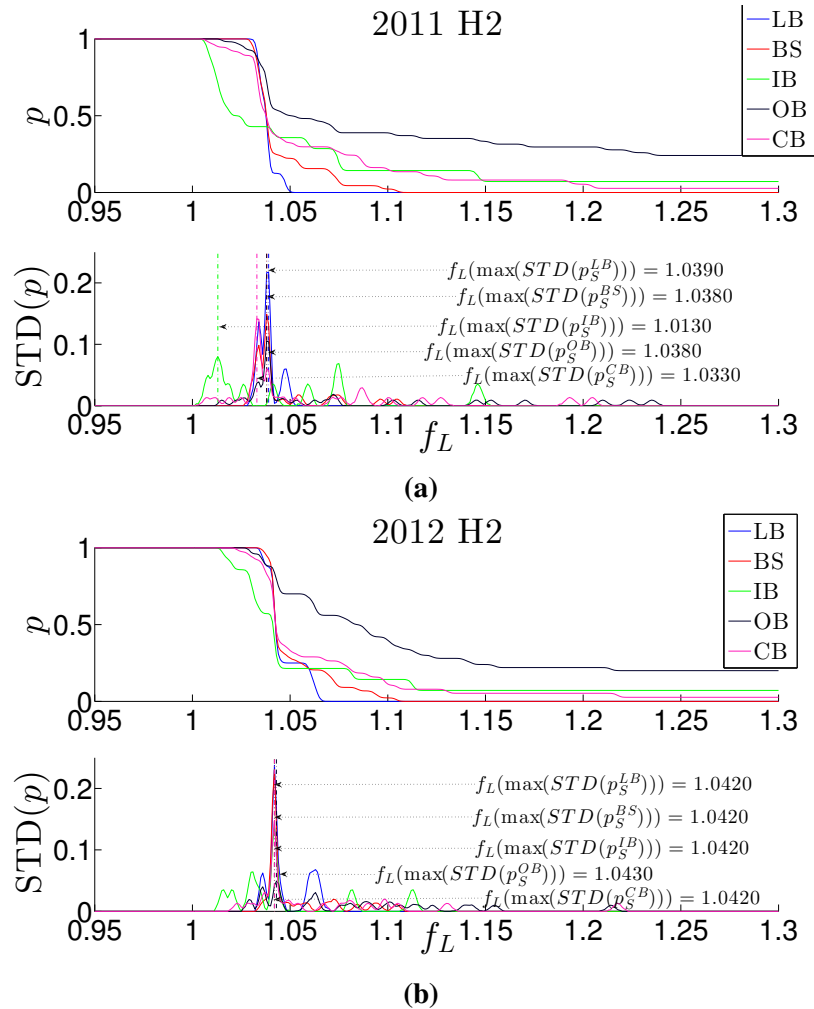


Figure C.2: To produce the plots in this figure, we use the same simulation set-up as was used to produce Figure 6.4. However, for the initialization of the models, we apply the 2011 H2 (a) and 2012 H2 (b) datasets for UK banks' balance sheets and interbank exposure data. In the first row of the figures, the mean fraction of surviving banks of 1'000 simulations of a particular bank type is plotted against the mean liabilities, f_L . In the second row, the STD of each fraction of surviving banks for the different bank types is plotted against the mean liabilities, f_L . The graphs are coloured blue for LB, red for BS, green for IB, black for OB and magenta for CB. Additionally, we marked the maximum STD of p_S for each bank type.

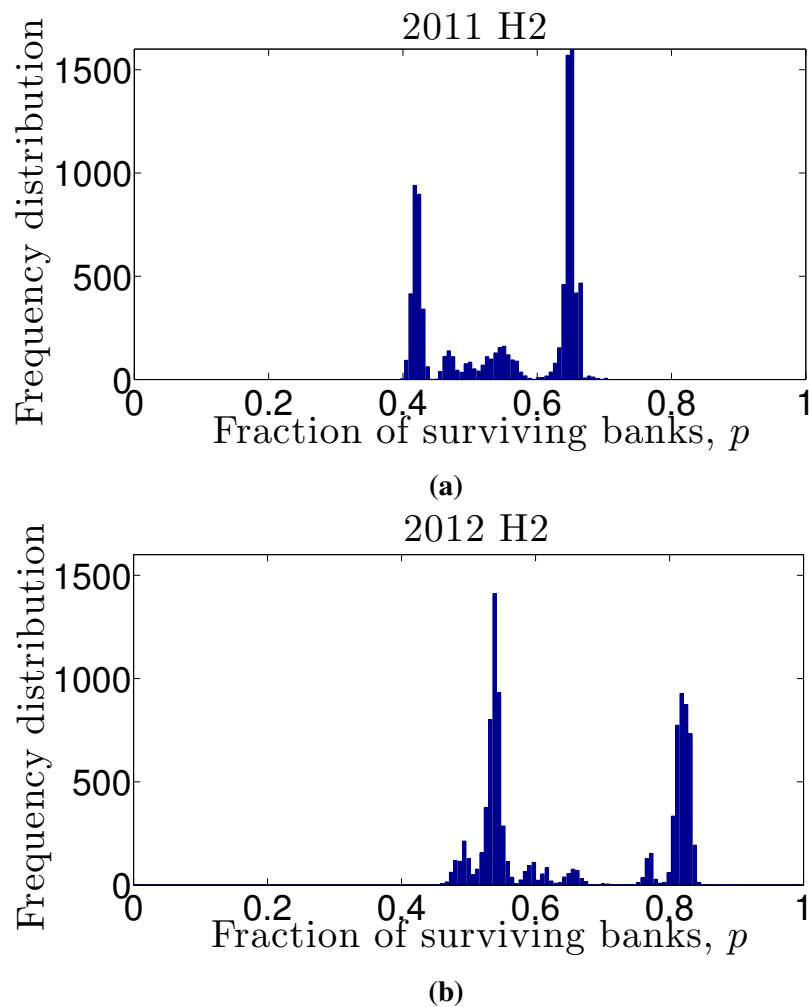


Figure C.3: To produce the plots in this figure, we use the same simulation set-up as was used to produce Figure 6.5. However, for the initialization of the models, we apply the 2011 H2 (a) and 2012 H2 (b) datasets for UK banks' balance sheets and interbank exposure data. The figures show the frequency distributions of 10'000 simulations for fixed values of f_L at 1.038 (2011 H2) and 1.042 (2012 H2). The parameter f_A was set to 0.001. Distinct peaks occur around 0.4 and 0.65 in 2011 H2, 0.5 and 0.8 in 2012 H2, and 0.45 confirming that the fragile state occurs for the fixed values of f_L .

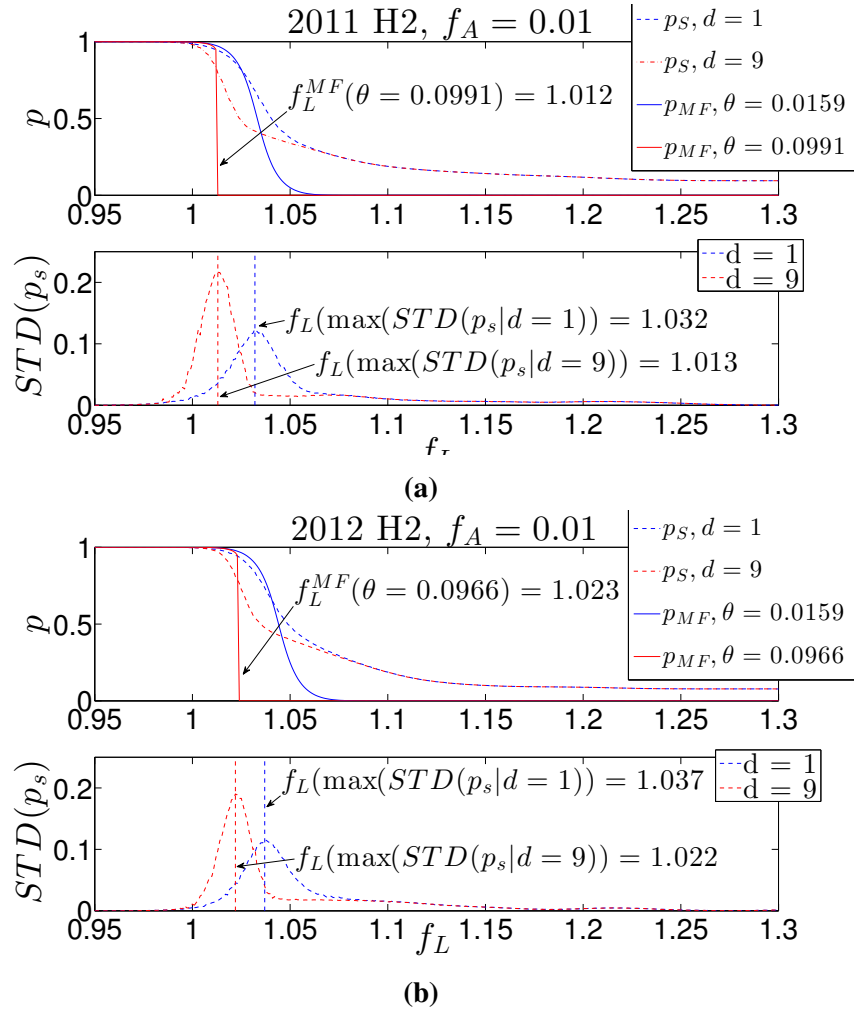


Figure C.4: To produce the plots in this figure, we use the same simulation set-up as was used to produce Figure 6.6. However, for the initialization of the models, we apply the 2011 H2 (a) and 2012 H2 (b) datasets for UK banks' balance sheets and interbank exposure data. As in Figure 6.3, the first row of each subplot shows the fraction of surviving banks, p , plotted against the fraction of the mean liabilities, f_L . The second row shows the STD of p_s plotted against f_L . The dotted lines are the average of 1'000 simulations and the solid lines indicate the solution of the Iteration Map ?? given $p_0 = 1$. The green lines use the original interbank network for each year. Whereas for the red line, the exposure of LB was multiplied by $d = 9$. Multiplying the exposure of LB by 9 increased θ from 0.0158 to 0.0991 in 2011 H2, from 0.0159 to 0.0966 in 2012 H2 and from 0.0159 to 0.0933 in 2013 H1. The parameter f_A for both simulation models as well as the mean-field model is set to 0.01. This causes θ for the original network to be smaller than θ_c and for the exposure network where LB exposure is multiplied by d equal to 9 to be larger than θ_c . As a result, for the green lines, we are not able to observe a jump but a smooth decline in p for increasing f_L , whereas for the red line, a jump can be observed.

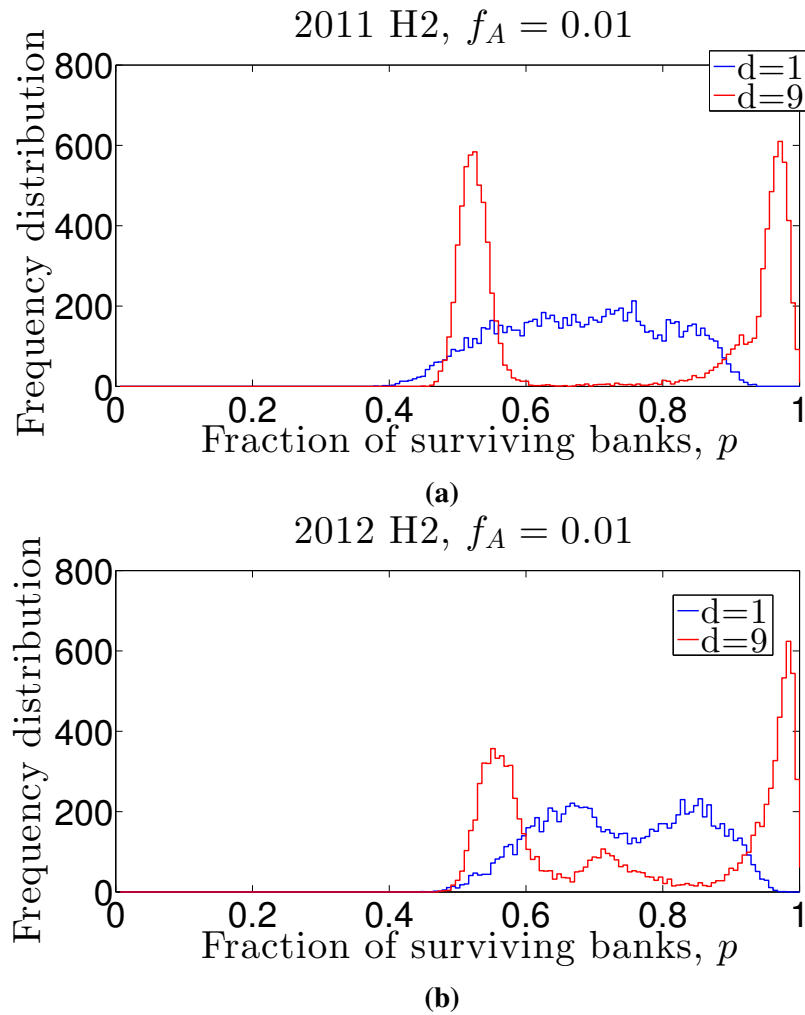


Figure C.5: To produce the plots in this figure, we use the same simulation set-up as was used to produce Figure 6.7. However, for the initialization of the models, we apply the 2011 H2 (a) and 2012 H2 (b) datasets for UK banks' balance sheets and interbank exposure data. The figures show the frequency distribution of the fraction of surviving banks, p , of 10^4 simulations. The parameter f_A is set to 0.01. For the blue line f_L was fixed at 1.032 for 2011 H2 (a), and at 1.037 for 2012 H2 (b) and the original interbank networks have been used during the simulations. For the red line, the exposure of LB was multiplied by a factor $d = 9$, and f_L was fixed at 1.013 for 2011 H2 (a), and 1.037 for 2012 H2 (b). For $d = 1$ (blue line), θ for all networks is below θ_c , and henceforth, no jump is visible. Instead the frequency distribution is almost bell shaped. For $d = 9$ (red line), θ is larger than θ_c , and peaks become visible around p approximately 0.5 and 0.95 confirming that the banking system can be in two states, where either most banks are operative or half of the banks are insolvent. These peaks cannot be observed for the frequency distribution when the original interbank network is used.

Appendix D

Variable Description

Variable	Variable description
α	Connection probability of two nodes.
β	Re-wiring probability for a link in the Small-World network .
γ	Leverage ratio.
γ_{\min}	Minimum leverage to ensure a stable system.
ϵ_i	Random variable drawn from a standard normal distribution.
μ_A	Location parameter of total assets.
$\mu_{\hat{A}}$	Location parameter of non-interbank assets.
μ_L	Location parameter of total liabilities.
μ	Difference between location parameter of liabilities and non-interbank assets.
θ	Fraction of interbank assets to total assets.
θ_c	Critical value of θ .
κ	Constant.
σ_A	Scale parameter of total assets.
$\sigma_{\hat{A}}$	Scale parameter of non-interbank assets.
σ_L	Scale parameter of liabilities.
σ	Scale parameter of the difference between the mean value of liabilities and non-interbank assets.
X	Adjacency matrix.
χ_{ij}	Element of Adjacency matrix X .

Variable	Variable description
$A_i(t)$	Total assets of bank i at time t .
$\hat{A}_i(t)$	Non-interbank assets of bank i at time t .
a	Mean-field value of the difference between the mean values of liabilities and non-interbank assets divided by the variance of the distribution of the difference of liabilities and non-interbank assets.
a_1	Value of a , at which the banking system changes from almost all banks insolvent to almost all banks solvent.
a_2	Value of a , at which the banking system changes from almost all banks solvent to almost all banks insolvent.
b	Mean-field value of interbank lending divided by the variance of the distribution of the
b_c	Critical value of b .
c	Neighbouring banks of all bank i in Small-World network.
f	Fraction by which the mean of Tier 1 capital is multiplied to resemble σ
f_A	Fraction by which the variance σ is multiplied to vary the occurrence of the fragile state.
f_L	Fraction that is multiplied to the mean value of liabilities to reduce or increase the overall average capital in the banking system.
f_L^*	Fraction that is multiplied to the mean value of liabilities at which the fragile state occurs.
G	Interbank exposure matrix.
$g_{ij}(t)$	Interbank exposure of bank i to bank j at time t .
g	Average interbank exposure.
$L_i(t)$	Total liabilities of bank i at time t .
$\hat{L}_i(t)$	Non-interbank liabilities of bank i at time t .
m	Location parameter.
N	Number of banks in the banking system.
Q	Recovery rate matrix.
$q_{ij}(t)$	Recovery rate of exposure of bank i to bank j at time t .
q	Average recovery rate.
s	Scale parameter.
$S_i(t)$	State of bank i at time t .
w_i	Fixed point, with $i \in \{1, 2, 3\}$.
x_i	Extrema of $x - F(x)$.
z	Average degree.
\bar{z}	Average degree of Erdős-Rényi network.
z_i	Degree of bank i .

Appendix E

Abbreviations

Abbreviation	Abbreviation description
<i>C</i>	Cauchy distribution.
<i>L</i>	Logistic distribution.
<i>LL</i>	Log-Logistic distribution.
<i>LN</i>	Log-Normal distribution.
<i>N</i>	Normal distribution.
<i>S</i>	Student's distribution.

Abbreviation	Abbreviation description
Annot.	Annotation.
2011 H2	Year 2011, second half.
2012 H2	Year 2012, second half.
2013 H1	Year 2013, first half.
BoE	Bank of England.
BS	UK building society.
CB	Other UK commercial bank.
CDS	Credit default swap.
CoVar	Conditional Value at risk.
ES	Expected Shortfall.
FWHM	Full width at half maximum.
IB	Investment bank.
LB	Large UK bank.
LHS	Left hand side.
PDF	Probability distribution function.
repos	Repayment products.
RFIM	Random Field Ising Model.
RHS	Right hand side.
RWA	Risk Weighted Assets.
OB	Oversea bank; subsidiaries of international banks regulated by the PRA.
OTC	Over the counter.
QE	Quantitative easing.
SES	Systemic Expected Shortfall.
STD	Standard deviation.
VaR	Value at Risk.

Bibliography

- Acharya, V., Engle, R., Pierret, D., 2014. Testing macroprudential stress tests: The risk of regulatory risk weights. *Journal of Monetary Economics* 65, 36–53.
- Acharya, V., Pedersen, L., Philippon, T., Richardson, M., 2010. Measuring systemic risk. http://papers.ssrn.com/sol3/papers.cfm?abstract_id=1573171, accessed: 2014-30-07.
- Adrian, T., Brunnermeier, M. K., Jan 2011. Covar. <http://www.princeton.edu/~markus/research/papers/CoVaR.pdf>, accessed July 21, 2014.
- Albert, R., Barabási, A.-L., 2002. Statistical mechanics of complex networks. *Reviews of modern physics* 74 (1), 47.
- Alessandri, P., Gai, P., Kapadia, S., Mora, N., Pühr, C., 2009. Towards a framework for quantifying systemic stability. *International Journal of Central Banking* 5 (3), 47–81.
- Allen, F., Carletti, E., Gale, D., 2009. Interbank market liquidity and central bank intervention. *Journal of Monetary Economics* 56 (5), 639–652.
- Allen, F., Gale, D., 2000. Financial contagion. *Journal of political economy* 108 (1), 1–33.
- Amini, H., Cont, R., Minca, A., 2012. Stress testing the resilience of financial networks. *International Journal of Theoretical and applied finance* 15 (01), 1250006.
- Amini, H., Cont, R., Minca, A., 2013. Resilience to contagion in financial networks. *Mathematical Finance* Preprint.
- Amundsen, E., Arnt, H., 2005. Contagion risk in the danish interbank market. <http://www.econstor.eu/handle/10419/82331>, accessed: 2014-30-07.

- Anand, K., Gai, P., Kapadia, S., Brennan, S., Willison, M., 2012. A network model of financial system resilience. *Journal of Economic Behavior and Organization* 85, 219–235.
- Arciero, L., Heijmans, R., Heuver, R., Massarenti, M., Picillo, C., Vacirca, F., 2014. How to measure the unsecured money market? The Eurosystem's implementation and validation using TARGET2 data. Social Science Research Network.
- Bank for International Settlement, 2014. Basel iii leverage ratio framework and disclosure requirements. <http://www.bis.org/publ/bcbs270.pdf>, accessed: 2014-07-10.
- Barabási, A.-L., Albert, R., 1999. Emergence of scaling in random networks. *science* 286 (5439), 509–512.
- Bargigli, L., Di Iasio, G., Infante, L., Lillo, F., Pierobon, F., 2015. The multiplex structure of interbank networks. *Quantitative Finance* 15, 673–691.
- Barrat, A., Barthelemy, M., Vespignani, A., 2008. Dynamical processes on complex networks. Vol. 1. Cambridge University Press Cambridge.
- Basel Committee on Banking Supervision, 2004. Basel ii: International convergence of capital measurement and capital standards: a revised framework. <http://www.bis.org/publ/bcbs107.htm>, accessed: 2013-05-04.
- Basel Committee on Banking Supervision, 2010. Basel iii: A global regulatory framework for more resilient banks and banking systems. http://www.bis.org/publ/bcbs189_dec2010.htm, accessed: 2013-05-04.
- Basurto, M. A. S., 2006. Portfolio credit risk and macroeconomic shocks: Applications to stress testing under data-restricted environments. No. 6-283. International Monetary Fund.
- Battiston, S., Delli Gatti, D., Gallegati, M., Greenwald, B., Stiglitz, J. E., 2012a. Liasons dangereuses: Increasing connectivity, risk sharing, and systemic risk. *Journal of Economic Dynamics and Control* 36 (8), 1121–1141.

- Battiston, S., Gatti, D. D., Gallegati, M., Greenwald, B., Stiglitz, J. E., 2012b. Default cascades: When does risk diversification increase stability? *Journal of Financial Stability* 8 (3), 138–149.
- Battiston, S., Puliga, M., Kaushik, R., Tasca, P., Caldarelli, G., 2012c. DebtRank: Too Central to Fail? Financial Networks, the FED and Systemic Risk. *Scientific Reports* 2, 1–5.
- Bech, M. L., Atalay, E., 2010. The topology of the federal funds market. *Physica A: Statistical Mechanics and its Applications* 389 (22), 5223–5246.
- Bhattacharya, S., Gale, D., 1985. Preference shocks, liquidity, and central bank policy. edited by William, in *New Approaches to Monetary Economics*.
- Billio, M., Getmansky, M., Lo, A. W., Pelizzon, L., 2012. Econometric measures of connectedness and systemic risk in the finance and insurance sectors. *Journal of Financial Economics* 104 (3), 535–559.
- Birch, A., Aste, T., 2014. Systemic losses due to counter party risk in a stylized banking system. *Journal of Statistical Physics* 156, 998–1024.
- BIS, 2011. International regulatory framework for banks (Basel III). <http://www.bis.org/bcbs/basel3.htm>, accessed: 2014-07-10.
- Blåvarg, M., Nimander, P., 2002. Interbank exposures and systemic risk. *Sveriges Riksbank Economic Review* 2, 19–45.
- Board of Governors of the Federal Reserve System, 2014. Fedwire Funds Service. http://www.federalreserve.gov/paymentsystems/fedfunds_about.htm, accessed Sep 22, 2014.
- Boss, M., Elsinger, H., Summer, M., Thurner, S., 2004. Network topology of the interbank market. *Quantitative Finance* 4 (6), 677–684.
- Boss, M., Krenn, G., Pühr, C., Summer, M., 2006. Systemic risk monitor: A model for systemic risk analysis and stress testing of banking systems. *Financial Stability Report* 11, 83–95.

- Bouchaud, J.-P., 2013. Crises and collective socio-economic phenomena: cartoon models and challenges. *Journal of Statistical Physics* 151, 567–606.
- Brain Connectivity Toolbox, 2010. Home. <https://sites.google.com/site/bctnet/>, accessed: 2014-30-07.
- Bruche, M., González-Aguado, C., 2010. Recovery rates, default probabilities, and the credit cycle. *Journal of Banking and Finance* 34 (4), 754–764.
- Bureau Van Dijk, Jan 2014. Bankscope. <https://bankscope2.bvdep.com/version-2014123/home.serv?product=scope2006>, accessed Jan 21, 2014.
- Caccioli, F., Catanach, T. A., Farmer, J. D., 2012. Heterogeneity, correlations and financial contagion. *Advances in Complex Systems* 15, 1–15.
- Caccioli, F., Shrestha, M., Moore, C., Doyne Farmer, J., 2014. Stability analysis of financial contagion due to overlapping portfolios. *Journal of Banking and Finance* 46, 233–245.
- Chessa, A., Marinari, E., Vespignani, A., Zapperi, S., 1998. Mean-field behavior of the sandpile model below the upper critical dimension. *Physical Review E* 57 (6), R6241.
- Chessa, A., Vespignani, A., Zapperi, S., 1999. Critical exponents in stochastic sandpile models. *Computer physics communications* 121, 299–302.
- Cifuentes, R., Ferrucci, G., Shin, H. S., 2005. Liquidity risk and contagion. *Journal of the European Economic Association* 3 (2-3), 556–566.
- Claessens, S., Kose, M. A., Laeven, L., Valencia, F., 2013. Understanding Financial Crises: Causes, Consequences, and Policy Responses. CAMA Working Paper.
- Cocco, J. F., Gomes, F. J., Martins, N. C., 2009. Lending relationships in the interbank market. *Journal of Financial Intermediation* 18 (1), 24–48.
- Cont, R., Moussa, A., Santos, E. B. e., 2010. Network structure and systemic risk in banking systems. Social Science Research Network.

- Craig, B. R., Von Peter, G., 2010. Interbank tiering and money center banks. Tech. rep., BIS Working Papers.
- Dahmen, K., Sethna, J. P., 1996. Hysteresis, avalanches, and disorder-induced critical scaling: A renormalization-group approach. *Physical Review B* 53 (22), 14872–14905.
- De Dominicis, C., Giardinà, I., 2006. Random fields and spin glasses. Cambridge University Press Cambridge.
- De Masi, G., Iori, G., Caldarelli, G., 2006. Fitness model for the Italian interbank money market. *Physical Review E* 74 (6), 066112.
- de Matos, J. A., Perez, J. F., 1991. Fluctuations in the curie-weiss version of the random field ising model. *Journal of Statistical Physics* 62 (3-4), 587–608.
- Degryse, H., Nguyen, G., 2007. Interbank exposures: An empirical examination of contagion risk in the belgian banking system. *International Journal of Central Banking* 3 (2), 123–171.
- Delpini, D., Battiston, S., Riccaboni, M., Gabbi, G., Pammolli, F., Caldarelli, G., 2013. Evolution of controllability in interbank networks. *Scientific reports* 3, 1626.
- Devaney, R. L., Devaney, L., Devaney, L., 2003. An introduction to chaotic dynamical systems. Vol. 6. Addison-Wesley Reading.
- Di Matteo, T., Aste, T., Gallegati, M., 2005. Innovation flow through social networks: productivity distribution in france and italy. *The European Physical Journal B-Condensed Matter and Complex Systems* 47 (3), 459–466.
- e MID, Sep 2014. e-MID. <http://www.e-mid.it/>, accessed Sep 22, 2014.
- ECB, June 2009. Press release, 4 June 2009 - Purchase programme for covered bonds. http://www.ecb.int/press/pr/date/2009/html/pr090604_1.en.html, accessed Jan 30, 2011.
- ECB, November 2011. Press release, 3 November 2011 - ECB announces details of its new covered bond purchase programme (CBPP2).

- http://www.ecb.int/press/pr/date/2011/html/pr111103_1.en.html, accessed Jan 30, 2011.
- Eisenberg, L., Noe, T. H., 2001. Systemic risk in financial systems. *Management Science* 47 (2), 236–249.
- Elsinger, H., Lehar, A., Summer, M., 2006. Risk assessment for banking systems. *Management science* 52 (9), 1301–1314.
- European Systemic Risk Board, 2015. Publications. <https://www.esrb.europa.eu/pub/html/index.en.html>, accessed: 2015-30-03.
- Farmer, J. D., Geanakoplos, J., 2009. The virtues and vices of equilibrium and the future of financial economics. *Complexity* 14 (3), 11–38.
- Fed, Nov 2011a. Credit and Liquidity Programs and the Balance Sheet. The Federal Reserve's response to the crisis. http://www.federalreserve.gov/monetarypolicy/bst_crisisresponse.htm, accessed Jan 30, 2011.
- Fed, Nov 2011b. Credit and Liquidity Programs and the Balance Sheet. The Federal Reserve's response to the crisis. http://www.federalreserve.gov/monetarypolicy/bst_crisisresponse.htm, accessed Jan 30, 2011.
- Financial Crisis Inquiry Commission and others, 2011. The financial crisis inquiry report. US Government Printing Office.
- Fique, J., Page, F., 2013. Rollover risk and endogenous network dynamics. *Computational Management Science* 10 (2-3), 213–230.
- Fleming, M. J., Sarkar, A., 2014. The Failure Resolution of Lehman Brothers. *Economic Policy Review*, Forthcoming.
- Fouque, J.-P., Langsam, J. A., 2013. *Handbook on Systemic Risk*. Cambridge University Press.

- Freixas, X., Parigi, B. M., Rochet, J.-C., 2000. Systemic risk, interbank relations, and liquidity provision by the central bank. *Journal of money, credit and banking*, 611–638.
- Fricke, D., Lux, T., 2015. Core-periphery structure in the overnight money market: Evidence from the e-mid trading platform. *Computational Economics* 45 (3), 359–395.
- FSA, Dec 2011. The failure of the Royal Bank of Scotland - Financial Services Authority Board Report. <http://www.fsa.gov.uk/pubs/other/rbs.pdf>, accessed Jan 21, 2014.
- Furfine, C. H., 2003. Interbank exposures: Quantifying the risk of contagion. *Journal of Money, Credit and Banking*, 111–128.
- Gai, P., 2013. *Systemic risk - the dynamics of modern financial systems*. Oxford University Press.
- Gai, P., Haldane, A., Kapadia, S., 2011. Complexity, concentration and contagion. *Journal of Monetary Economics* 58 (5), 453–470.
- Gai, P., Jenkinson, N., Kapadia, S., 2007. Systemic risk in modern financial systems: analytics and policy design. *Journal of Risk Finance* 8 (2), 156–165.
- Gai, P., Kapadia, S., 2010. Contagion in financial networks. *Proceedings of the Royal Society A: Mathematical, Physical and Engineering Science* 466, 2401–2423.
- Garlaschelli, D., Di Matteo, T., Aste, T., Caldarelli, G., Loffredo, M. I., 2007. Interplay between topology and dynamics in the world trade web. *The European Physical Journal B* 57 (2), 159–164.
- Garnier, J., Papanicolaou, G., Yang, T.-W., 2013. Diversification in financial networks may increase systemic risk. In: Fouque, J.-P., Langsam, J. A. (Eds.), *Handbook on Systemic Risk*. Cambridge University Press.
- Geanakoplos, J., Karatzas, I., Shubik, M., Sudderth, W. D., 2014. Inflationary equilibrium in a stochastic economy with independent agents. *Journal of Mathematical Economics* 52, 1–11.

- Glasserman, P., Young, H. P., 2015. How likely is contagion in financial networks? *Journal of Banking & Finance* 50, 383–399.
- Gleeson, J. P., Hurd, T., Melnik, S., Hackett, A., 2013. Systemic risk in banking networks without monte carlo simulation. In: *Advances in Network Analysis and its Applications*. Springer, pp. 27–56.
- Goode, R., 2010. *Principles of corporate insolvency law*, 4th Edition. Sweet and Maxwell.
- Griessen, R., 1983. Phase separation in amorphous metal hydrides - a stoner-type criterion. *Physical Review B* 27 (12), 7575.
- Haldane, A. G., 2009. Rethinking the financial network. In: Speech presented at the Financial Student Association.
- Haldane, A. G., Madouros, V., 2012. The dog and the frisbee. In: Speech presented at the Federal Reserve Bank of Kansas City's Jackson Hole economic policy symposium.
- Haldane, A. G., May, R. M., 2011. Systemic risk in banking ecosystems. *Nature* 469 (7330), 351–355.
- Hale, G., Candelaria, C., Caballero, J., Borisov, S., 2011. Global banking network and cross-border capital flows. Tech. rep., Mimeo. Federal Reserve Bank of San Francisco, and University of California, Santa Cruz.
- Hatchett, J., Kuehn, R., 2009. Credit contagion and credit risk. *Quantitative Finance* 9 (4), 373–382.
- Hatzopoulos, V., Iori, G., Mantegna, R. N., Micciché, S., Tumminello, M., 2014. Quantifying preferential trading in the e-mid interbank market. *Quantitative Finance* (ahead-of-print), 1–18.
- Heise, S., Kühn, R., 2012. Derivatives and credit contagion in interconnected networks. *The European Physical Journal B* 85 (4), 1–19.
- Helbing, D., 2012. Systemic risks in society and economics. Springer, pp. 261–284.

- Hommes, C., 2006. Interacting agents in finance. Tech. rep., Tinbergen Institute Discussion Paper.
- Huang, X., Zhou, H., Zhu, H., 2009. A framework for assessing the systemic risk of major financial institutions. *Journal of Banking & Finance* 33 (11), 2036–2049.
- Huang, X., Zhou, H., Zhu, H., 2012. Assessing the systemic risk of a heterogeneous portfolio of banks during the recent financial crisis. *Journal of Financial Stability* 8 (3), 193–205.
- Hull, J., Nelken, I., White, A., 2004. Merton’s model, credit risk, and volatility skews. *Journal of Credit Risk* Volume 1 (1), 05.
- Hurd, T. R., Gleeson, J. P., 2011. A framework for analyzing contagion in banking networks. arXiv preprint arXiv:1110.4312.
- Iori, G., De Masi, G., Precup, O. V., Gabbi, G., Caldarelli, G., 2008. A network analysis of the italian overnight money market. *Journal of Economic Dynamics and Control* 32 (1), 259–278.
- Iori, G., Jafarey, S., Padilla, F. G., 2006. Systemic risk on the interbank market. *Journal of Economic Behavior and Organization* 61 (4), 525–542.
- Iori, G., Kapar, B., Olmo, J., 2012. The cross-section of interbank rates: A nonparametric empirical investigation. <http://openaccess.city.ac.uk/1613/>, accessed Jun 11, 2015.
- Ising, E., 1925. A contribution to the theory of ferromagnetism. *Z. Phys* 31 (1), 253–258.
- Klimek, P., Poledna, S., Farmer, J. D., Thurner, S., 2014. To bail-out or to bail-in? answers from an agent-based model. arXiv preprint arXiv:1403.1548.
- Kolb, R., 2010. *Lessons from the financial crisis: Causes, consequences, and our economic future*. John Wiley & Sons.
- Kollewe, J., July 2011. ECB raises interest rates despite debt crisis. <http://www.guardian.co.uk/business/2011/jul/07/ebc-raise-interest-rates-debt-crisis>, accessed Jan 30, 2011.

- Langfield, S., Liu, Z., Ota, T., 2014. Mapping the UK interbank system. *Journal of Banking and Finance* 45, 288–303.
- Langfield, S., Soramäki, K., 2014. Interbank exposure networks. *Computational Economics*, 1–15.
- Lublóy, Á., 2005. Domino effect in the hungarian interbank market. *Hungarian Economic Review* 52 (4), 377–401.
- Lux, T., Marchesi, M., 2000. Volatility clustering in financial markets: A microsimulation of interacting agents. *International Journal of Theoretical and Applied Finance* 3 (04), 675–702.
- Martínez-Jaramillo, S., Alexandrova-Kabadjova, B., Bravo-Benítez, B., Pablo Solórzano-Margain, J., 2014. An empirical study of the mexican banking system's network and its implications for systemic risk. *Journal of Economic Dynamics and Control* 40, 242–265.
- Mastromatteo, I., Zarinelli, E., Marsili, M., 2012. Reconstruction of financial networks for robust estimation of systemic risk. *Journal of Statistical Mechanics: Theory and Experiment* 2012 (03), P03011.
- May, R. M., Arinaminpathy, N., 2010. Systemic risk: the dynamics of model banking systems. *Journal of the Royal Society Interface* 7 (46), 823–838.
- May, R. M., Levin, S. A., Sugihara, G., 2008. Complex systems: Ecology for bankers. *Nature* 451 (7181), 893–895.
- Memmel, C., Stein, I., 2008. Contagion in the german interbank market. Tech. rep., Deutsche Bundesbank.
- Merton, R. C., 1973. An intertemporal capital asset pricing model. *Econometrica: Journal of the Econometric Society*, 867–887.
- Mistrulli, P. E., 2005. Interbank lending patterns and financial contagion. Online verfügbar unter <http://www.efmaefm.org/OEFMAMEETINGS/EFMA%20ANNUAL%20MEETINGS/2008-athens/Memmel.pdf>.

- Mistrulli, P. E., 2011. Assessing financial contagion in the interbank market: Maximum entropy versus observed interbank lending patterns. *Journal of Banking and Finance* 35 (5), 1114–1127.
- Müller, J., 2006. Interbank credit lines as a channel of contagion. *Journal of Financial Services Research* 29 (1), 37–60.
- Musmeci, N., Battiston, S., Caldarelli, G., Puliga, M., Gabrielli, A., 2012. Bootstrapping topology and systemic risk of complex network using the fitness model. arXiv preprint arXiv:1209.6459.
- Newman, M., 2010. *Networks: an introduction*. Oxford University Press.
- Newman, M. E., 2002. Spread of epidemic disease on networks. *Physical review E* 66 (1), 016128.
- Nier, E., Yang, J., Yorulmazer, T., Alentorn, A., 2007. Network models and financial stability. *Journal of Economic Dynamics and Control* 31 (6), 2033–2060.
- Poledna, S., Thurner, S., 2014. Elimination of systemic risk in financial networks by means of a systemic risk transaction tax. arXiv preprint arXiv:1401.8026.
- Pozzi, F., Di Matteo, T., Aste, T., 2013. Spread of risk across financial markets: better to invest in the peripheries. *Scientific reports* 3, 01665.
- Pricewaterhouse Coopers, 2014. IFRS and US GAAP: similarities and differences. http://www.pwc.com/en_US/us/issues/ifrs-reporting/publications/assets/ifrs-and-us-gaap-similarities-and-differences-2014.pdf, accessed: 2014-17-10.
- RBS, 2014. Annual Report and Accounts 2013. <http://www.investors.rbs.com/media/Files/R/RBS-IR/2013-reports/annual-report-and-accounts-2013.pdf>, accessed March 11, 2015.
- Richards, P. M., 1984. Lattice gas with random-site energies and theory of novel amorphous metal hydride phase. *Physical Review B* 30 (9), 5183.

- Rinne, H., 2011. Location-scale distributions. In: *International Encyclopedia of Statistical Science*. Springer, pp. 752–754.
- Rochet, J.-C., Tirole, J., 1996. Interbank lending and systemic risk. *Journal of Money, credit and Banking*, 733–762.
- Rørørdam, K. B., Bech, M. L., 2008. The topology of Danish interbank money flows. Tech. rep., University of Copenhagen. Department of Economics. Finance Research Unit.
- Roukny, T., Bersini, H., Pirotte, H., Caldarelli, G., Battiston, S., 2013. Default cascades in complex networks: Topology and systemic risk. *Scientific Reports* 3, 1–8.
- Rubinov, M., Sporns, O., 2010. Complex network measures of brain connectivity: uses and interpretations. *Neuroimage* 52 (3), 1059–1069.
- Ryan, J., November 2011. Bank of England Keeps Asset Purchase Program Steady, Holds Benchmark Rate. <http://www.bloomberg.com/news/2011-11-10/bank-of-england-keeps-asset-purchase-program-steady-holds-benchmark-rate.html>, accessed Jan 30, 2011.
- Segoviano, M. A., Goodhart, C. A. E., 2009. Banking stability measures. No. 627. International Monetary Fund.
- Sethna, J. P., Dahmen, K., Kartha, S., Krumhansl, J. A., Roberts, B. W., Shore, J. D., 1993. Hysteresis and hierarchies: Dynamics of disorder-driven first-order phase transformations. *Physical Review Letters* 70 (21), 3347.
- Singh, R. K., 2010. The Role of Central Bank in Crisis Management. Social Science Research Network.
- Smith, H. L., 1995. *Monotone Dynamical Systems - An Introduction to the Theory of Competitive and Cooperative Systems*, 4th Edition. American Mathematical Society.
- Smith, H. L., 2008. *Monotone Dynamical Systems: An Introduction to the Theory of Competitive and Cooperative Systems*, 41st Edition. American Mathematical Soc.

- Solorzano-Margain, J. P., Martinez-Jaramillo, S., Lopez-Gallo, F., 2013. Financial contagion: extending the exposures network of the mexican financial system. *Computational Management Science*, 1–31.
- Soramäki, K., Bech, M. L., Arnold, J., Glass, R. J., Beyeler, W. E., 2007. The topology of interbank payment flows. *Physica A: Statistical Mechanics and its Applications* 379 (1), 317–333.
- Staum, J., 2013. Counterparty contagion in context: Contributions to systemic risk. In: Fouque, J.-P., Langsam, J. A. (Eds.), *Handbook on Systemic Risk*. Cambridge University Press.
- The Federal Reserve Board, August 2011. 2 Monetary Policy and the Economy. http://www.federalreserve.gov/pf/pdf/pf_2.pdf, accessed Jan 30, 2011.
- Thurner, S., Poledna, S., 2013. Debtrank-transparency: Controlling systemic risk in financial networks. *Scientific reports* 3.
- Toivanen, M., 2009. Financial interlinkages and risk of contagion in the finnish interbank market. Tech. rep., Suomen Pankki.
- Tsatskis, I., 2012. Systemic losses in banking networks: indirect interaction of nodes via asset prices. Available at SSRN 2062174.
- UK parliament, 2013. 4 capital and loss absorbency. <http://www.publications.parliament.uk/pa/jt201213/jtselect/jtpcb/126/12606.htm>, accessed: 2014-30-07.
- Upper, C., 2011. Simulation methods to assess the danger of contagion in interbank markets. *Journal of Financial Stability* 7 (3), 111–125.
- Upper, C., Worms, A., 2004. Estimating bilateral exposures in the german interbank market: Is there a danger of contagion? *European Economic Review* 48 (4), 827–849.
- Van Lelyveld, I., Liedorp, F., 2006. Interbank contagion in the dutch banking sector: A sensitivity analysis. *International Journal of Central Banking* 2 (2), 99–133.

- van Lelyveld, I., et al., 2012. Finding the core: Network structure in interbank markets. Tech. rep., De Nederlandse Bank.
- Viegas, E., Takayasu, M., Miura, W., Tamura, K., Ohnishi, T., Takayasu, H., Jensen, H. J., 2013. Ecosystems perspective on financial networks: diagnostic tools. arXiv preprint arXiv:1301.5821.
- Watts, D. J., 2002. A simple model of global cascades on random networks. *Proceedings of the National Academy of Sciences* 99 (9), 5766–5771.
- Watts, D. J., Strogatz, S. H., 1998. Collective dynamics of ‘small-world’ networks. *Nature* 393 (6684), 440–442.
- Webber, L., Willison, M., 2011. Systemic capital requirements. Bank of England Working Paper.
- Weidlich, W., 1971. The statistical description of polarization phenomena in society. *British Journal of Mathematical and Statistical Psychology* 24 (2), 251–266.
- Weidlich, W., 1994. Synergetic modelling concepts for sociodynamics with application to collective political opinion formation. *Journal of Mathematical Sociology* 18 (4), 267–291.
- Wetherilt, A., Soramaki, K., Zimmerman, P., 2010. The sterling unsecured loan market during 2006-08: insights from network theory. Bank of England Working Paper.